Molecular Characterisation and Modelling for Refining Processes

A thesis submitted to the University of Manchester for the degree of

Doctor of Philosophy

in the Faculty of Engineering and Physical Sciences

2015

Luyi Liu

Under the supervision of

Dr. Nan Zhang

Centre for Process Integration

School of Chemical Engineering and Analytical Science

Table of Contents

List of Tables

List of Figures

Abstract

The highly competitive market in the oil refining industry forces refiners look for more detailed information of both feedstocks and products to achieve the optimal economic performance. Due to stricter environmental legislations, the molecular level characterisation has been investigated by various researchers and shows promising advantages in modern refinery design and operation. Although various molecular characterisation methods have been developed, there is an unavoidable trade-off between keeping astronomical molecule details and practicality in industrial applications. In the meantime, many of these methodologies have different characteristics and different focuses according to a particular application purpose. Our aim is hence to tackle the problems of developing manageable and practical technical solutions for molecular characterisation of petroleum fractions for vary refinery processes.

A pseudo-component based approach is developed within a modified MTHS (Molecular Type Homologous Series) matrix framework (Peng, 1999) to represent the molecular information of a particular refining stream. This proposed methodology incorporates both molecular type and pseudo-component information by the conjunction of homologous series and boiling points in the matrix framework. To increase the usability of this method, a 3-parameter gamma distribution function is introduced to describe the composition of each structural molecular type. Typical PIONA (paraffin, iso-paraffin, olefin, naphthene, aromatic) analysis, ratios between each homologous types and the percentage of particular carbon type are considered as well as the distillation curve and the density of a stream.

More strict product specifications and environmental legislations make strong

restriction to the benzene and aromatics content in gasoline products, which motivate refiners to understand, characterise and simulate gasoline catalytic reforming on molecular-level. In this work, kinetic and reactor model of naphtha catalytic reforming is developed based on the proposed MTHS method. The naphtha feedstock composition is represented by the MTHS matrix, and a kinetic network is constructed according to conversions among matrix elements. A process model proposed by Wu (2010) is employed for reforming modelling. The proposed model is then applied to a bench-scale semi-regenerative catalytic reforming unit, which contains 3 fixed-bed reactors, for validation. The influences of essential operating conditions, such as reactor inlet temperature, pressure and weight hourly space velocity (WHSV), on the product distribution and quality are explored.

The developed characterisation is also applied in gasoline blending modelling. A molecular-level nonlinear gasoline blending model is developed based on proposed MTHS method with validation. Key properties such as Octane Numbers (ONs) and RVP are blended by molecular matrix elements, and the influence of molecular composition on bulk properties is obvious. A case of recipe optimisation is studied to show the applicability of the proposed method.

The implementation of the developed MTHS method for catalytic reforming and gasoline blending demonstrates the compatibility when characterising different petroleum streams, and provides a common platform to simulate and optimise refining operations on the same molecular basis.

DECLARATION

No portion of the work referred to in the thesis has been submitted in support of an application for another degree or qualification of this or any other university or other institute of learning.

Luyi Liu

Manchester, 2015

Copyright Statement

i. The author of this thesis (including any appendices and/or schedules to this thesis) owns any copyright in it (the "Copyright") and she has given The University of Manchester the right to use such Copyright for any administrative, promotional, educational and/or teaching purposes.

ii. Copies of this thesis, either in full or in extracts, may be made only in accordance with the regulations of the John Rylands University Library of Manchester. Details of these regulations may be obtained from the Librarian. This page must form part of any such copies made.

iii. The ownership of any patents, designs, trademarks and any and all other intellectual property rights except for the Copyright (the "Intellectual Property Rights") and any reproductions of copyright works, for example graphs and tables ("Reproductions"), which may be described in this thesis, may not be owned by the author and may be owned by third parties. Such Intellectual Property Rights and Reproductions cannot and must not be made available for use without the prior written permission of the owner(s) of the relevant Intellectual Property Rights and/or Reproductions.

iv. Further information on the conditions under which disclosure, publication and exploitation of this thesis, the Copyright and any Intellectual Property Rights and/or Reproductions described in it may take place is available from the Head of School of Chemical Engineering & Analytical Science.

Dedicated to my dearest parents

Acknowledgement

I would like to express my sincere gratitude towards my supervisor Dr. Nan Zhang for his guidance, advice, support and encouragement throughout my research period.

Thanks all members of the Centre for Process Integration, for providing a friendly international environment. Special thanks to Dr. Lluvia Ochoa-Estopier, Maria, Fei, Shixun, Kunpeng, Chengjun, Luwen for their kind help and cheerful spirit.

My deepest thanks to my parents, grandparents, and my uncle's family for their endless love and support through my life. I would like to thank Feixue and Elsa for their company during my life in Manchester. I am grateful to my friends Echo, Rui and Likun in China for their understanding and encouragement.

Last but not least, I wish to acknowledge the help and the inspiration provided by Dr. Yongwen Wu, and Dr. Linzhou Zhang in my PhD study.

Chapter 1 Introduction

1.1 Introduction to Petroleum Refining Scheme

The petroleum refining industry is essential to the modern society. It produces not only fuels of transportation, but also some feedstocks for the chemical industry. Although the oil consumption percentage in world energy consumption has been decreased due to the increasing use of new energy sources such as hydroelectricity, wind, solar and biomass, 33% of world energy consumption was still made by oil in 2012. Table 1.1 shows the consumption comparison of different energy sources in total world energy (BP, 2013).

Table 1. 1 Consumption comparison of different energy sources

Million tonnes oil equivalent	2002	2007	2012
Oil	3640.2	4009.7	4130.5
Natural gas	2276.7	2647.3	2987.1
Coal	2411.0	3199.8	3730.1
Nuclear	610.5	621.8	560.4
Hydroelectricity	598.5	700.7	831.1
Renewable energy	60.9	108.1	237.4
Total	9597.8	11287.5	12476.6

Crude oil is a very complex mixture of hydrocarbon compounds with heteroatoms. These compounds have varying molecular weight, structure and corresponding properties. Some of them are undesirable for petroleum products, so that a series of refining processes are needed to produce different products or mid-products that can

meet the specifications and market demand.

The history of the refining industry started in the 19th century. At that time, refineries only comprised simple distillation units that converted crude oil to kerosene, gas oil, and fuel oil (Maples, 2000). In the 20th century, the invention of combustion engines and the development of the automobile industry lifted the demand of diesel and gasoline and promoted the development of the refining industry with process of cracking.

Nowadays, modern refineries become a very complex system that produce various fuels, lubricants and petrochemical products, and it basically comprises various refining processes and utilities (Hu, and Zhu, 2001). Refining processes can be roughly classified into 6 types according to different purposes: crude oil distillation unit, heavy oil conversion unit, upgrading unit, blending unit, light ends processes, supporting units and petrochemical plants (Lin, 2000). A distillation unit is the first process in a refinery that separates crude oil into several distillates and residues for further processing. A crude oil distillation unit typically contains an atmospheric section and a vacuum section. To improve the recovery rate of light fractions, heavy oil conversion units are utilised to convert vacuum distillates and residues into light fractions via cracking processes, for instance, catalytic cracking, hydrocracking, and coking. Upgrading processes including catalytic reforming, hydrotreating, hydrofining et al, can improve the quality of oil products to meet the property requirements. Normally several mid-product oils need to be blended together with some additives to meet the product specifications in a blending unit. The optimisation of oil products blending scheme could affect the profit of a refinery. Light ends processes include the isomerisation of C_5/C_6, and supporting processes include hydrogen plants, sulphur plants etc. A simplified flow diagram of a fuel refinery is shown in Figure 1.1 to show one combination of possible processes (Gary and Handwerk, 1994).

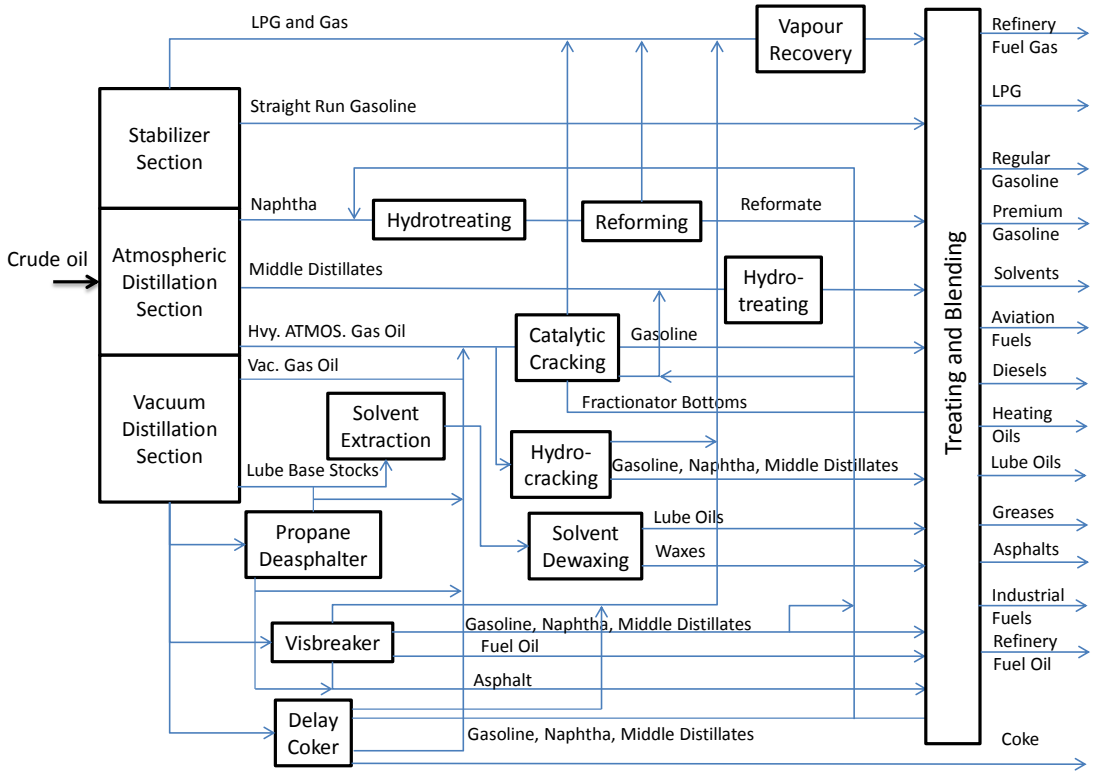

Figure 1. 1 Flowsheet of a refinery

The crude oil is fed to an atmospheric distillation unit (ADU) and separated into several cuts according to their boiling temperature ranges such as liquefied petroleum gas (LPG) and gas, straight run gasoline, light/heavy naphtha, kerosene, and diesel. The bottom distillates from the atmospheric distillation unit are fed to the vacuum distillation unit to retrieve gas oil which needs to be further converted to light and high value products in processes such as catalytic cracking, hydrocracking, delayed coking, etc.

1.2 Current Trends in the Refining Industry

Throughout the history of the oil refining industry, the aim of refining technologies is to produce products that can meet the stricter and stricter specifications and the higher and higher demand of petroleum products from crude oil.

Due to the background that crude oil is getting heavier and containing less volatile

fractions and the increasing demand of high-value lighter products, heavy fraction conversion processes have attracted more and more attentions. For example, in China, the content of vacuum residue with corresponding boiling temperature above 500˚C can reach around 40% - 50% in most crude oils (Lin, 2000). The involvement of these secondary conversion processes could lead to a more complex refinery configuration and introduce more interactions among process units.

The factor needs to be mentioned is that modern refineries are getting bigger and bigger in scale with the capacities from a few million to tens of million tons of crude oil annually. Although the total number of refineries decreased due to the limited profit margin, the average refinery capacity increased to 6.72 Mt/a in 2011(Li and Wang, 2013). It is reported that the average capacity of the largest 10 refineries in the U.S. is 10.32 Mt/a (U.S. Energy Information Administration, 2013), while the aggregate capacity of largest refinery of the world (Reliance Jamnagar Refinery, India) reaches 60 Mt/a (The Indian Express, 2008).

Another factor that forces the industry to modify its processes is the more and more rigid environmental legislations. Environmental issues have caused extensive public concern, especially the air quality problem. The increasing number of vehicles has become a major factor that caused the air quality problem due to car exhaust and secondary pollutants from their photochemical reactions in big cities since 1940s and 1950s (Haagen-Smit, 1956). These car exhaust pollutants include CO; some hydrocarbon compounds; nitrogen oxides such as NO, NO_2; SO_2; some metallic compounds such as lead and manganese from additives, etc (Twigg, 2007). Motor vehicle exhaust has been considered as a cause of many diseases (Marcqb, 2014) and correlated with breast cancer incidence (Park, 2014).

Environment concerns require cleaner oil products, so the product specifications are becoming more and more stringent and putting more emphasis on specific

compounds that can cause air and other environmental pollution. Table 1.2 and Table 1.3 list European Union and the U.S. gasoline specifications. Maximum limitations of benzene, total aromatics, oxygenates and olefins have been phased in since 1993. Especially for benzene content, the maximum limitation decreases from 5 vol% to 1 vol% in Europe, and from 2 vol% to 0.8 vol% in the U.S. during the past two decades. Similar product specifications have also been adopted in other countries of the world.

To achieve the environmental and product quality requirements, upgrading processes such as hydrotreating unit have become more crucial in a refinery. Besides, component limitations could force refiners to track and control these molecules throughout the clean fuel producing scheme, and which is one of the reason that promote the molecular-level refining technology.

Table 1. 2 European Union specifications for gasoline (Official Journal of the European Communities)

	EN228	Dir. 98/70	Dir. 98/70	Dir.98/70
Entry to force	1993/1995	2000	2005	2009
Vehicle emission Standard equivalent	Euro II	Euro III	Euro IV	Euro V
Sulphur [ppm] max	500	150	50	10
RVP [kPa] summer	35-100	60/70	60/70	60/70
Distillation [% v/v] min				
E100℃	-	46	46	46
E150℃	-	75	75	75
Hydrocarbon analysis				
Olefins [% v/v] max	-	18	18	18
Aromatics [% v/v] max	-	42	35	35
Benzene [% v/v] max	5.0	1.0	1.0	1.0
Oxygen [% m/m] max	-	2.7	2.7	2.7
Oxygenates [% v/v] max				
Methanol	-	3	3	3
Ethanol	-	5	5	10
Iso-propyl alcohol	-	10	10	12
Tert-butyl alcohol	-	7	7	15
Iso-butyl alcohol	-	10	10	15
Ethers containing 5 or more carbon atoms	-	15	15	22
Other oxygenates	-	10	10	15
Use of additives				MMT* banned from 2010

MMT: Methylcyclopentadienyl Manganese Tricarbonyl

Table 1. 3 Clean Air Act and CARB specifications (U.S.A.)

	1990	Clean Air Act			CARB*			
		Simple	Complex		Phase2 (1996)		Phase3 (2003)	
			I	II	Limit	Average	Limit	Average
Benzene [% v/v] max	2.0	1.0	1.0	1.0	1.0	0.8	0.8	0.7
Oxygen [% m/m] min	0.2	2.0	2.0	2.0	1.8	N/A	1.8	No change
Oxygen [% m/m] max	-	2.7	-	-	2.2		2.2	
Sulphur [ppm] max	150.0	-	-	-	40.0	30.0	20.0	15.0
Aromatics [% v/v] max	32.0	-	-	-	25.0	22.0	No change	No change
Olefins [% v/v] max	9.9	-	-	-	6.0	4.0	No change	No change
RVP [psi]	8.0	55.8	-	-	7.0	N/A	7.0	No change
(During VOC control period)	-	49.6	-	-				
50% evaporated [°F] max	-	-	-	-	210.0	200.0	211.0	201.0
90% evaporated [°F] max	170	-	-	-	300.0	290.0	305.0	295.0

CARB: California Air Resources Board

The development of the petrochemical industry is also influencing refineries especially on the quantity and species of feedstocks. In addition to lubricating oils and fuels, some refiners prefer to produce chemical materials to realise the optimum utilisation of oil resources. These by-products from refining units can be further processed to some high value chemical products, for example, ethylene could be used to produce plastic material, propylene could be used to produce polypropylene,

acrylonitrile or isopropyl alcohol, etc. The integration of refineries and petrochemical plants provides more flexibility for refiners to increase their economic margins, which is one of the main trends of the oil refining industry.

1.3 Challenges in Refinery Modelling

Refinery modelling becomes a very important approach for refinery process design, advanced control and optimisation in the strong integrated system of a modern refinery. The network among refining processes correlates a vast number of outputs from different units. Even a little change of feedstocks, operating conditions or other factors in a unit could lead to a significant influence on the performance of other units and the whole refinery. For instance, the vacuum product of a distillation unit could be fed to catalytic cracking; the light cycle oil (LCO) from catalytic cracking could be the feedstock to a hydrotreating process etc. As a consequence of the feed quality change in catalytic cracking, the product composition and the yields of gasoline and LCO would be affected, and would have a further impact on hydrotreating unit output.

The aim of refinery modelling is to predict bulk properties and yields of different products which could be subject to process operation conditions, which can then be used as basis for refinery optimisation, catalyst, properties and sources of feedstocks.

In addition, due to the huge capacity of modern refineries, the investment factor of such large plants must be considered. Hence, accurate modelling not only can improve the performance of refinery integration, but also can provide a solution to reduce the facilities investment and to maximise the profit.

With the rapid development of computer technology, refinery modelling is becoming more and more practical and detailed. Figure 1.2 illustrates the evolution of fluidised

catalytic cracking (FCC) modelling techniques (Christensen, 1999) during the past half century: from a very simple 3-lump model to composition based molecular models.

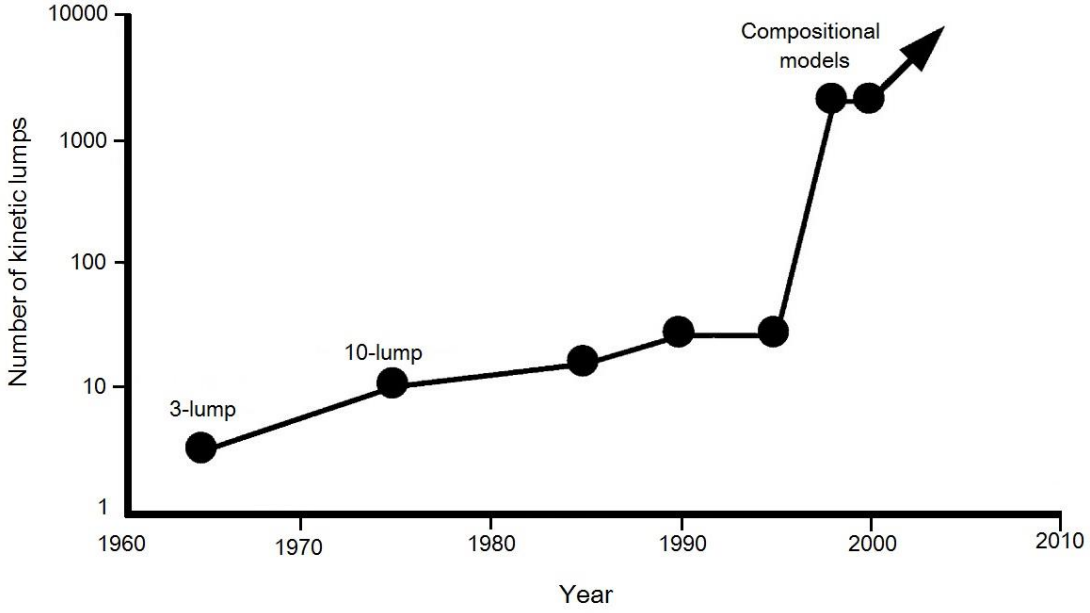

Figure 1. 2 The development of FCC modelling techniques

However, two technical challenges are remaining in this area according to the problem nature of refinery modelling: to characterise refining feedstocks and products with accuracy and appropriate representation framework to be adopted in process modelling; to build up consistent reaction and separation models that based on physical chemical rearrangement of petroleum molecules when processing. Therefore, an accurate and compatible characterisation method is the key starting point in better refinery modelling.

1.4 Introduction and Challenges in Molecular Characterisation of Petroleum Fractions and Its Application

1.4.1 Complexity of Petroleum Mixtures

As mentioned before, petroleum fractions are very complex mixtures of hydrocarbon compounds with enormous number of molecules. A crude oil composition schematic (Figure 2.1) shows the composition of typical petroleum hydrocarbon type analysis for Arabian heavy crude (Speight, 1998).

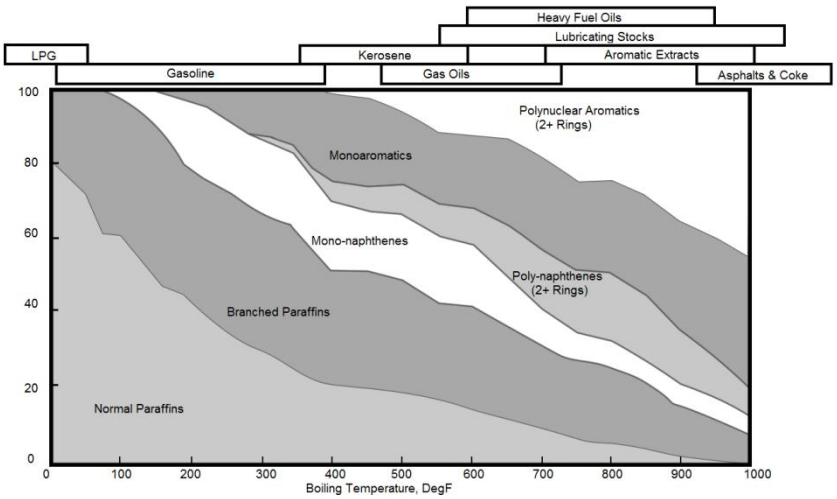

Figure 1. 3 Complexity of typical petroleum hydrocarbon type with boiling point (Speight, 1998)

With increasing boiling temperature and carbon number of petroleum fractions, the number of structural isomers grows exponentially as shown in Figure 1.4 (Read, 1976). The number of paraffin isomers increases from 75 for C_{10} to 4347 for C_{20}, and when carbon number goes higher to 40+, the paraffin isomers number could reach multi trillion, which is impossible to analysis by existing approaches. Besides,

undesirable heteroatoms including sulphur, nitrogen, oxygen and metal elements (nickel, iron, vanadium, calcium and etc.) of the petroleum fractions strongly coupling to hydrocarbons are very difficult to describe according to their various possible positions in molecules. Elements analysis of Orinoco VR stream (Table 1.4) shows the complexity of high boiling point fractions.

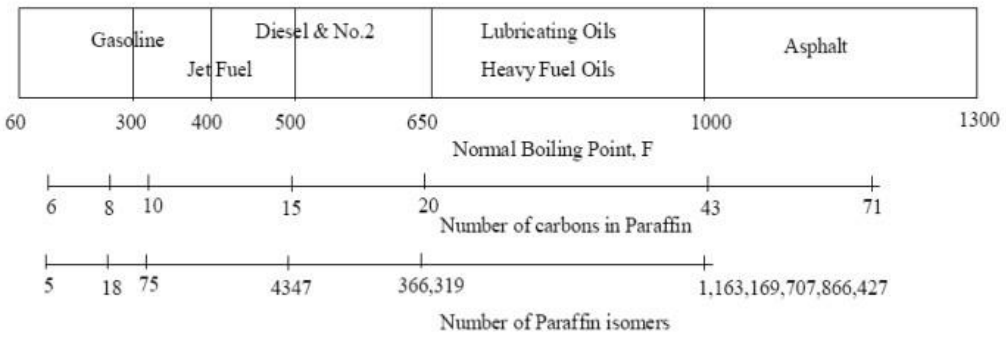

Figure 1. 4 Chemical complexity of petroleum fractions (Read, 1976)

Although such molecule by molecule analysis might not be essential, but to comply with the environmental regulations and further understand the nature of streams, molecular analysis to a certain extent is necessary.

The complex composition of petroleum fractions makes it extremely difficult to keep molecular information in a certain characterisation framework. Therefore, previous researchers working on this area focus on limited characters that might be only essential in a particular process model, which could be far from adequate for an overall characterisation and restrict their methods to a narrow application.

1.4.2 Introduction of Petroleum Characterisation

In the early stage, due to the lack of integration methodology and the computation power, characterisation methods were mainly developed for a particular process model, and without considerations of changes in feedstock composition and operating conditions. As a consequence, petroleum fractions are lumped into several

simple chemical groups for further simulation use.

Table 1. 4 Element analysis of Orinoco VR (Zhang, 2014)

Property		Orinoco VR
Content of Elements, wt%	C H S N	82.69 9.68 4.8 1.09
H/C Atomic		1.4
Content of Metal Elements, wppm	Ni V Ca Fe	175.5 751.7 12.8 16.7

Recently, along with the increasing crude oil price and the stringent environmental legislation, getting higher product quality with less property give-away becomes more and more important. And behind it, the idea of process optimisation and integration is coming to modern refiners' sight. To achieve goals of predicting process product properties and yield with high accuracy, monitoring and controlling operation conditions throughout processes, molecular level process modelling is necessary. Moreover, the molecular level characterisation on both feedstock and products could be the first essential step as molecular composition could determine bulk property of petroleum mixtures, process chemistry, and affect reaction kinetics and thermodynamics. The summarised molecular technique procedure for molecular conversion modelling could be seen in Figure 1.5 (Klein et al., 2006)

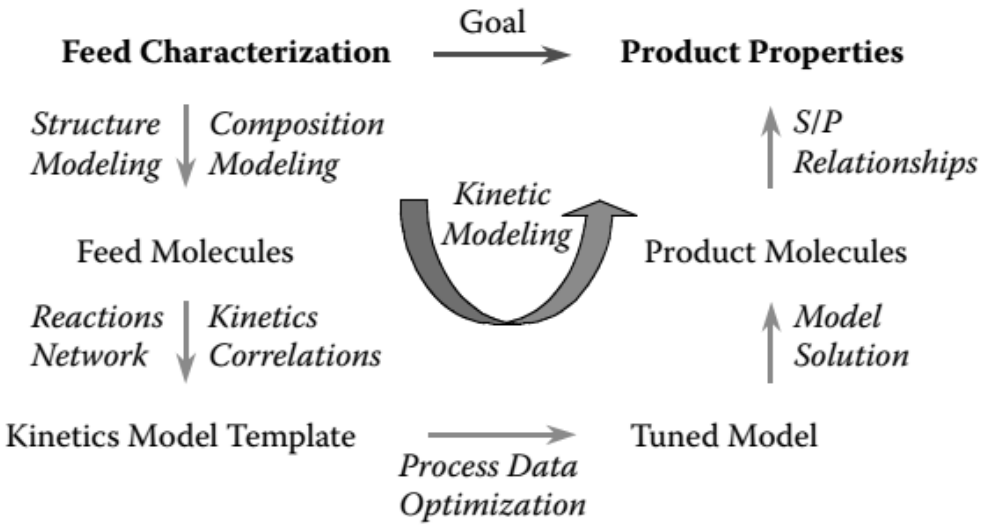

Figure 1. 5 An overall procedure for molecular conversion modelling

1.4.3 Challenges in Petroleum Characterisation

As illustrated in Figure 1.1, the feedstock of a processing unit could be a mixture of several refining streams in a modern refinery. That means the characterisation of a processing feedstock is facing the challenges of not only the varying bulk properties from day to day but also numerous molecular information of the highly complicated petroleum mixture from various upstream processes. A simple example could be given as FCC unit feedstocks. In an integrated refinery, the feedstock of a FCC unit could comprise gas oil from atmospheric/vacuum distillation sections, and products from delay coker, hydrotreating and visbreaking unit. Two factors must be taken into consideration when predicting the FCC yield: crude oil resource and upstream processing scheme.

Conventional characterisation methods mainly focus on bulk properties or some indices that can indicate the average properties of a petroleum mixture such as API gravity, carbon residue, element analysis, SARA analysis, UOP *K* and distillation information, etc. The shortcomings of these conventional methods could be roughly classified into two aspects: the first is that petroleum mixtures with the same bulk

properties could have distinct molecular composition, so property based methods could be misleading when representing streams from different origins; the other drawback is each of these methods has its own points of focus so that they could not have universal applicability for all range oil fractions.

Although molecular characterisation of petroleum streams, as the first essential stage of molecular management, has been investigated by various researchers, the complex nature of petroleum composition restricts the application of laboratory analysis approaches, and forms challenges on both characterisation and simulation methodologies. Separation and upgrade of petroleum fractions, especially heavy fractions, could be extremely difficult to describe in a molecular level due to the enormous number of involved molecules, reactions and equations-of-state (EOS). The trade-off between keeping astronomical molecular details and practicality in industrial applications is remaining unsolved in this area. On the other hand, even researches on refining processes modelling are more and more depending on this composition information, it is still extremely difficult to monitor, track and control this large number of components in refining processing.

1.5 Motivation and Objective of Present Research

The motivation of this work is to help refiners to improve their competitiveness with molecular management. And a successful molecular management targets right molecules at the right place, at the right time and at the right price (Aye and Zhang, 2005), makes it possible to track the path of each molecular species as they are processed, could achieve more profitable exploitation of crude oil through better yield of high value products and more profitable interface with petrochemicals. It consists of molecular characterisation of refining streams, molecular modelling of refining processes, process level optimisation and overall refinery optimisation on the molecular level. An appropriate characterisation method can provide reliable

input information for accurate modelling as mentioned before. And accurate modelling of refining processes not only can provide reliable prediction of product yield, properties and composition, but also can lead to an efficient process integration and refinery optimisation.

Our aim is to provide the refiners with a proper molecular-level characterisation approach and corresponding process models to satisfy the need for a better and more accurate characterisation of petroleum fractions and refining processes, and the need to close the gap between reaction modelling and separation modelling. In this work, we are focusing on molecular characterisation of light and middle distillates. And due to high profit and importance of gasoline product in fuel market, refining processes of gasoline manufacture will be selected for modelling. Besides, to explore the feasibility of the present characterisation methodology, an extension of present framework will be applied to diesel range fractions. And eventually, we wish to provide a consistent platform for characterising different refining streams and modelling various refining processes with reliable petroleum characterisation and process models.

1.6 Structure of the Thesis

This thesis comprises six chapters, and a brief overview of each chapter could be seen as follows.

Chapter 2. A Review of Molecular Characterisation of Petroleum Fractions

Laboratory analytical methods as well as existing characterisation lumping and molecular-level methods are reviewed. Technical challenges of petroleum characterisation are drawn from the review. The molecular type homologous series (MTHS) matrix method and its development, as well as its applications in refining

process modelling, are then presented.

Chapter 3. New Molecular Characterisation Methodology with Modified MTHS Matrix

A new methodology of petroleum characterisation in molecular level is represented in this chapter. The procedure as well as the mathematical model is illustrated in detail. The feasibility and reliability could be verified by two case studies.

Chapter 4. Molecular Modelling of Catalytic Reforming

In this chapter, the catalytic reforming process is briefly introduced, and a review of existing researches on catalytic reforming modelling is given. A modified reaction network of catalytic reforming is proposed and kinetic parameters are regressed based on the combination of pseudo-component information and MTHS matrix. A process optimisation model is then developed to optimise operating conditions.

Chapter 5. Molecular Modelling of Gasoline Blending

A brief introduction of gasoline blending background and principle is presented along with the review existing gasoline blending models. A molecular model of gasoline blending based on the proposed characterisation method is developed with a modified non-linear Octane blending model. Two case studies of gasoline blending recipe simulation and optimisation are chosen to validate the new method.

Chapter 6. Conclusions and Future Work

Conclusions are drawn from this work, and some suggestions are given for future research.

Chapter 2 Existing Work on Petroleum Characterisation and Its Applications

2.1 Introduction

Molecular-level refining modelling is providing modern refiners more competitive ways of operation because of not only the stricter and stricter environmental legislations and oil product specifications, but also the diminishing profit margins in the refining industry. The first step in the development of convincing molecular level refining modelling is to determine an accurate molecular representation of the feedstock. Although researches on analytical techniques have made a significant contribution to petroleum characterisation, not all are useful to determine the molecular representation. Table 2.1 summarises several common analytical methods used to identify molecular structure in petroleum fractions (Klein, 2006).

In this chapter, current practices in petroleum characterisation from modern laboratory methods to non-experimental methods are discussing. Considering that molecules are the basis for feedstock/product composition, property calculation, reactor kinetics and process chemistry, a molecular-level characterisation is necessary for modern refiners. The development of representation and transformation methodologies of a molecular characterisation method is reviewed in this chapter, as well as its applications in refining modelling.

Table 2. 1 Common Analytical Methods Used to Elucidate Molecular Structures (Klein, 2006)

Characteristics	Analytical Methods
H/C ratio	Elementary analysis
Boiling point (BP)	Distillation
	Gas chromatography (GC)–simulated distillation (SimDis)
	Gas chromatography–mass spectrometry (GC-MS)
Compound class	High performance liquid chromatography (HPLC)
	PIONA (paraffin, isoparaffin, olefin, naphthene, aromatic)
	SARA (saturates, aromatics, resins, asphaltenes)
Molecular weight	Vapor pressure osmometry (VPO)
	Cryoscopy
	Gel permeation chromatography (GPC)
	Field ionization mass spectrometry (FIMS)
Atomic connectivity	^{1}H-, ^{13}C-NMR

2.2 Modern Analytical Laboratory Methods

With the development of modern instrumental analysis technology, molecular-level composition analysis can be achieved by various laboratory methods such as GC, HPLC, MS, NMR and etc. The analytical results are essential to molecular-level characterisation methodologies because they provide the basis and the reference values when developing a new characterisation method. Hence, the basic principles and the range of applications will be briefly introduced in the following sections.

2.3.1 GC

Typical uses of GC are separating and analysing light and middle distillates that can be vaporised without decomposition. Essentially, GC separates molecules according to their boiling points. A gas chromatograph contains a sampler, an injector, a separation column, several detectors and a temperature controller. Coupled with different detectors, such as FID, SCD and NCD, GC based techniques have the capacity of characterising hydrocarbon, sulphur and nitrogen compounds. Traditional gas chromatography, also known as one dimensional GC (1D GC) is mainly used in the analysis of gasoline range as it could identify and quantify hundreds of hydrocarbon components in the temperature range below 200℃. But for the compounds of higher boiling point range, the enormous number of compound types creates difficulties for the identification of all isomers. Recent applications of two dimensional GC (2D GC or GCxGC) increased the separation efficiency by adding a second column. Thus the quantitative analysis of hydrocarbon and sulphur composition is extended to VGO. For heavier fractions (e.g. vacuum resid), it cannot be analysed by GC since its boiling points is too high. The GC is invented by Martin and Synge, who suggested its possibility in a paper on liquid chromatography published in 1941 (Martin and Synge, 1941). Teng, S. T. (1994) developed a gas chromatography-mass spectrometric (GC-MS) method to analyse hydrocarbons by structural group types in gasoline and distillates. It is one of the few methods capable of distinguishing between paraffins and naphthenes, thus providing a true PONA analysis.

2.3.2 HPLC

HPLC is widely used in separation of middle distillates and high boiling fractions with saturated hydrocarbons (paraffins and naphthenes), aromatics and resin.

Petroleum mixture separation and analysis utilising HPLC are based on the principle that different compounds have different polarities. The HPLC is in principle similar to GC, but has several notable differences. The main distinction is that the process of compounds separation in a mixture is carried out between a solid stationary phase and a liquid mobile phase, whereas in GC the stationary phase is a liquid and the mobile phase is a gas. The application of HPLC includes aromatic ring number (AR) group type analysis and saturates / aromatics / resins / asphaltenes (SARA) compositional analysis for middle and heavy fractions.

2.3.3 MS

Mass spectrometer is usually served as a detector in GC and HPLC systems. With the development of refining process technologies, hydrocarbon compositional information from liquid chromatography could not satisfy the process requirement. MS analyses compounds according to their molecular weight and chemical formula CnH2n+ZX, where C is carbon, H is hydrogen, X refers to heteroatoms while n is the number of carbon and Z is the hydrogen deficiency (Sun, 2004). Mass spectrometry has been widely adopted in obtaining the information of molecular weight distributions with boiling range from about 200℃ to more than 500℃. This method combined with HPLC or GC by far provides the most detailed information on the compositions such as normal-paraffins, iso-paraffins, naphthenes with 1, 2, 3 or more rings, single-ring aromatics and polycyclic aromatics, etc. Although it could provide essential information about the detailed molecular structure, its application is limited to light petroleum fractions such as that of gasoline.

2.3.4 NMR

NMR spectroscopy is one of the principal techniques used to obtain physical, chemical, electronic and structural information about molecules due to either the

chemical shift, Zeeman effect, or the Knight shift effect, or a combination of both, on the resonant frequencies of the proton and ^{13}C nuclei present in different chemical groups. NMR spectroscopy can measure directly aromatic and aliphatic carbons; hydrogen distributions and the concentration of various structural groups can be determined when combined with elemental analysis. Different from GC or HPLC methods which provide information on structural distribution, ^{1}H and ^{13}C are responsible for revealing the averaged structures of petroleum fractions.

Modern laboratory analytical approaches such as gas chromatography (GC), high performance liquid chromatography (HPLC), nuclear magnetic resonance (NMR), mass spectroscopy (MS), and other combined approaches can identify and quantify hundreds of petroleum molecules. Analytical results from laboratory approaches provide a reliable basis for petroleum characterisation which is vital at the beginning of methodology development to setup connections between properties and compositions and to avoid misleading correlations.

However, disadvantages of these approaches are also very noteworthy. These complex laboratory works must be done sample by sample manually, which means the time-consuming training and operating, and the restriction of co-operation with process modelling. Another common disadvantage is the high capital and operating cost.

2.3 Review of Existing Characterisation Work

Characterisation of petroleum fractions is the starting point of refining process modelling. Studies of characterisation model have been taking place in the past several decades. And its development has been closely related to the development of modern computer technology.

2.3.1 Lumping Methods

Lumping methods are widely accepted for traditional process simulation and still playing a significant role in the industry. One of the most well-known lumping methods could be pseudo-component method which is defined to transfer ASTM (American Society for Testing and Materials) curves into a representative series of components (Katz and Brown, 1933). These narrow-boiling cuts divided from petroleum fraction or crude oil true boiling point curves are then treated as pure components with corresponding properties in the next process modelling. This method has been adopted in separation unit modelling of commercial software tools such as PROII (Simulation Sciences, Brea CA), HYSYS (AspenTech, Cambridge MA), AspenPlus (AspenTech, Cambridge MA). A simple case generated from HYSYS in Table 2.2 can demonstrate the pseudo-components list that represents the known hydrocarbon fraction (Aye, 2003).

Table 2. 2 Pseudo-components information from Hysys

Comp Name	NBP (°C)	Mole Wt.	Density (kg/m^3)	Viscosity (cP) (@ 37.78°C)	Viscosity (cP) (@ 98.89°C)
NBP_43	43.43	72.87	641.77	0.28719	0.15048
NBP_59	58.82	79.28	618.64	0.32879	0.16983
NBP_73	72.99	85.41	634.21	0.26816	0.16913
NBP_87	86.50	91.50	647.67	0.28636	0.18367
NBP_100	100.49	98.34	660.51	0.32825	0.20438
NBP_114	114.38	105.54	672.05	0.37727	0.22777
NBP_128	128.29	113.29	682.58	0.43493	0.25407
NBP_142	142.20	121.55	692.18	0.48801	0.27751
NBP_156	156.08	130.28	700.98	0.56098	0.30840
NBP_170	169.80	139.37	708.96	0.65149	0.34507
ETC ….					

Another major type of lumping methods is called compound class method. This kind of methods is based on chromatographic separation and describes oil mixtures in terms of operationally defined fractions (Gray et al., 1989). A particular example of this approach is the SARA (S="saturate", A="aromatics", R="resins", A="asphaltenes") method. The n-d-M method, the refractivity intercept-density method and Riazi and Daubert correlations are also such compound class methods.

By adopting lumping methods, the complexity of reaction kinetic networks can be reduced to overcome the limitation of computation power, the high-cost instrumental analysis and the complicated molecular composition characterisation. With these advantages, lumping methods have received wide application in product yield prediction and for almost all upgrading processes. As lumping methods commonly classifies petroleum fractions based on their physical properties, the limitation is also obvious. The lack of molecular information could restrict the property prediction and the extrapolation range. Moreover, the process-focused model development makes it difficult to be applied in an integrated modern refinery simulation. To be more specific, petroleum fractions are represented by pseudo-components in separation unit models while lumped by chemical classes in reaction unit models.

2.3.2 Molecular-level Characterisation Methods

With the development of computer technology, molecular composition based characterisation methodologies have attracted many attentions during the past two decades. More and more molecular-level approaches have been developed. Liguras and Allen (1987) developed a carbon centre based framework to represent petroleum mixtures. Compounds in the mixture are divided into 4 classes (normal paraffins, branched paraffins, cyclic paraffins and aromatics), and described as a collection of carbon centres.

Shariati (1999) used the chain of rotators group contribution EOS (CORGC EOS)

for characterising the C6+ fractions. However, the model with three compounds (n-alkanes, n-cyclopentanes, and n-alkylbenzenes) in Shariati's work is inadequate for molecular simulation. Jabr et al. (1992) characterised petroleum mixtures by pseudo-components from the physical properties and fractional composition of paraffins, naphthenes, and aromatics. A naphtha stream is divided into 5 cuts with unified boiling ranges with assumed chemical components. Albahri (2005) modified Jabr's work and selected 68 molecular species for petroleum naphtha simulation with PNA components. Bulk properties of a petroleum fraction such as ASTM D86 curves, API gravity, RVP and properties of pure components are used as input data. However, the preselected components, which highly affect the accuracy of prediction results, would be hard to decide for different fractions.

2.4 The Development of the MTHS Matrix Method

The molecular type homologous series matrix method was developed by Peng in 1999. The representation framework shown in Figure 2.1 incorporates Molecular type and molecular size into one MTHS matrix. In the matrix, the rows represent carbon numbers and the columns represent the homologous series. Homologous series, which is a key concept of the MTHS method, is used to lump molecular species with the same structure base. An example is shown in Figure 2.2 to explain the concept. These listed molecules are lumped into the column of 1A because they have the same structure base of single aromatic ring. Molecules belonging to a homologous series with the same number of carbon atoms are lumped into one matrix element. The elements of the MTHS matrix represent volume/molar/weight fraction of each lump.

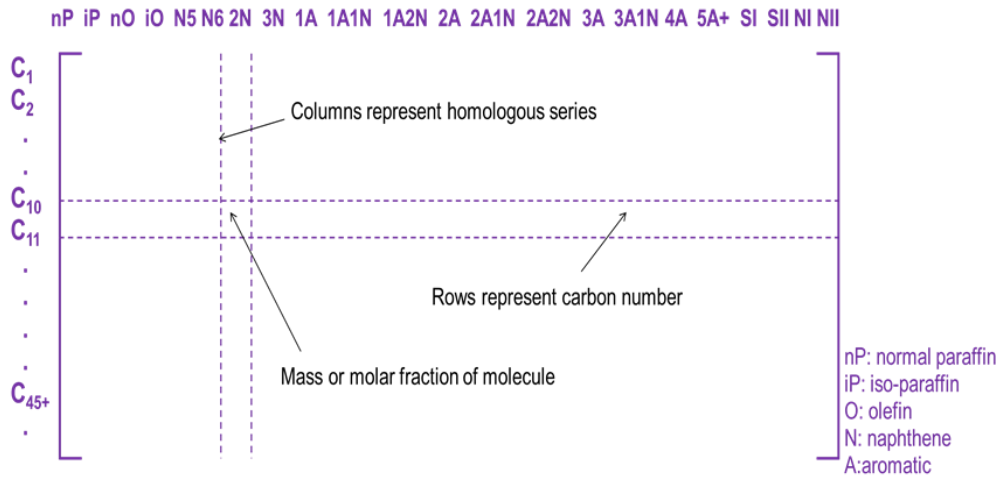

Figure 2. 1 MTHS matrix representation framework

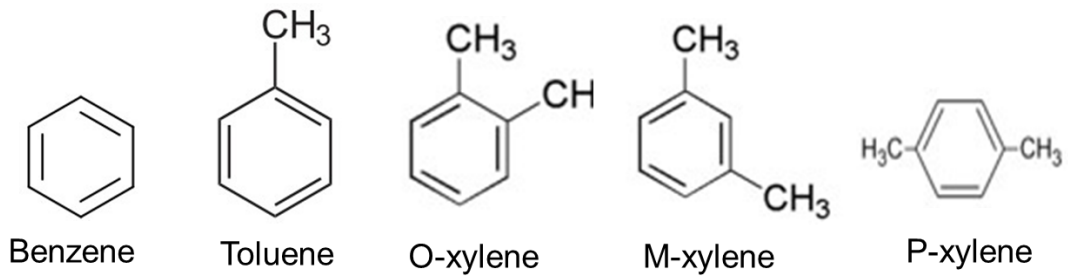

Figure 2. 2 Several molecules that lumped into homologous series of 1A (single-ring aromatic)

This carbon number based MTHS matrix can provide sufficient chemical information, and to some extent, reduce the complexity of a molecular model. But the representation framework could restrict the application of the method when dealing with heavier petroleum fractions.

Based on the matrix framework, Zhang (1999) correlated bulk properties with molecular composition. Aye (2003) considered the influence of isomers and generated several databases for characterising petroleum fractions from different processes. Wu (2010) further divided iso-paraffins into 3 categories with different number of branches for gasoline characterisation according to their different contribution to ON of a gasoline product. A statistic method was introduced to

describe the distribution of each homologous series. The MTHS matrix method provides molecular level structural information that is essential to modern refining process modelling. On the other hand, the representation framework with carbon number is no longer suitable for heavy fractions because of the complex nature and the difficulty of required input data generation. Gomez-Prado (2007) developed a modified MTHS representation approach based on temperature. A good feasibility was achieved when applied to hydrocarbon streams with a wide boiling range from diesel to residue. Characterisation parameters were used instead of direct physical properties in his work that caused massive boundary setting work due to the mass conservation principle.

2.4.1 Transformation to Predict Molecular Composition

In the transformation step, a petroleum fraction with its bulk properties is characterised into molecular composition with a matrix form. The composition of the fraction is dispersed represented in each entry of the matrix. Several researchers have worked on this difficulty and developed three main approaches.

Zhang (1999) introduced the property prediction and transformation method to characterise hydrocarbon samples up to diesel range. In her work, carbon number and homologous series are correlated with boiling point, molecular weight and density. For example, in her work, Fisher's (1982) correlations are modified to correlate homologous series of the MTHS matrix and carbon number (C) with boiling points (T) as Eq.2.1. Coefficients of and b are regressed and shown in Table 2.3.

$$\frac{C}{T} = a + b \times C \tag{2.1}$$

Table 2. 3 Coefficients for Eq. 2.1 for boiling points of homologous seires in MTHS matrix Zhang (1999)

Molecular type	Coefficients		Carbon number range
	a	b	
nP	0.011649200	0.001069240	9-14
	0.013570300	0.000938137	15-27
	0.015470300	0.000866235	28-45
iP	0.010565789	0.001231172	
O	0.011797460	0.001069430	9-14
	0.013701933	0.000939431	15-27
	0.015591169	0.000867916	28-45
1N	0.011503720	0.001068970	9-14
	0.013440561	0.000936825	15-27
	0.015350833	0.000864554	28-45
2N	0.011319370	0.001067810	10-14
	0.013267521	0.000935016	15-27
	0.015190967	0.000862273	28-45
3N	0.012992552	0.000935394	14-27
	0.014992624	0.000859394	28-45
1A	0.011002080	0.001067410	9-14
	0.012988684	0.000931960	15-27
	0.014932077	0.000858504a	28-45
1A1N	0.010366860	0.001061190	10-14
	0.012377015	0.000924613	15-27
	0.014358493	0.000849808	28-45
1A2N	0.011549258	0.000917387	14-27
	0.013638978	0.000838189	28-45
2A	0.010065040	0.001058270	10-14
	0.012089615	0.000920842	15-27
	0.014086224	0.000845507	28-45
3A	0.010638163	0.000903088	14-27
	0.012758921	0.000822816	28-45

And the molecular structure-property correlations for density is also developed based on the same principle that properties could be correlated with carbon number and homologous series. Other properties are then calculated from boiling point and density by empirical correlations. However, without considering the contribution of isomers within the lump of each matrix entry, the influence of molecular structures

on properties such as octane number and vapour pressure is neglected.

Further extension of the MTHS framework is proposed by Aye (2003) that isomers have been considered, and the transformation method is enhanced in Aye's work (2003) by obtaining sample streams database considering the processing history as shown in Figure 2.3. The properties of isomers can be calculated by the group contribution methodology. The procedure to calculate the isomer distributions in a petroleum fraction is divided into two categories: (1) For gasoline fractions, the detailed information from chemical component analysis can be obtained from the open literature, and this data is used to build a series of sample streams database (e.g. straight-run gasoline, FCC gasoline, reforming gasoline) according to the thermodynamic equilibrium assumption. (2) For LCO or heavier fractions, due to the lack of analysis results in the literature, the assumption that the carbon number distribution of isomers follows a gamma distribution is made.

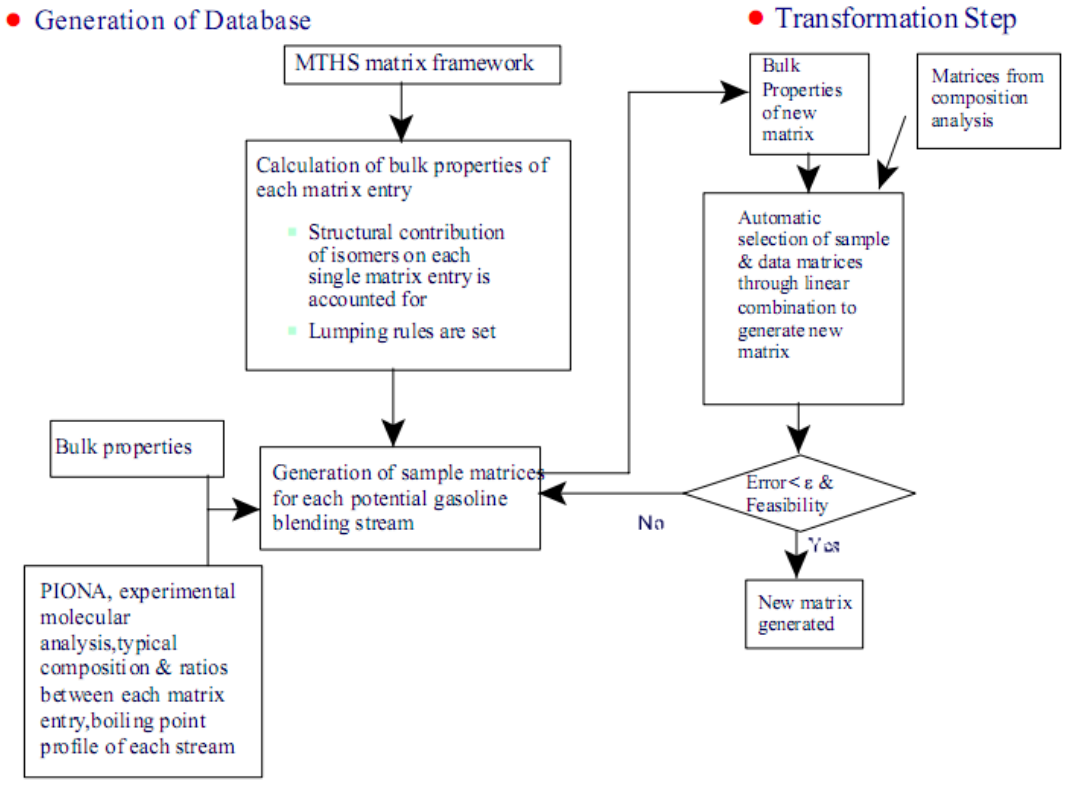

Figure 2. 3 Schematic representation of the methodology (Aye, 2003)

However, several inherent limitations of the existing MTHS methodology reduce the accuracy and applicability. Considering the transformation methodology, first, a huge amount of well-characterised samples are required for various refining processes, and the accuracy of a new composition prediction highly depends on the size of database, which is difficult to obtain; second, because of the assumption that the predicted streams are the blend of several well-characterised streams, the molecular composition of predicted streams could not be predicted accurately if the properties of sample streams do not cover the properties of the predicted streams; last, different molecular compositions could be achieved based on the same bulk properties due to the similarity of properties between some compound.

Wu (2010) considered the influence of different branched paraffins on octane number and further divided iso-paraffins into mono-methyl, di-methyl, and tri-methyl paraffins and lumped olefins into two series, normal and branched olefins to construct a modified MTHS gasoline model. His work is based on two assumptions. One is that the molecular composition within each homologous series follows a statistical distribution against a certain property. The other follows a general belief that the bulk properties of a petroleum fraction are close to the calculated from the composition of pure compounds based on mixing rules. And he introduced a stochastic optimisation algorithm of simulated annealing for diesel range fraction characterisation. The procedure of his work could be seen in Figure 2.4. The separation of isomers could enhance the accuracy to some extent for octane number calculation. However, it also increases the problem size and the difficulty of preparative analytical work. The optimisation engine of simulated annealing (SA) algorithm could introduce undesired solutions as the random nature of the algorithm.

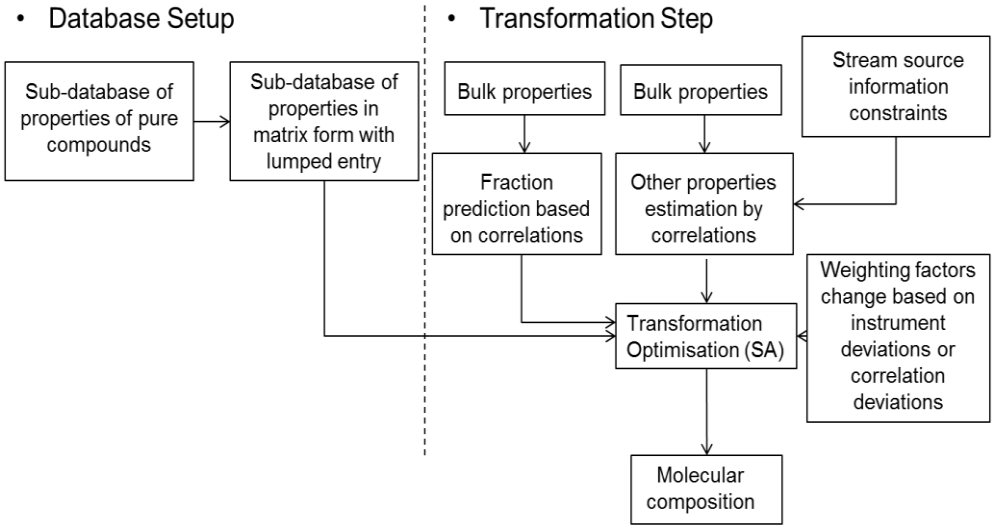

Figure 2. 4 Wu's MTHS framework for the characterisation of refining streams (2010)

2.4.2 Representation Methods

According to the existing researches of the molecular type homologous series (MTHS) matrix, modifications of representation methodology mainly focus on the lumping rules of isomers (Wu, 2010). However, the main challenge is that the combination of carbon number and homologous series cannot appropriately describe wide temperature range distillates especially in fractions heavier than diesel. The main reason is the high carbon number lumping is hard to be divided.

Gomez-Prado (2007) proposed the modified MTHS (mMTHS) matrix, where the molecular size of each cut is represented via its boiling point instead of carbon number. This new compound class approach can be used to represent hydrocarbon streams with the boiling range up to 700℃. In Prado's work, components are lumped together in sub-cuts of 10℃ at low temperature range up to 320℃. For higher boiling range (gas oil and residue fraction), each cut is sub-divided into 30℃ and 50℃ temperature range for gas oil and residue, respectively. Although this method showed good agreement with the experimental data in the case study of FCC feedstock, some molecular structures such as aromatic-naphthenic rings are not included in this representation and the optimisation steps for each narrow fraction produce a huge

number of parameters within the whole mixture.

2.5 The Application of Existing MTHS Matrix Method

As molecular characterisation is the first level of refinery molecular management, many efforts have been made to extend the existing MTHS matrix representation to refining modelling, and furthermore, integrated refinery optimisation.

Peng (1999) proposed reaction and separation modelling methods based on the initial MTHS framework, and validated with a catalytic reforming case study. A molecular kinetic model considering reactions of hydrodesulphurisation, hydrogenitrogenation and aromatics hydrogenation is also developed for VGO hydrotreating process. Hu (2001) adopted Peng's work and applied the reactor model in a combined unit of catalytic reforming and gasoline stabiliser. Aye (2003) validated the feasibility of the modified MTHS method in gasoline and diesel blending processes. Wu (2010) investigated three different processes including gasoline blending, catalytic reforming, and diesel hydrotreating, and considered the economic performance with the molecular level processes optimisation.

The application of existing MTHS method in gasoline catalytic reforming, refining product blending, and diesel hydrotreating illustrates the feasibility and reliability of this novel molecular characterisation method. Although studies of process modelling based on the MTHS characterisation method are focusing on limited refining processes, researchers have made their efforts to incorporate molecular characterisation and modelling into the overall refinery optimisation. However, the insufficient of existing characterisation and modelling methods could be obviously seen: (1) existing applications are focusing on processes dealing with petroleum fractions up to diesel range, which is far from enough for modern refiners; (2) existing process models based on MTHS method are not covering all important

refining processes; (3) the difference in representation and transformation methodologies of MTHS matrix could lead to a different reactor model and further influence the process modelling and optimisation, that could cause the incompatibility between process models developed by different researchers and restrict application for later researches to some extent.

2.6 Summary

Several experimental and non-experimental methods of characterisation of petroleum fractions are reviewed in this chapter. With the development of modern computing and analysis technologies, it is possible to analyse single component of the petroleum fraction up to middle distillates by laboratory approaches as mentioned previously. This specific molecular information can not only provide the foundation of the characterisation methodology, but also guide the refining production and operation. On the other hand, it also means time consuming and high capital cost on equipment, operating, maintenance and training for refiners that to some extent could restrict the application of laboratory approaches.

According to the level of lumping detail, characterisation methodologies for petroleum streams can be divided into two categories: molecular-level and lumping methods. In molecular-level models, molecular identities are kept and the detail composition and properties of fractions can be obtained. As all molecular information can be retained throughout mechanism simulation, molecular methods are suitable for all refining processes. The disadvantage of the molecular model is the high requirement of computer power when dealing with a complex system. And the more complex of a petroleum mixture, the more computation time will be needed. Lumping methods such as pseudo-component method may more appropriate for simulation with incomplete chemical information. Although these lumping methods have been widely accepted in the industry due to their simplicity and

moderate accuracy achieved, the lack of chemical information makes them process specified. In addition to this, process simulation with lumping methods can only predict product yield and the detail molecular composition is lost. The trade-off between keeping astronomical molecule details and practicality in industrial applications is remaining unsolved in this area.

Moreover, two technical challenges should be taken into consideration when developing a molecular characterisation methodology: representation and transformation. The representation methodology is the way used to generalise petroleum fractions. Molecules or lumps of compounds or pseudo-components are selected to describe petroleum mixtures in a characterisation method according to different focuses. Even the molecular-level approaches cannot represent all molecules of a petroleum mixture. Compound classification in a characterisation method could be the first challenge to be dealt with. For example, the types of compounds that used to define petroleum fractions in SARA characterisation are saturate, aromatics, resins and asphaltenes, and in total there are 4 lumps of compounds involved. An appropriate representation framework is the essential start of a petroleum characterisation methodology.

If the representation framework is determined, another technical challenge is waiting ahead. Transformation in the characterisation could be regarded as the bridge between the information we have known and that we want to know. For molecular-level characterisation methods, it means the correlation between bulk properties of a mixture and molecular information of every single molecule or molecular lump. The transformation step is the core of a molecular-level characterisation method, as it has the conclusive effect on accuracy and reliability.

In this work, a non-experimental molecular approach is chosen for further research to overcome these weaknesses and challenges. The development of the MTHS matrix method and its application are briefly introduced in this chapter.

Chapter 3 New Molecular Characterisation Method with Modified MTHS Matrix

3.1 Introduction

According to the previous review of existing characterisation methodologies, two technical challenges are rising from two main areas: representation and transformation. To handle these challenges, a molecular-level characterisation method was developed (Peng, 1999), which was applicable to reaction kinetic modelling but not suitable for separation. For purposes of better process integration and easier application, a new methodology is developed that combines the pseudo-component method, which has been successfully used in separation process modelling, with the MTHS matrix that keeps essential chemical information of each molecular species. The method is explained in detail in Sections 3.2 and 3.3.

3.2 New Molecular Characterisation Method with Modified MTHS Matrix: Representation Framework

According to previous researches on the MTHS method, technical challenges of both representation and transformation have been studied extensively. To some extent, the representation model could affect the development of transformation, as molecules/lumps used to represent a petroleum stream are determined in the representation framework before transformation. On the other hand, the transformation step determines the accuracy and the practicality of the characterisation methodology.

The new matrix framework is shown in Figure 3.1. It should be noticed that the

matrix in Figure 3.1 is a general framework. For different refining stream, the matrix size could be modified. For example, for gasoline range stream, the matrix homologous series column could reduce to 5 (nP, iP, O, 1N, 1A) and around 10 pseudo-components are used. This modified matrix incorporates both molecular types and temperature ranges. Rows in the matrix represent pseudo-component cuts and columns represent homologous series. In the matrix, the molecules belonging to a pseudo-component cut within the same homologous series are lumped into one entry. On the right side, properties of each pseudo-component cut could be generated by correlations from distillation curve and density. It is important to note that this combination provides a consistent starting point for simulation and optimisation of most refinery processes, since the method can estimate quantities of all the matrix elements that further affect results of petroleum stream representation and reaction-related unit simulation.

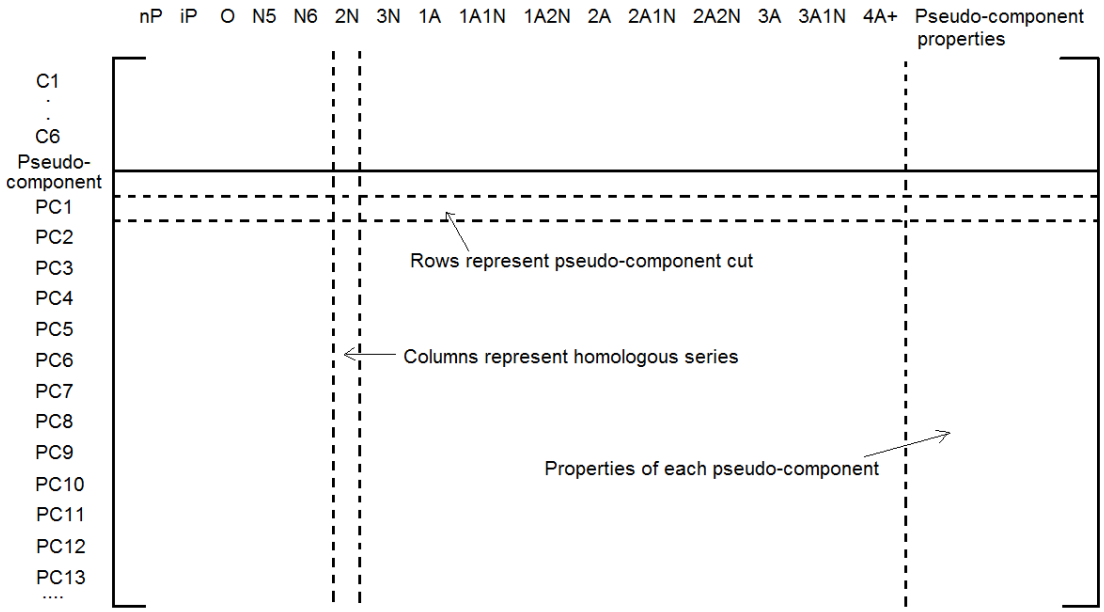

Figure 3. 1 The modified MTHS matrix framework

The flexible matrix framework makes it possible to characterise full range distillates with adequate chemical information. For different temperature range fractions,

corresponding modifications of the initial framework are necessary. The temperature range of pseudo-component cuts for petroleum streams varies as streams from different operation units have different distillation profiles. However, the MTHS matrix size and the general applicability need to be taken into consideration when deciding the number of pseudo-components. The actual pseudo-component cutting temperatures of gasoline and diesel range petroleum fractions will be given with case studies in Section 3.4. For heavier petroleum fractions, more homologous series columns are needed due to the sharp increase in molecule number. In this work we will focus on refining products of gasoline and diesel streams in terms of hydrocarbon components.

For gasoline fractions, the common homologous series classification is NP, IP, O, N, and A, in which NP stands for normal-paraffin that contains only straight chain paraffins; IP stands for iso-paraffins that includes all branched chain paraffins; O stands for olefins; N stands for naphthenes (also known as cycloparafins), and A represents aromatic compounds. The gasoline fraction is divided into several pseudo-components according to its TBP curve. The generation of pseudo-components will be illustrated in Section 3.3.4.2. However, due to the lack of light-end processing techniques, components with low boiling temperature may not be dealt with properly. It could affect the performance of a process model and/or the predictive accuracy of characterisation in some ways (Hay, 2013). Therefore, pure component information within available light end information is recommended to be involved during the molecular characterisation if possible. The matrix representation of an FCC stream with available pure component information is shown in Table 3.1.

The MTHS matrix size could be different when representing petroleum fractions with higher boiling temperature ranges than gasoline. In this work, the representation framework of diesel fractions has also been studied. The typical boiling temperature range of a diesel stream is from 180^{o}C to 350^{o}C, and it could contain millions of

different molecules. Therefore, more homologous series and more pseudo-components are necessary when determining an MTHS matrix.

Table 3. 1A modified MTHS matrix used to represent an FCC stream (vol%)

Pure component	NP	IP	O	N	A	density
C4	1.17	0.70	2.25			
C5	2.66			0.31		
C6					0.49	
Pseudo-component cut						
pc1	0.00	8.99	7.17	0.00	0.00	677.95
pc2	1.44	7.09	5.26	0.00	0.00	702.10
pc3	1.02	5.28	3.35	0.00	0.00	716.19
pc4	0.71	3.80	3.11	2.83	0.71	729.50
pc5	0.48	2.89	2.32	2.52	3.26	742.50
pc6	0.35	2.13	1.73	1.78	6.15	755.36
pc7	0.19	1.60	1.30	0.98	5.60	767.32
pc8	0.18	1.20	0.97	0.47	3.20	778.82
pc9	0.11	0.86	0.70	0.08	1.16	784.43

The number of pseudo-components is decided according to the distillation curve of a diesel stream, and the homologous series involved in the matrix are presented as the following with examples:

NP: normal paraffins with straight chain;

IP: iso-paraffins with branched chain;

O: olefins;

N, 2N, 3N: single-ring, double-ring, and triple-ring naphthenes

e.q. 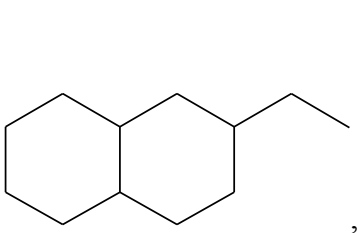 , 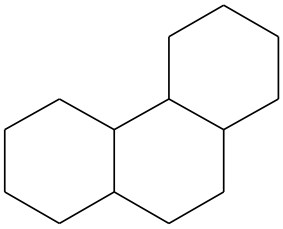 ;

A, 2A, 3A: single-ring, double-ring, and triple-ring aromatic compounds

e.g. 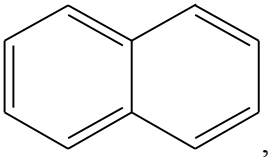 , 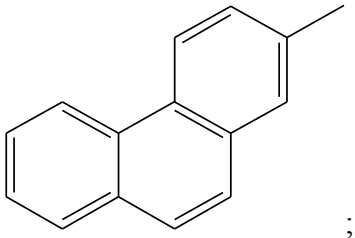 ;

1A1N, 1A2N: single-ring aromatics with naphthenic rings

e.g. 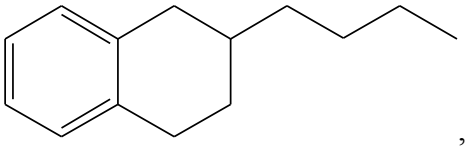 , 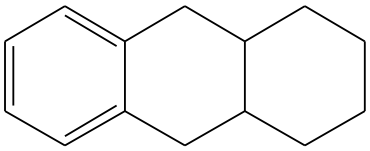 ;

AA: biphenyls:

e.g. 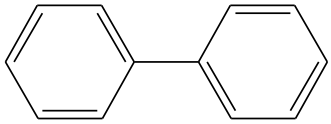 ;

2A1N: double-ring aromatics with a naphthenic ring

e.g. 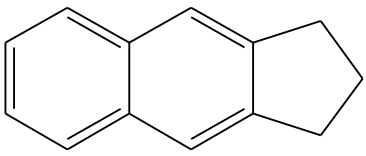 .

To summarise, the common concept of pseudo-components has been adopted together with the existing homologous series in the modified MTHS matrix representation model of petroleum fractions. Because of this combination, both physical information such as molecular size and chemical information such as molecular structure, as well as composition of each single molecular lump could be found in the proposed matrix of a petroleum stream.

An example of representation matrix for diesel range fraction is shown as Table 3.2.

Table 3. 2 A modified MTHS matrix used to represent an diesel range stream

PC	NP	IP	N	A	2A	1A1N	2N	3A	2A1N	1A2N	3N
PC1											
PC2											
PC3											
PC4											
PC5											
PC6											
PC7											
PC8											
PC9											
…											
PC_n											

Also due to the combination of these two concepts, the transformation behind the representation model has been changed significantly. The explicit transformation methodology will be presented by Section 3.3.

3.3 New Molecular Characterisation Method with Modified MTHS Matrix: Transformation methodology

3.3.1 General procedure

Figure 3.2 shows the general procedure of the proposed molecular-level characterisation methodology. It can be roughly divided into 2 moves: preparative calculation and molecular transformation. In the preparation part, information including bulk properties of petroleum streams (distillation profile, density, PIONA composition, et al.), and available pure component properties needs to be saved as initial input data. Other properties can be estimated via correlations if needed. Once

the distillation profile and the density of a petroleum stream are obtained, pseudo-components together with their corresponding properties can be estimated. In the meantime, homologous series division is made to form the matrix frame with determined boiling temperature cuts. After the determination of certain MTHS matrix, the essential properties of each matrix entry can be estimated via correlations from the literature. All estimation methods adopted in this work could be found in Table 3.4.

The next step comprises the transformation from bulk properties to molecular composition and the transformation from molecular composition to bulk properties. By adopting some assumptions (Section 3.3.2), a mathematical model is set up for the regression of composition distribution of a matrix. Bulk properties obtained from measurement/correlations and those calculated from the MTHS matrix method are compared, and the difference between them is minimised via optimisation. Once the matrix is established, its bulk properties could be predicted via blending mixing rules. After all, the comparison of predicted bulk properties and measured ones is given to show the accuracy and reliability of the proposed methodology. The procedure is illustrated step by step in Section 3.3.4 to Section 3.3.5, and demonstrated in detail with a SRN gasoline case in Section 3.4.

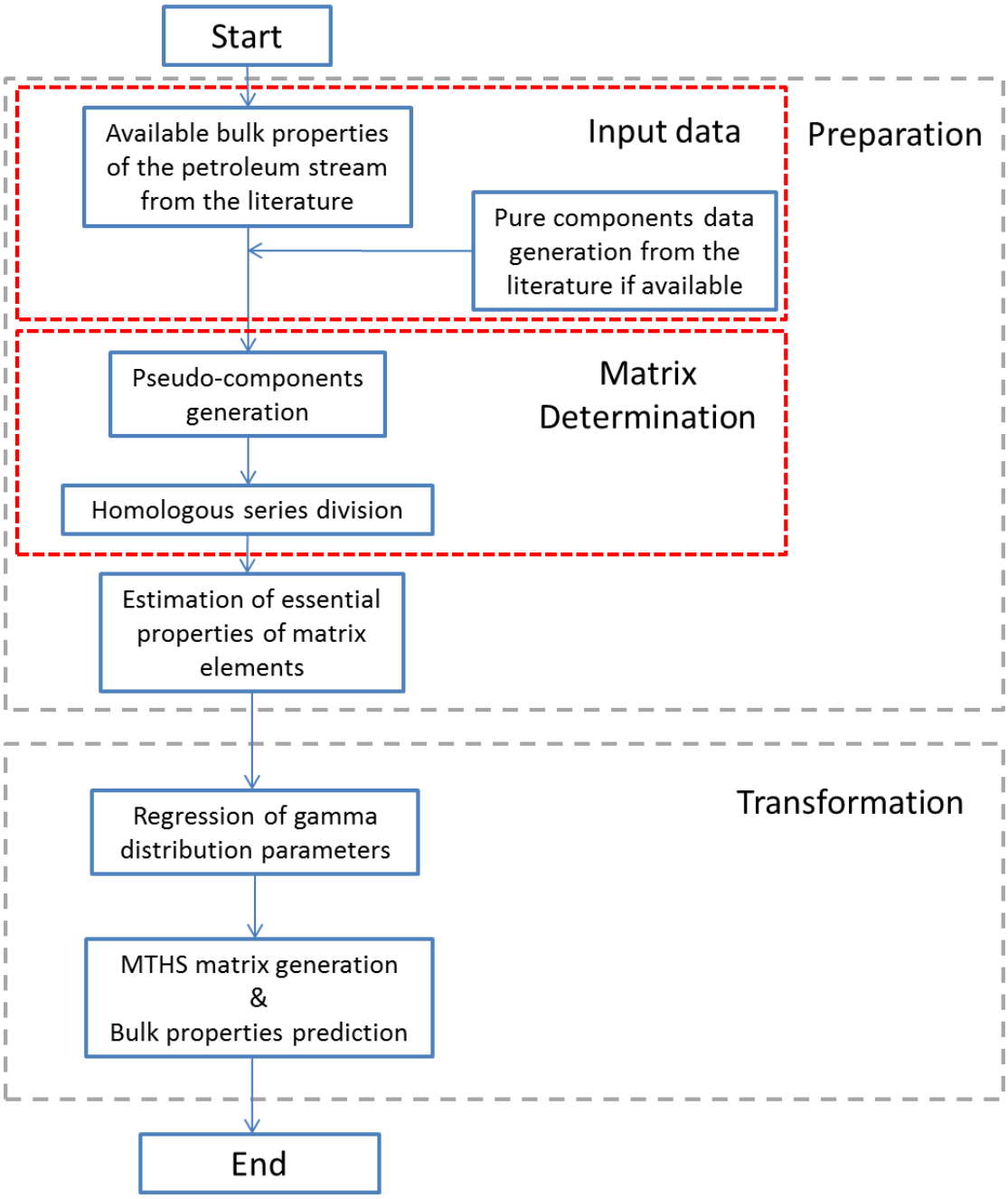

Figure 3. 2 Development procedure of the proposed method

3.3.2 Key assumptions

A fundamental assumption made in this work is that the bulk properties of the predicted stream estimated by mixing rules and correlations are accurate enough. The bulk properties of a petroleum fraction are determined based on the molecular

composition. Thus we assume that the properties calculated from MTHS matrix via mixing rules must be equivalent to those obtained from correlations. This assumption is verified in the literature (Albahri, 2005; Wu, 2010; Zhang, 2014). An example of gasoline properties calculation is selected from Albahri (2005) to prove this assumption in Table 3.3.

Table 3. 3 Properties comparison of a gasoline stream based on both correlations and mixing rules

Properties	**Mixing rules**	**Correlation**	**Error%**
Volume average boiling point (°C)	112.48	113.23	0.67
Specific gravity	0.76	0.76	0.00
Reid vapour pressure (kPa)	13.31	13.17	-1.04
Watson K	11.58	11.55	-0.26
CH weight ratio (wt/wt)	6.66	6.31	-5.26
Cloud Point (°C)	-104.41	-102.66	-1.68
Kinematic viscosity (100^{o}F) (cSt)	0.42	0.40	-4.76

Another assumption adopted in this work is that the molecular composition within each homologous series follows a statistic distribution against certain properties. This statistic methodology provides a simple way to represent molecules when analytical approaches are not available to analyse petroleum molecules directly. Campbell (1998) proposed the overall steps of such an approach to transfer analytical data such as bulk properties, PONA composition, H/C ratio and NMR etc. to molecular composition information.

3.3.3 Properties of interest and their calculations

It is common to use product properties as the indices of process performance to control and optimise process operations in refineries. As one of our targets is to help refiners to monitor, track and control molecules of refining streams as they are processed to meet product specifications, the bulk properties that are of interest are based on their importance on the specification. Therefore, in this work, bulk properties taken into consideration for the gasoline range fractions are:

1. Research Octane Number (RON),
2. Motor Octane Number (MON),
3. Reid Vapour Pressure (RVP),
4. Specific Gravity/Density,
5. Boiling Point Temperature,

Bulk properties taken into consideration for diesel range fractions are:

1. Cetane number,
2. Flash point,
3. Viscosity at 37.8 and 98.9°C,
4. Specific Gravity/Density,
5. Boiling Point Temperature,
6. Pour point.

Intensive correlations for pure component and mixtures, as well as mixing rules for properties calculation are developed in the past, and most are available from API TDB (1986, 1997) and Riazi (2005) with discussions of applicable range and error of as listed in Table 3.4.

Table 3. 4 Properties estimation methodology for pure compounds and mixtures, mixing rules

Properties	Pure component	Correlations	Mixing rules
Volume/weight/molar average boiling point (^oC)	Experimental/Group contribution method	API 2B 1.1	Eq. 3.45
Molecular weight (g/mol)	Eq. 2.40	API 2B 2.1	Eq. 3.45
Specific gravity	Experimental/ Group contribution method	Experimental	Eq. 5.126
API Gravity	Eq. 2.4	Eq. 2.4	N/A
Research octane number (RON)	Experimental	Experimental	Ghosh, 2006
Motor octane number (MON)	Experimental	Experimental	Ghosh, 2006
Reid vapour pressure (RVP)(kPa)	Eq. 3.102	Eq. 3.103	API 5B 1.3
Kinematic viscosity (100^oF) (cSt)	Eq. 2.128	Wauquier, 1995	Eq. 3.45
CH weight ratio (wt/wt)	Calculated	Eq. 2.120	Calculated
Watson K	Eq. 2.13	Eq. 2.13	API 2-0.9
Pour Point (K)	Experimental	Eq. 3.119	Eq. 3.120 & Eq. 3.117
Flash Point	Experimental	Eq. 3.114	Eq. 3.116 & Eq. 3.117

* Eq: equations in the reference (Riazi, 2005)

*API: methods in the reference (API. TDB, 1997)

3.3.4 Transformation preparation

3.3.4.1 Input information generation

The first step is the generation of input information. The information of a petroleum stream, including bulk properties such as distillation profile, density/SG, PIONA analysis, as well as properties of pure components, is employed as the initial input data. Other properties of interest can be estimated by correlations that available in Table 3.4. For light fractions such as gasoline, pure components data are key constraints of important components such as benzene and light-ends. Therefore, it could be necessary for us to incorporate such information in our representation matrix whenever it is available. Table 3.5 lists some pure component placements in PIONA groups. And the pure component information also shows a clear value of benzene content, which is one of the gasoline specifications.

Table 3. 5 Pure components adopted in modified MTHS matrix

Carbon Number	NP	IP	O	N	A
4	N-butane	Iso-butane	1-butene, 2-butene, isobutene	N/A	N/A
5	N-pentane	Iso-pentane	PC*	Cyclopentane	N/A
6	PC*	PC*	PC*	Methylcyclopentane, cyclohexane	Benzene

* The pseudo-component (PC) they could be lumped into is according to their boiling points and the pseudo-component temperature cut range.

3.3.4.2 Pseudo-components generation and corresponding properties estimation

❖ **Pseudo-components generation**

The petroleum stream is characterised in order to obtain its bulk properties along the boiling point range. To achieve this target, a set of narrow boiling range fractions should be generated according to the distillation profile and the density of the stream by the pseudo-component approach. These pseudo-components are considered as pure components with their average boiling temperatures and densities, and then used in a series of correlations to calculate other bulk properties.

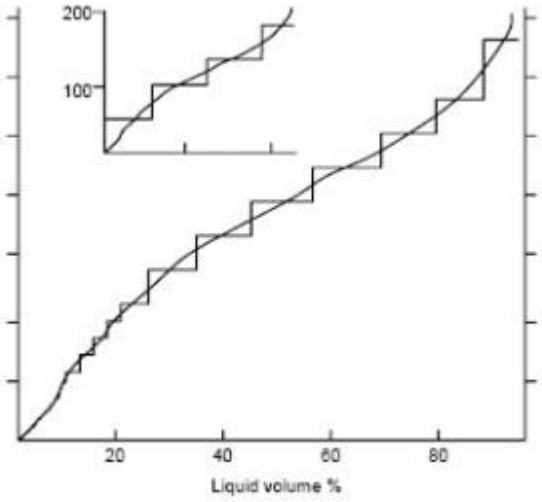

Figure 3. 3 Pseudo-components generation

The second step in the procedure comprises transferring ASTM curves to pseudo-components and their corresponding properties. The temperature range of pseudo-components can be cut differently for different fractions.

To generate pseudo-components from a distillation profile, the D86 curve needs to be converted to a TBP curve first. Daubert's (1997) conversion method is introduced to generate TBP (True Boiling Point) from ASTM-D86 distillation temperature points. Firstly, a TBP distillation temperature at 50vol% point in Kelvin can be

calculated from the 50vol% D86 distillation temperature by Eq.3.1.

$$TBP(50\%) = 255.4 + 0.8851[ASTM\ D86(50\%) - 255.4]^{1.0258} \quad (3.1)$$

Other TBP curve points can be estimated based on the $TBP(50\%)$ temperature by the following equations (eq.3.2 – eq. 3.8)

$$TBP(0\%) = TBP(50\%) - Y_4 - Y_5 - Y_6 \quad (3.2)$$

$$TBP(10\%) = TBP(50\%) - Y_4 - Y_5 \quad (3.3)$$

$$TBP(30\%) = TBP(50\%) - Y_4 \quad (3.4)$$

$$TBP(70\%) = TBP(50\%) + Y_3 \quad (3.5)$$

$$TBP(90\%) = TBP(50\%) + Y_3 + Y_2 \quad (3.6)$$

$$TBP(100\%) = TBP(50\%) + Y_3 + Y_2 + Y_1 \quad (3.7)$$

$$Y_i = AX_i^B \quad (3.8)$$

Where Y_i is the difference in TBP temperature between two cut points, Kelvin or ^oC; X_i is observed difference in ASTM D86 temperature between two cut points, Kelvin or ^oC; A and B are constants varying for each cut point and are given in Table 3.4 together with the maximum allowable temperature of each cut point range.

Table 3. 6 constants A, B and their maximum allowable temperature (Riazi, 2005)

i	Cut point range, %	*A*	*B*	Maximum allowable X_i, °C
1	100-90	0.1403	1.6606	-
2	90-70	2.6339	0.7550	55
3	70-50	2.2744	0.8200	85
4	50-30	2.6956	0.8008	140
5	30-10	4.1481	0.7164	140
6	10-0	5.8589	0.6024	55

The obtained TBP temperatures are used to regress the distillation curve by a cubic polynomial model in Eq. 3.9 with 4 parameters of *a, b, c,* and *d* to be determined.

$$T_{cal} = ax^3 + bx^2 + cx + d \tag{3.9}$$

Where *x* is the percentage cumulative volume fraction on the distillation curve, T_{cal} is the corresponding temperature.

The objective function of the distillation curve regression is to minimise the summation of square differences between calculated and measured TBPs. The objective function is presented by the following Eq. 3.10:

$$OBJ = \sum w_T (T - T_{cal})^2 \tag{3.10}$$

Where *T* is the measured temperature on the distillation curve; T_{cal} is the calculated temperature from the distribution model; w_T is the weight factor for each temperature point. The regressed TBP curve is then divided into several cuts with same temperature range and their pseudo-component temperature T_{pc} and volume fraction v_{pc} could be obtained.

❖ **Specific Gravity (SG) of each pseudo-component**

and their corresponding specific gravity and Watson K can be calculated via the regression based on Equations 3.11 and 3.12:

$$(1.8T_{pc})^{1/3} = SG_{pc} \times Kw \tag{3.11}$$

$$\mathrm{SG}_{cal} = \sum v_{pc} SG_{pc} \tag{3.12}$$

Where Eq. 3.11 is the definition of the UOP characterisation factor Waston K. The objective function of the SG generation is to minimise the difference between the predicted and measured SG of the petroleum stream shown as Eq. 3.13.

$$OBJ = \sum (SG - SG_{cal})^2 \tag{3.13}$$

Where *SG* is the measured specific gravity; SG_{cal} is the calculated specific gravity of the stream.

On the other hand, there is another way to generate pseudo-components of a petroleum stream with a general process simulation software package such as Aspen Hysys or ProII when it is available. In this work, the generation of pseudo-components is completed in GAMS (Appendix 1).

❖ **Other properties of each pseudo-component**

In this work, we only consider average boiling point and SG for pseudo-components. Properties other than temperature and SG can be calculated by correlations in Table 3.4 and briefly introduced in this section in case they are needed for fellow researchers.

The formula used to calculate properties of pseudo-components is presented in Eq. 3.14. This general correlation developed by Riazi and Daubert (1987) can be used to

predict properties such as boiling point temperature T_b, critical properties T_C and P_C, molecular weight MW, specific gravity SG, C/H ratio, and viscosity by various characterisation parameters.

$$\theta = a \cdot \exp[b \cdot \theta_1 + c \cdot \theta_2 + d \cdot \theta_1\theta_2]\theta_1^e\theta_2^f \quad (3.14)$$

Where a, b, c, d, e and f are constants obtained from properties of hydrocarbons within a carbon number range from C5 to C20 through linear regression of the logarithmic form of the above equation. However, it should be noticed that as these two parameters are independent, they should represent molecular energy and molecular size. Table 3.7 lists properties that may be used as parameters (θ_1, θ_2) in the above equation and the value of constants could be found in the literature (Riazi, 2005).

Table 3. 7 Parameters of Riazi's equation for properties calculation

θ	Tc(K), Pc(bar), Vc(cm^3/g), M, Tb(K), SG, I(20^oC), CH
(θ_1, θ_2)	(Tb, SG), (Tb, I), (Tb, CH), (M, SG), (M, I), (M,CH)
Pairs	(v38(100), SG), (v38(100), I), (v38(100), CH)

This method is suitable for hydrocarbon systems with molecular weight range from 70 to 280, which is approximately equivalent to the boiling range of 30-350℃.

3.3.4.3 Homologous series division

In the pseudo-components generation step, a petroleum stream is divided into several pseudo-components with their corresponding temperature, volume fraction, and specific gravity. Then it is further divided into several homologous series depending on its origin. For example, straight-run naphtha can be divided into NP (normal paraffin) IP (iso-paraffin) N (single-ring-naphthene) and A (single-ring-aromatic),

while FCC gasoline needs at least two extra classes of MO (mono-olefin) and DO (di-olefin). The involved homologous series of gasoline and diesel have been discussed in Section 3.2. Hence the matrix size expands with the boiling temperature increase of a fraction. The more homologous series used, the more composition information needs to be determined.

3.3.4.4 Properties estimation of matrix entries

The shape and size of the proposed MTHS matrix are decided in previous matrix determination steps by far.

For different petroleum streams, a distillation cut with the same boiling temperature could have different molecular composition and bulk properties. Estimation of the bulk properties of each matrix is crucial to the following characterisation steps, as it is the first step to transfer the bulk properties of a whole stream into more detailed properties of each lump of the matrix. Every single entry in the matrix is a mixture of molecules within a temperature range and homologous series. And hence average properties are necessary to represent all lumped molecules of an entry.

The calculation of matrix entries' properties could be more complex then pseudo-components' as the correlations may not be suitable for molecule lumps under the homologous series divisions. In addition, the interior relation between the temperature-based matrix and the carbon-number-based matrix should be taken into consideration to keep the versatility and consistency. Correlations adopted to estimate properties of each matrix entry are given as follows.

❖ **Estimation of the average carbon number of each matrix entry**

The principle of this step is to transfer generated pseudo-component information of matrix rows to chemical information of matrix entries. Therefore, the carbon number of each matrix within should be estimated first.

Average carbon number of each pseudo-component within normal paraffin column (entries of NP column) is obtained based on the correlations (Glinzer, 1985) in Eq. 3.15:

$$T_P = 266.5 \times \ln n - 456.5 - 213.37 \times F\left(-\frac{n}{6}\right) \tag{3.15}$$

where $F\left(-\frac{n}{6}\right)$ is the integral-exponential function:

$$F\left(-\frac{n}{6}\right) = \int_{-\infty}^{-n/6} e^x \, d(\ln x) \tag{3.16}$$

This correlation could be extended to heavy oil fractions and shows an acceptable accuracy when dealing with gasoline range fractions. (Zhang, 1999)

The double-bond equivalent (DBE) concept (Korsten, 1997) is used to estimate the average carbon number of matrix entries of olefin, naphthene and aromatic columns. Hydrocarbons can be represented by the structural formula of C_nH_{2n+z}, where n is the carbon number and z is the hydrogen deficiency. The definition of DBE is: $DBE = 1 - \frac{z}{2}$. The boiling temperature of hydrocarbons other than paraffins can be calculated by the addition of temperature of normal paraffins T_p and the excess temperature T_E.

$$T=T_p+T_E \tag{3.17}$$

The excess temperature T_E is estimated as Eq.3.17 and Eq. 3.18:

$$T_E = (2.450 \times DBE + 0.53163 \times DBE^2) \times \theta_T \tag{3.18}$$

$$\theta_T = \frac{DBE - 2 \times DB_o}{|DBE - 2 \times DB_o|} \tag{3.19}$$

where DB_o is the number of olefinic double bond. The value of DB_o for each

homologous series could be found in Table 3.8.

Table 3. 8 DBE Characteristics of Homologous Series of Hydrocarbons

Hydrocarbon	Formula	DBE	H/C	DB_O	R	DB_R
Paraffins	C_nH_{2n+2}	0	2<H/C<4	0	0	0
Naphthenes	C_nH_{2n}	1	2	0	1	0
Monoolefins	C_nH_{2n}	1	2	1	0	0
Diolefins	C_nH_{2n-2}	2	4/3<H/C<2	2	0	0
Alkylbenzenes	C_nH_{2n-6}	4	1≤H/C<2	0	1	3
Alkylnaphthalenes	C_nH_{2n-12}	7	0.8≤H/C<2	0	2	5

Table 3.8 shows the DBE information of each chemical family. Where $\mathrm{DBE} = 1 - \frac{z}{2}$; DB_O is the number of olefinic double bonds; R is the number of rings; DB_R is the number of aromatic double bonds.

Average carbon number of each entry within iso-paraffin columns is calculated via a group contribution method proposed by Cordes and Rarey (2002). The model is based on the boiling point database of 2550 components of the Dortmund Data Bank (DBB) and proposed to describe the NBP for molecules with varying sizes by adjustable parameters and structural groups.

$$T_b = \frac{\sum_k N_k(tbk)}{n^a + b} + c \tag{3.20}$$

Where N_k is the number of groups of type k, tbk is the group contribution (K), n is the number of atoms in the molecule (except hydrogen), and a, b and c are the adjustable parameters with the values used in this work of 0.6713, 1.4442, and 59.334 K, respectively. The definitions of groups are revised in order to consider

other special effects that may lead to large deviations, which could be found in Appendix 2. Therefore the molecular fragment groups used in this method contain both the structure information of molecular fragments and chemical environment around them.

According to different contribution to bulk properties from paraffin isomers, the distribution of branched paraffins has been taken into consideration by thermodynamic equilibrium calculation in this work. Sull and Edgar (1969) compared the composition distribution of C_8 aromatics in different gasoline products from several refining processes shown in Table 3.7. From the comparison, it can be seen that the distribution calculated from thermodynamic equilibrium is very close to the measured distribution at the process temperature (755-810^{o}K). And Rossini (1950) noted that the distribution is found very similar in the C_8 aromatics in crude petroleum. Therefore, we could assume isomers that lumped into a matrix entry are in thermodynamic equilibrium (Aye, 2003). The thermodynamic equilibrium calculation of distribution between isomers could be found in Section 4.6.2.

Table 3.9 Volume Distribution of C_8 aromatics in different gasoline fractions (Sull and Edgar, 1969)

Compound	Platforming	Catalytic Cracking	Virgin Petroleum	Thermodynamic Equilibrium
o-xylene	23	20	20	23
m-xylene	40	50	50	47
p-xylene	21	20	20	21
Ethyl-benzene	16	10	10	9
Total	100	100	100	100

* In volume percent (=mole or weight percent)

The composition distribution between paraffin isomers is not only a fundamental basis when calculating properties of the elements in IP column, but also an important constraint for characterisation of petroleum mixtures from different refining processes.

These carbon-number-and-chemical-structure-based correlations are introduced for the regression of the average carbon number of each matrix entry with its pseudo-component temperature and homologous series division.

❖ **Properties estimation of each matrix entry**

Once the average carbon number is determined, the average molecular weight and H/C ratio can be obtained via molecular formula, C/H atomic weight and the homologous series information.

For example, molecules in nP and iP columns have the same chemical formula as C_nH_{2n+2}, so their H/C ratio can be calculated by the equation: 1.00794*(2n+2) / (12.0107*n).

And estimation of other average properties of interest for gasoline and diesel range streams can be carried out by the correlations from Riazi's book (2005) (Table 3.4).

3.3.5 Transformation methodology

After setting up the representation framework with property calculations behind each pseudo-component matrix entry, the next step is the transformation, in which the molecular composition information of the whole matrix is to be determined. To do so, gamma distribution within homologous series is assumed to predict the molecular composition of the MTHS matrix.

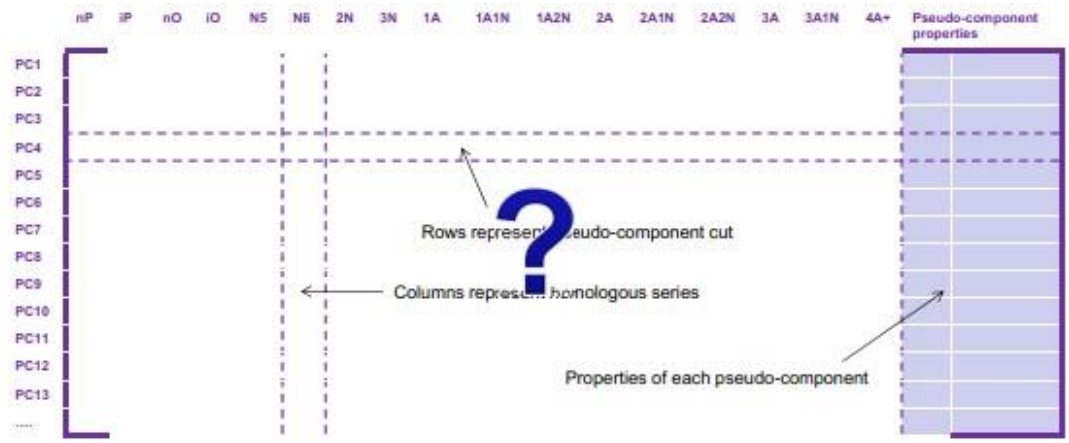

Figure 3. 4 Completed part and undo part in new MTHS matrix

3.3.5.1 Gamma Distribution

As mentioned in Section 3.3.2, the assumption that the molecular composition within each homologous series follows a statistical distribution against a certain property has been adopted to predict composition information within each column.

The continuous distribution includes normal distribution, gamma distribution, and exponential distribution. It is important to choose a proper distribution function form to model hydrocarbon mixtures.

The gamma distribution function, an independent probability density function (PDF), has been widely accepted to characterise petroleum fractions according to its flexibility (Klein, 2006). Flory (1936) developed a modified gamma distribution to describe the molecular size distribution of condensation polymers. Whitson (1983) used a gamma distribution to fit the molar and weight distribution of the C7+ fraction of crude oil.

The expression of the 3-parameter gamma distribution function is shown in Eq. 3.21.

$$p(x) = \frac{(x-\eta)^{\alpha-1} e^{-(x-\eta)/\beta}}{\beta^{\alpha}\Gamma(\alpha)} \tag{3.21}$$

A continuous (any real value of x) probability density functions (PDF) is defined as

p(x) by the following equations:

$$0 \leq p(x) \leq 1 \tag{3.22}$$

$$\int_{-\infty}^{\infty} p(x)dx = 1 \tag{3.23}$$

Where x indicates a certain property, α, β, and η are the shape, scale and location parameters of gamma distribution, and p is the probability density function. The Γ(α) is the gamma function with parameter α, given by,

$$\Gamma(\alpha) = \int_{0}^{\infty} e^{-u} u^{\alpha-1}\, du \tag{3.24}$$

The cumulative probability function is given by,

$$P(X \leq x) = \int_{0}^{x} p(x)dx \tag{3.25}$$

Some boundaries can be taken into consideration to control the shape of the composition distribution curves. For example, the amount of C_8 and C_9 content is usually the highest in gasoline streams which could be written as Eq.3.26.

$$T_{C8} \leq (\alpha - 1)\beta + \eta \leq T_{C9} \tag{3.26}$$

To verify this assumption, a PIONA homologous series distribution of an FCC gasoline stream from Chen (1995) and a weight fraction density curves of a Griffin crude oil (Behrenbruch, 2007) are given in Figures 3.5 and 3.6. Both of them show good agreement between the predicted data by the gamma distribution and the measured data.

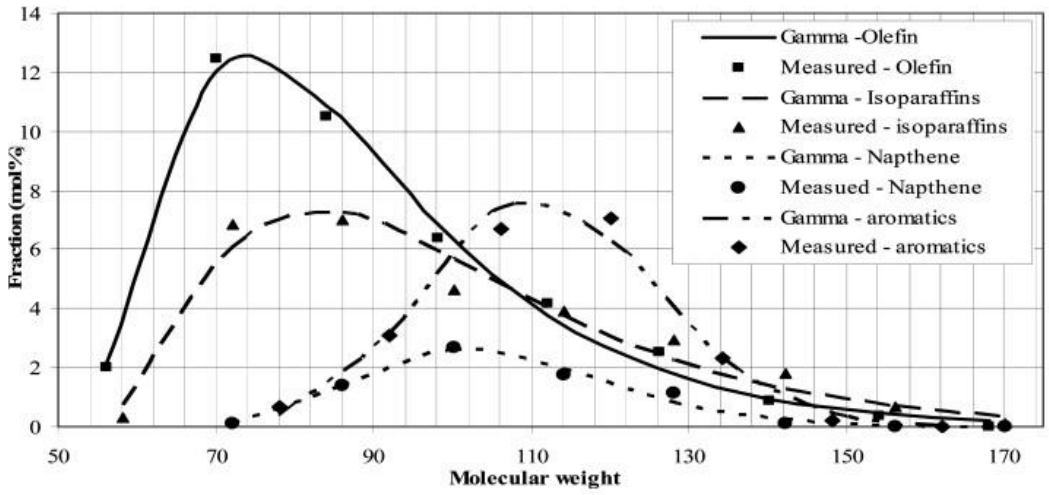

Figure 3. 5 Gamma distribution fitted fractions within PIONA of an FCC gasoline stream

By the assumption that the identities of matrix elements within each homologous series follow a gamma distribution, several benefits can be obtained. First of all, the difficult step of generating the sample matrices database in Aye's (2003) work can be removed. Secondly, the extrapolation capability of the modified MTHS characterisation method is highly enhanced based on this kind of statistic assumption. Another advantage is that the new methodology is able to deal with the challenge that the fractions with significantly different molecular compositions may have similar bulk properties, according to the consideration of internal distribution of molecules within each homologous series. Furthermore, the degrees of freedom (DOF) of the molecular composition representation are reduced dramatically to three within each homologous series. Besides, this distribution form is easily controlled as integrated into a mathematical model (Wu, 2010).

Although gamma distribution has been successfully applied in existing work and the MTHS method, the nature of gamma distribution function may make considerable deviations when fitting the composition distribution that have more than one compositional peak (Figure 3.6 (b)). Therefore, chemical structural characteristics (such as homologous series in this work) should be selected carefully for gamma

distribution to be used in heavy oil characterisation. Hou (2014) adopted the gamma distribution for vacuum gas-oil (VGO) characterisation considering the influence of sulphur content. Another fact that should be noted is that the gamma distribution model can be applied to both molecular weight (MW) and T_b (as adopted in this work), but for SG (Riazi, 2005). There are some alternative statistic distribution models that could be adopted for future research, such as the generalised distribution, the exponential model, etc.

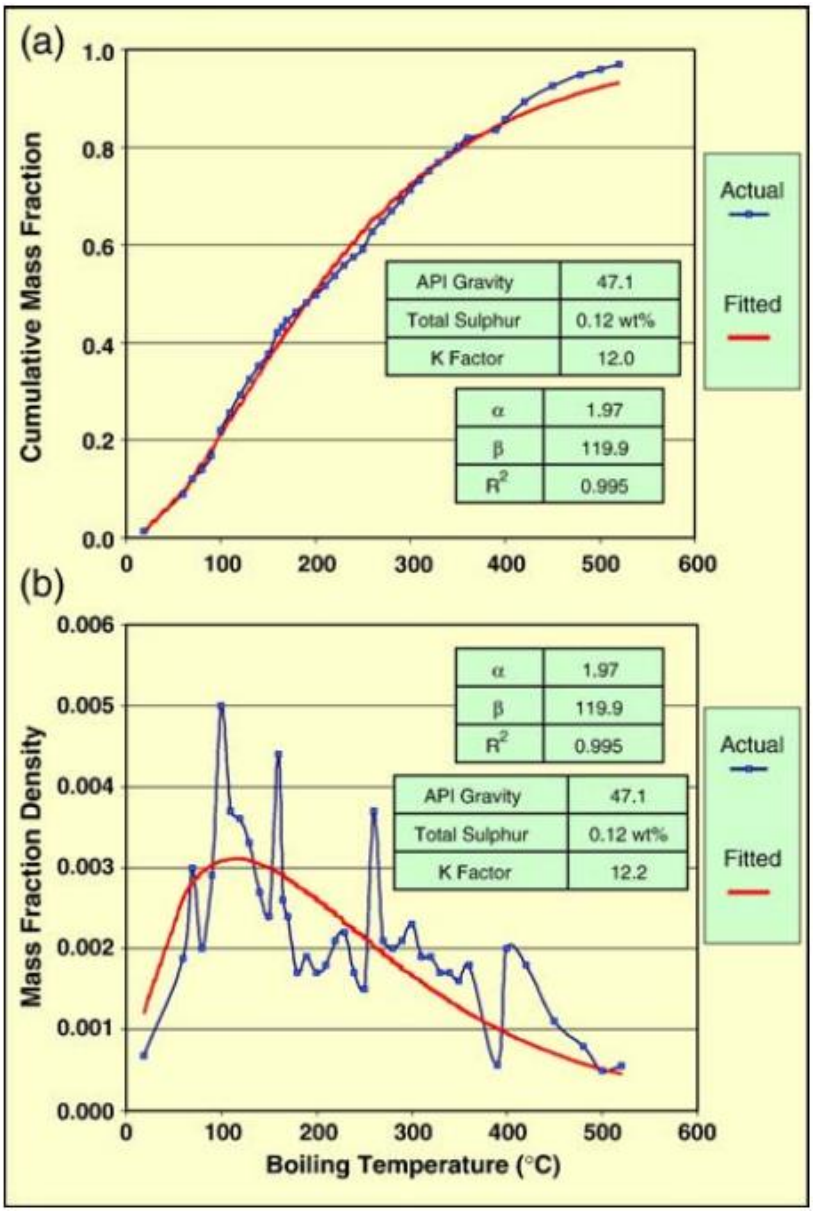

Figure 3. 6 Cumulative weight fraction and weight fraction density curves of a Griffin crude oil (Behrenbruch, 2007)

3.3.5.2 Mathematical Model

The next step is to estimate gamma distribution parameters, which are needed to estimate the distribution of matrix elements.

The procedure of mathematical model is shown in Figure 3.7.

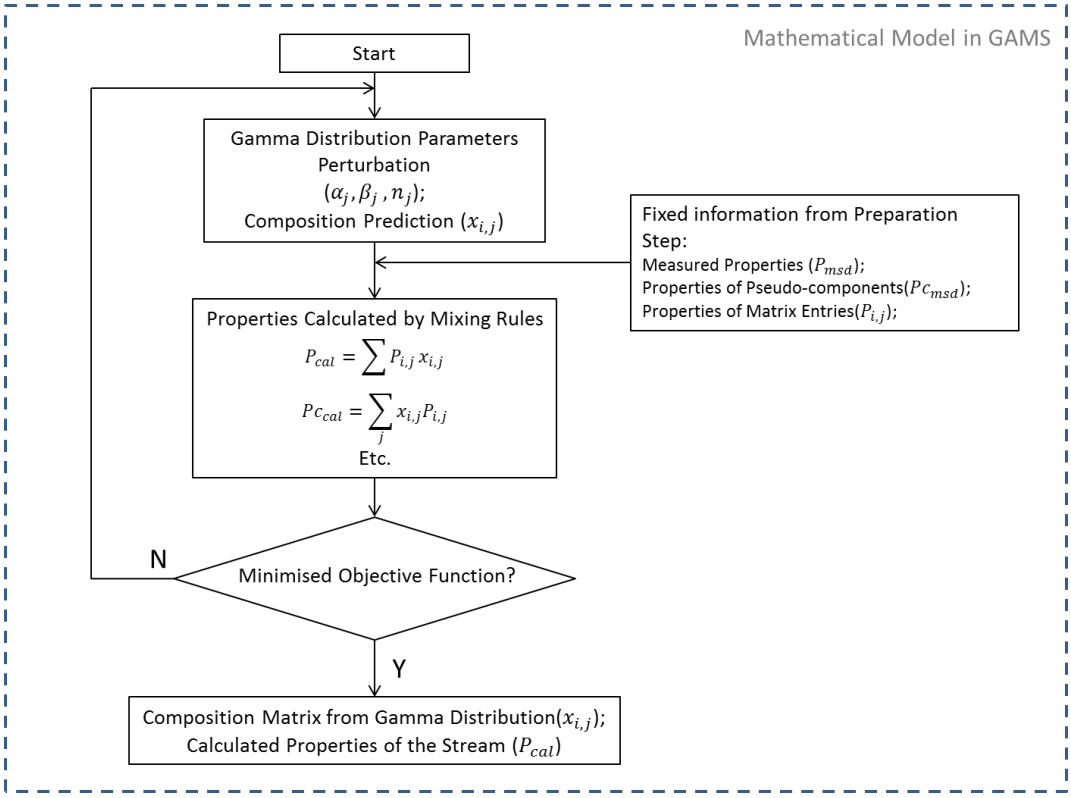

Figure 3.7 The procedure of mathematical model for gamma distribution parameters regression in GAMS

The objective function shown in Eq. 3.27 is to minimise the sum of the percentage deviation between the input properties and predicted ones from the MTHS matrix.

$$\mathrm{Obj} = \sum_{\mathrm{T}}\left(w_{1,\mathrm{T}} \times \frac{V_{\mathrm{T}}^{\mathrm{in}} - V_{\mathrm{T}}^{\mathrm{pred}}}{V_{\mathrm{T}}^{\mathrm{in}}}\right)^2 + \sum_{\mathrm{P}}\left(w_{2,\mathrm{P}} \times \frac{p_{\mathrm{P}}^{\mathrm{in}} - p_{\mathrm{P}}^{\mathrm{pred}}}{p_{\mathrm{P}}^{\mathrm{in}}}\right)^2 + \sum_{\mathrm{f}\in \mathrm{PIONA}}\left(w_{3,\mathrm{j}} \times \frac{C_{\mathrm{f}}^{\mathrm{in}} - C_{\mathrm{f}}^{\mathrm{pred}}}{C_{\mathrm{f}}^{\mathrm{in}}}\right)^2 \quad (3.27)$$

where superscripts of in and pred indicate the input and the predicted data,

respectively; and subscripts of T, P, and f stand for measured temperature of a distillation profile, properties, the measured homologous series respectively; w_1 to w_3 are weighting factors. The objective function contains three parts in this work. The first is the difference between the measured distillation profile and the calculated ones from the prediction molecular composition. The second part of the objective function is the deviation between all the measured and predicted properties except distillation profile and homologous series composition. The third part of the objective function is the homologous series composition difference. We should notice that the more properties included, the more accuracy could be achieved (ignore the deviations caused by mixing rules).

The composition of each homologous series described by the 3-parameter gamma distribution could be written as the following (Eq. 3.28 – Eq. 3.29):

For i = 1,

$$Y_{1,j} = F\left(T_{1,j}^{b}\right) = \frac{\gamma\left(\alpha_j, \frac{T_{1,j}^{b} - \eta_j}{\beta_j}\right)}{\Gamma(\alpha_j)} \tag{3.28}$$

For i > 1,

$$Y_{i,j} = F\left(T_{i,j}^{b}\right) - F\left(T_{i-1,j}^{b}\right) = \gamma\left(\alpha_j, \frac{T_{i,j}^{b} - \eta_j}{\beta_j}\right)/\Gamma(\alpha_j) - \gamma\left(\alpha_j, \frac{T_{i-1,j}^{b} - \eta_j}{\beta_j}\right)/\Gamma(\alpha_j) \tag{3.29}$$

where the subscripts i, j denote the pseudo-components and the homologous series of an MTHS matrix respectively; $F\left(T_{1,j}^{b}\right)$ denotes the cumulative distribution function of gamma distribution at normal boiling point $T_{i,j}^{b}$ of the matrix entry (i,j); $\Gamma(s, x)$ is the incomplete gamma function; $Y_{i,j}$ stands for the fraction of the entry (i,j) of the modified MTHS matrix.

The weight fraction of a matrix element can be calculated by the weight fraction of

homologous series x_j^w to be optimised.

$$x_{i,j}^w = (x_j^w \times \frac{y_{i,j}}{\sum_{ii} y_{ii,j}} + \varepsilon) \tag{3.30}$$

$$x_j^w = \sum_i x_{i,j}^w \tag{3.31}$$

$$\sum_j x_j^w = 1 \tag{3.32}$$

Where ε is the tolerance that allows the small deviation between the optimal and the calculated molecular composition based on the gamma distribution.

The inter-conversion between the weight fraction and the volume fraction is as following Eq. 3.33:

$$x_{i,j}^v = \frac{x_{i,j}^w / SG_{i,j}}{\sum_{ii} \sum_{jj} x_{ii,jj}^w / SG_{ii,jj}} \tag{3.33}$$

where $x_{i,j}^v$, $x_{i,j}^w$ denote the volume and weight fraction of the matrix entry (i,j) respectively; $SG_{i,j}$ stands for the specific gravity of the matrix entry (i,j).

The properties are calculated based on the fundamental properties such as Tb, SG, and CH ratio by correlations and mixing rules from the literature (Riazi, 2005; API handbook, 1997; Korsten, 1997) are summarised in Table 3.4. These methods may not be suitable for other cases and could be changed depending on the available information. For further study on heavier petroleum fractions with hetero-atoms, more constraints are necessary.

3.4 Case studies

Three cases are chosen to verify the reliability and usability of the proposed approach, including a straight-run naphtha (SRN) characterisation without pure component information, an FCC product characterisation with pure component information, and a straight-run gas oil stream characterisation.

Case study 1: Straight-run naphtha (SRN)

The case from Ancheyta (2000) is chosen to validate the proposed characterisation approach in detail. The hydrodesulfurised straight-run naphtha from a commercial naphtha HDS unit with available bulk properties information listed in Table 3.10.

Table 3. 10 Input property and component information of the SRN stream

SG*	0.74
RVP *(psi)	3.11
RON*	62.76
MON*	58.95
Benzene (vol%)	0.48
P (vol%)	69.24
N (vol%)	17.11
A (vol%)	13.65
Distillation* (^{o}C)	
10 vol%	48.03
30 vol%	88.50
50 vol%	114.52
70 vol%	138.20
90 vol%	162.57

*The properties are calculated from the molecular composition in the literature based on mixing rules.

Based on the distillation information, the distillation curve is regressed via the cubic polynomial model in Eq. 3.9 to Eq. 3.10. Once the formula of distillation curve is obtained, it is divided into series of pseudo-components and the SG of each pseudo-component is calculated by Eq. 3.11 to Eq. 3.13. The programming code could be

found in Appendix 1.

Table 3. 11 Pseudo-components generation results from GAMS

No. of PC	vol%	midT in K
PC1	1.39	282.15
PC2	3.95	293.15
PC3	5.41	313.15
PC4	8.22	333.15
PC5	12.48	353.15
PC6	14.52	373.15
PC7	16.30	393.15
PC8	20.23	413.15
PC9	10.56	433.15
PC10	5.53	453.15
PC11	0.42	464.26

After the pseudo-components generation step, the stream is further divided by homologous series. Due to the nature of straight-run naphtha, no olefins are included. Therefore, the composition matrix could be determined comprising 11 pseudo-components and 4 homologous series of NP, IP, N and A, as shown in Table 3.12. Our objective is to fill all blanks in the composition matrix.

Table 3. 12 The composition matrix framework determination

No. of PC	Temperature	NP	IP	N	A
1					
2					
3					
4					
5					
6					
7					
8					
9					
10					
11					

As we know, a refining stream is a mixture of molecules. Hence, the bulk property of the stream could be regarded as the blended property of properties of all the molecules, and it could be calculated by mixing rules. A simple example is given as a linear blending property in Eq.3.35, where P is a bulk property of a stream, P_i is the property of matrix entry i, X_i is the molar composition of matrix entry i. The bulk property is available, and if we can determine property of each matrix entry, the composition could be calculated.

$$\mathrm{P} = \sum_i X_i P_i \tag{3.35}$$

Therefore, the next step is to calculate properties of each matrix entry. Firstly, the chemical information of carbon number of each entry is calculated by the DBE method (Section 3.3.4.4). In this case, the calculated average carbon number of each matrix entry could be found in Table 3.13.

Table 3. 13 Average carbon number of each MTHS matrix entry for a SRN stream calculated by the DBE method (Korsten, 1997)

No. of PC	Temperature in K	NP	IP	N	A
1	282.15	4.14	4.47	N/A	N/A
2	293.15	4.55	4.90	N/A	N/A
3	313.15	5.12	5.49	N/A	N/A
4	333.15	5.72	6.12	5.63	N/A
5	353.15	6.37	6.79	6.27	5.92
6	373.15	7.06	7.50	6.95	6.58
7	393.15	7.79	8.26	7.67	7.28
8	413.15	8.56	9.07	8.44	8.02
9	433.15	9.39	9.92	9.26	8.81
10	453.15	10.26	10.83	10.13	9.65
11	464.26	10.77	11.36	10.63	10.14

So far, properties of boiling point and carbon number are estimated, chemical formula of each homologous series is available. Other properties such as molecular weight, C/H ratio, SG, RVP etc. could be calculated by correlations in Table 3.8.

After the preparation calculation work, the only missing information is the molecular composition. As mentioned in Section 3.3.4, the gamma distribution assumption is used to fit the composition within each homologous series against temperature. By this assumption, the number of variables decreased from 44 to 16 for the whole matrix. Information from preparation work is applied in a regression program in GAMS. The objective function is shown as:

$$\text{Obj} = \sum_{10,50,90} \left(\frac{V^{msd}_{10,50,90} - V^{pred}_{10,50,90}}{V^{msd}_{10,50,90}}\right)^2 + \left(100 \times \frac{0.74 - p^{pred}_{SG}}{0.74}\right)^2 \quad (3.36)$$

$$+ \left(100 \times \frac{3.11 - P^{pred}_{RVP}}{3.11}\right)^2 + \left(\frac{0.48 - C^{pred}_{benzene}}{0.48}\right)^2$$

$$+ \sum_{pc} \left(\frac{C^{msd}_{pc} - C^{pred}_{pc}}{C^{msd}_{pc}}\right)^2 + \sum_{ONs} \left(\frac{P^{msd}_{ONs} - P^{pred}_{ONs}}{P^{msd}_{ONs}}\right)^2$$

$$+ \sum_{PIONA} \left(\frac{C^{msd}_{P,I,N,A} - C^{pred}_{P,I,N,A}}{C^{msd}_{P,I,N,A}}\right)^2$$

The first part in the objective function includes 3 deviations of distillation points of 10 vol%, 50 vol%, and 90 vol%; the second part is the SG difference with weighting factor of 100; the third part is the RVP difference with weighting factor of 100; the fourth part is difference of benzene content; the fifth part is the differences of volume fraction of pseudo-components; the next part is the Octane Number (RON and MON) differences; and the last part includes content differences of normal-paraffin, iso-paraffin, naphtha, and aromatic. It should be noted that the superscript of msd indicates the input properties of the stream, and the superscript of pred indicates the predicted properties of the stream by mixing rules that use composition and properties of matrix entries for calculation.

By minimising the objective function, which is the total difference between measured properties and calculated properties by mixing rules as well as PINA components, the new MTHS matrix and predicted bulk properties of the fraction can be obtained. The predicted volume composition is given in Table 3.14.

Table 3. 14 The new generated MTHS matrix for SRN

	temperature in K	n-paraffins	i-paraffins	naphthenes	aromatics	vol%	0.65
PC1	282.15	0.21	0.15			0.36	0.67
PC2	293.15	1.45	2.12			3.57	0.69
PC3	313.15	1.55	2.12			3.67	0.71
PC4	333.15	1.67	2.14	0.50		4.31	0.72
PC5	353.15	2.39	2.23	2.84	0.55	8.01	0.73
PC6	373.15	3.28	3.74	3.74	2.05	12.80	0.74
PC7	393.15	5.46	7.48	3.71	2.87	19.51	0.76
PC8	413.15	6.51	8.92	3.25	3.10	21.78	0.77
PC9	433.15	4.73	6.48	2.67	2.65	16.54	0.78
PC10	453.15	2.42	3.32	2.09	1.84	9.67	0.79
PC11	464.26	0.09	0.12	0.10	0.08	0.39	0.65

The measured and the predicted distillation profiles and several key properties are compared in Figure 3.8 and Table 3.15. The biggest deviation of property comparison is 1.72 vol% in naphthene prediction. Other properties show good agreement between the measured values and the predicted values. A verification property of Waston K which is not used in the regression model is predicted. The small difference between the input value and the predicted one shows the feasibility of the proposed method.

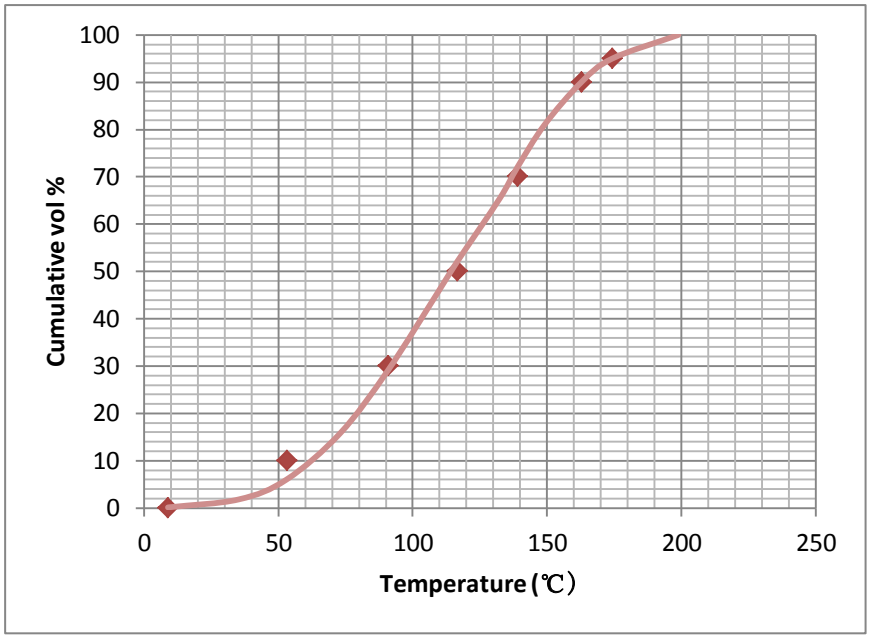

Figure 3. 8 Comparison of measured and predicted distillation profile

Table 3. 15 Comparison of measured and predicted properties

Properties	Measured	Calculated	Absolute Error
SG	0.74	0.74	0.13
RVP (psi)	3.11	3.23	0.12
RON	62.76	61.69	1.07
MON	58.95	58.40	0.55
Benzene (vol%)	0.48	0.55	0.07
P (vol%)	69.24	68.03	1.21
N (vol%)	17.11	18.83	1.72
A (vol%)	13.65	13.13	0.52
Watson K*	11.93	12.01	0.08

* Watson K is predicted from the result of the proposed model, not the regression.

The following two cases are based on the same methodology and procedure of calculation. Therefore, the step by step explanation as case study 1 is unnecessary for case study 2 and case study 3. And the feasibility and reliability could be illustrated by the result comparison.

Case study 2: An FCC product gasoline

Compared to the SRN stream studied in the previous case, the FCC gasoline product contains more iso-paraffinic and olefinic contents. The composition difference is further reflected on the bulk properties. For example, FCC gasolines always have higher octane number than SRNs, as iso-paraffins and olefins could make positive contribution to octane numbers.

Measured bulk properties and light-end information are available as initial input data.

Table 3. 16 The measured distillation and density information

density(20℃), kg/m^3		729.5
Distillation (℃)	IBP	37
	10%	53
	30%	70.5
	50%	96.5
	70%	131.5
	90%	169.5
	FBP	198

The MTHS matrix is divided into columns of NP, IP, O, N, and A for this FCC gasoline characterisation. As the light-end composition is available, pure components

are present in the MTHS matrix. The predicted molecular composition matrix is shown in Table 3.17.

Table 3. 17 Predicted composition matrix of the FCC stream

Pure component	Normal-paraffin	Iso-paraffin	Olefin	naphthene	aromatics	density
C4	1.16	0.70	2.24			
C5	2.65			0.31		
C6					0.49	
Pseudo-component cut						
pc1	0.00	8.94	7.13	0.00	0.00	677.95
pc2	1.43	7.05	5.23	0.00	0.00	702.10
pc3	1.01	5.25	3.33	0.00	0.00	716.19
pc4	0.71	3.78	3.09	2.81	0.71	729.50
pc5	0.48	2.87	2.31	2.51	3.24	742.50
pc6	0.35	2.12	1.72	1.77	6.12	755.36
pc7	0.19	1.59	1.29	0.97	5.57	767.32
pc8	0.18	1.19	0.96	0.47	3.18	778.82
pc9	0.11	0.86	0.70	0.08	1.15	784.43

Predicted bulk properties are calculated through this matrix by mixing rules, and the results are compared with measured bulk property values.

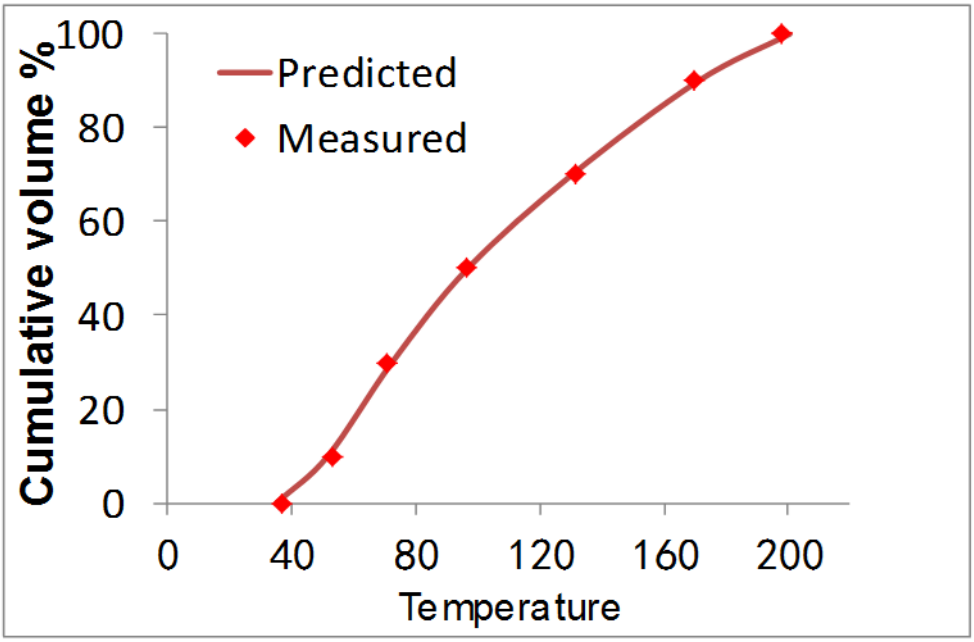

Figure 3. 9 Comparison of distillation profiles between the measured and the predicted

Table 3. 18 Comparison of measured and predicted bulk properties

	Measured	Predicted	Absolute Error	Relative Error %
nP(vol%)	8.25	8.26	0.01	0.18
iP(vol%)	34.29	34.35	0.06	0.18
O(vol%)	28.03	28.01	0.02	0.09
N(vol%)	8.95	8.92	0.03	0.32
A(vol%)	20.48	20.46	0.02	0.11
Benzene (vol%)	0.49	0.49	0.00	0.41
Density kg/m^3	729.5	729.7	0.20	0.03
RON	89.7	89.9	0.20	0.22
MON	80.4	80.5	0.10	0.12

Figure 3.9 exhibits the comparison of distillation profile between the measured and calculated values by the proposed methodology. The predicted distillation profile fits well with the measured distillation points. The comparison of other bulk properties such as PIONA composition, Benzene content, density, RON and MON is shown in Table 3.18. A good agreement is achieved in all the property comparisons.

Case study 3: Straight run gas oil characterisation

A straight-run gas oil from one of Kuwait crudes (Marafi, 2007) is applied to generate an MTHS matrix. The information available for the SRGO fraction regarding the physical properties and compositions is shown in Table 3.19.

Table 3. 19 Properties of a SRGO stream

Feed properties	
density @15°C (g/cm^3)	896.2
total aromatics (% wt)	45.68
monoaromatics (% wt)	19.47
polyaromatics (% wt)	26.21
cetane index	38.2
Distillation (°C)	
IBP	236
10 vol%	261
30 vol%	288
50 vol%	314
70 vol%	340
90 vol%	366
95 vol%	375

In this case, it is assumed that the weight fractions of the MTHS matrix entries within each homologous series follow a gamma distribution against boiling point. Since the complexity of middle petroleum fractions and the lack of compositional information, some constraints are applied to control the shape and location of distribution curves.

The initial and end temperatures of each homologous series should be considered:

$$T^{b}_{initial,j} \leq (\alpha_j - 1)\beta_j + \eta_j \leq T^{b}_{end,j} \tag{3.37}$$

To avoid the distribution within each homologous series too narrow or too wide, the shape parameter α_j and the scale parameter β_j of the gamma distribution has its individual limits.

$$1 \leq \alpha_j \leq 20 \tag{3.38}$$

$$19 \leq \beta_j \leq 100 \tag{3.39}$$

These equations and terms are not necessarily the same for different cases, and could be changed depending on the available information.

As the straight-run gas oil is an olefin-free fraction, homologous series considered in this problem are divided as normal paraffin (NP), iso-paraffin (IP), naphthenic compounds containing up to three rings (N,2N,3N), aromatic compounds containing up to three aromatic rings (A, 2A, 3A), and also compounds containing both naphthenic and aromatic rings (1A1N, 2A1N, 1A2N). In this case, only hydrocarbon mixtures without heteroatoms are considered.

The composition matrix is shown in Table 3.20.

Table 3. 20 MTHS matrix generated for SRGO (wt%)

PC temperature °C	NP	IP	N	A	2A	1A1N	2N	3A	2A1N	1A2N	3N	SG
209.1	0.70	1.95		0.71			0.01		0.02			0.84
224.2	0.78	2.16		0.78		0.00	0.20		0.08			0.85
239.3	0.68	1.87		0.67		0.15	0.88		0.23		0.03	0.86
254.5	0.57	1.57	0.00	0.56		1.34	1.53		0.47		0.43	0.87
269.6	0.45	1.25	0.03	0.45	0.01	2.86	1.37	0.02	0.66	0.01	1.30	0.87
283.5	0.39	1.07	0.22	0.38	0.09	2.86	0.90	0.18	0.78	0.09	1.76	0.88
299.2	0.33	0.90	1.02	0.32	0.35	1.60	0.40	0.79	0.80	0.35	1.37	0.89
314.2	0.26	0.73	2.39	0.26	0.70	0.56	0.13	1.77	0.66	0.70	0.66	0.90
329.2	0.21	0.59	3.88	0.21	0.97	0.15	0.04	2.76	0.50	0.97	0.24	0.91
344.3	0.17	0.49	4.68	0.18	0.99	0.03	0.01	3.20	0.34	0.99	0.07	0.92
359.5	0.14	0.39	4.33	0.14	0.78	0.01	0.00	2.84	0.21	0.78	0.01	0.92
373.9	0.11	0.32	3.43	0.11	0.53			2.17	0.12	0.53	0.00	0.93
389.0	0.09	0.25	2.27	0.09	0.30			1.38	0.07	0.30		0.94
403.1	0.08	0.22	1.45	0.08	0.16			0.85	0.04	0.16		0.94
419.6	0.05	0.14	0.59	0.05	0.06			0.33	0.01	0.06		0.95
total	5.00	13.90	24.29	5.00	4.95	9.54	5.47	16.28	4.98	4.95	5.88	

Figure 3.10 shows the comparison of distillation profile between the measured and the predicted and a comparison of the SRGO density and calculated cetane index is given in Table 3.21 and shows an acceptable accuracy.

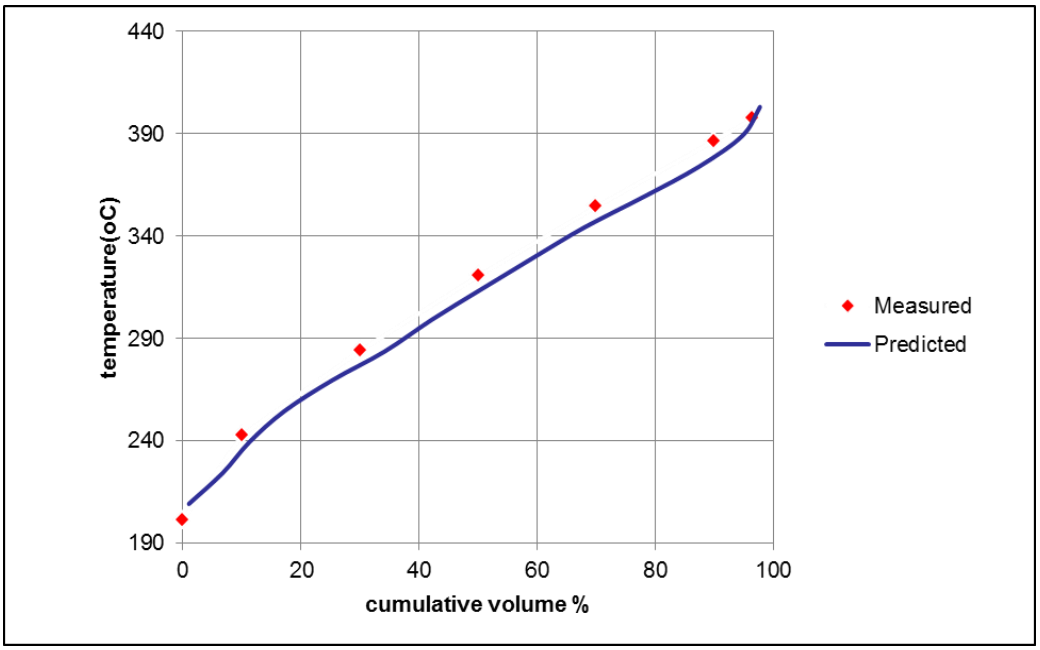

Figure 3. 10 Comparison of distillation profile of a SRGO stream

Table 3. 21 Comparison of measured and predicted properties of a SRGO stream

Properties	Measured	Predicted	Absolute Error	Relative Error %
Density (kg/m^3)	896.2	895.8	0.40	0.04
CCI*	40.42	40.04	0.38	0.91
Flash point °C *	105.72	103.53	2.19	2.07
Viscosity at 37.8 °C (cSt)*	0.88	0.84	0.04	4.55
Pour point °C *	-7.43	-8.70	1.27	17.09

* Measured properties are calculated via correlations

The calculated cetane index (CCI) is estimated based on the following equation (Riazi, 2005).

$$CCI = 454.74 - 1641.416SG + 774.74SG^2 - 0.554T_{50} + 97.083(log_{10}T_{50})^2 \quad (3.40)$$

Where T_{50} is the ASTM D86 temperature at 50 vol% in ^{o}C.

3.5 Summary

In this work, a non-experimental characterisation methodology is developed to obtain molecular level information of petroleum fractions by using the proposed MTHS matrix framework, which takes advantages of both pseudo-component and molecular modelling methodologies. By introducing pseudo-components instead of carbon numbers in the matrix framework for easier extraction of essential data, the matrix can be extended to heavier fractions for consistency. The corresponding transformation method behind the new matrix framework has been presented step by step in this chapter, and good accuracy and reliability can be seen through several case studies of different petroleum fractions up to middle distillates.

One key benefit with the proposed characterisation framework is that the method provides a compatible characterisation tool that could be adopted among reaction, separation, and blending models, which is demonstrated in Chapters 4 and 5 respectively, providing a common platform for overall simulation and optimisation of refining processes.

3.6 Nomenclature

List of sets

k	group type
n	carbon number
i	pseudo-component
j	homologous series

List of symbols

T	boiling point temperature
w	weight factor
v_{pc}	volume fraction of a pseudo-component
Kw	UOP characterisation factor Waston K
SG	specific gravity
θ	properties
N_k	number of groups of type k
tbk	group contribution
z	hydrogen deficiency

Chapter 4 Molecular Modelling of Catalytic Reforming

4.1 Introduction

Catalytic reforming is a very important refining process to enhance gasoline product quality, provide aromatics (BTX: benzene, toluene, xylene) to the petrochemical industry, and is also treated as one of primary sources of hydrogen. Reformers typically contribute for 50 vol % to the gasoline pool by transforming straight-run naphtha with a low octane number of 50-60 into high-octane gasoline compounds of 90-105 (Sotelo-Boyas and Froment, 2009). The octane number increase is mainly achieved by conversions of normal paraffins and naphthenes to corresponding isoparaffins and aromatics. Recently, new environmental legislations demand the reduction in emissions of volatile, toxic, and polluting components in gasoline, especially the limitation of benzene and aromatics content in commercial gasoline. As reformates are a major source of aromatics in gasoline, the trade-off between high-octane-number products and the specification of aromatics limit should be explored. Because of these reasons, it is very necessary to apply an appropriate kinetic model capable of predicting the detailed reformate composition for further processing use, in combination with a catalytic reforming reactor model for simulation and optimisation. For such a process clearly in need of accurate modelling at the detailed molecular level, it is a good candidate to test the proposed molecular characterisation method.

This chapter firstly gives a brief introduction of catalytic reforming process and discusses some influential process variables, followed by the review of previous works on catalytic reforming modelling. Main chemical reactions occurred in catalytic reforming and the reaction network are illustrated respectively to build up a molecular level reaction model. A case study demonstrates the accuracy of the proposed model based on the developed molecular characterisation method.

4.2 Catalytic Reforming Process

According to the frequency and mode of catalyst regeneration, catalytic reforming processes are commonly classified into three types:

(1) Semi-regenerative

(2) Continuous regeneration

(3) Cyclic regeneration

Semi-regenerative units generally involve three of four reactor (Chang, et al., 2012) and need to shut-down at intervals of 3 to 24 months for catalyst regeneration (Wu, 2010). It is the most commonly used process worldwide with the advantages of lower capital cost (Rodriguez and Ancheyta, 2011) and relatively simple process flow schemes. A severe operating condition of high pressure and hydrogen recycle rate is necessary to minimise coke laydown and catalyst deactivation rate.

The continuous process can maintain high catalyst selectivity and activity by the construction of a special reactor that allows continuous catalyst withdrawal and regeneration while the reactor is on-stream. The operating cost of a continuous process is lower than other processes due to lower operation pressure and hydrogen recycle rate needed for acceptable rate of coke laydown. Recently, catalytic reformers are mostly designed with continuous regeneration (Wu, 2010).

Cyclic process units have several additional swings or spare reactors so it can regenerate the catalyst without shutting the whole unit down. It is a compromise between semi-regenerative and continuous processes.

Figure 4.1 shows a simplified process flow diagram of a semi-regenerative catalytic reforming unit. Hydrotreated naphtha feed is combined with recycle hydrogen, heated first by reactor effluent for heat recovery. Then the mixture stream is further heated up by a fired heater to reaction temperature and fed into the first fixed-bed reactor. The major reaction in this reactor is strongly endothermic and very fast, causing a sharp drop in temperature. The effluent from the first reactor is then reheated before entering the second one to maintain necessary operating temperature and for required reaction rate. This sequence is repeated for one or more extra reactors before the effluent from the last reactor is cooled and enters a separator. As

conversions of feedstock proceeds through a series of heating and reacting, reactions become less and less endothermic and temperature differential across the reactors decreases. A part of hydrogen-rich stream separated in the separator is compressed and recycled back to join the fresh naphtha feed. The remaining hydrogen by-product is supplied to other hydrogen users in the refinery or used as fuel. Liquid products from the separator are condensed and fractionated into a stabilised reformate as well as a stream of butanes and lighter materials. Reformate is sent to storage for gasoline blending. The catalyst is regenerated intermittently, whenever its activity falls to a predetermined level or sometimes when the unit is down for other reasons (Maples, 2000).

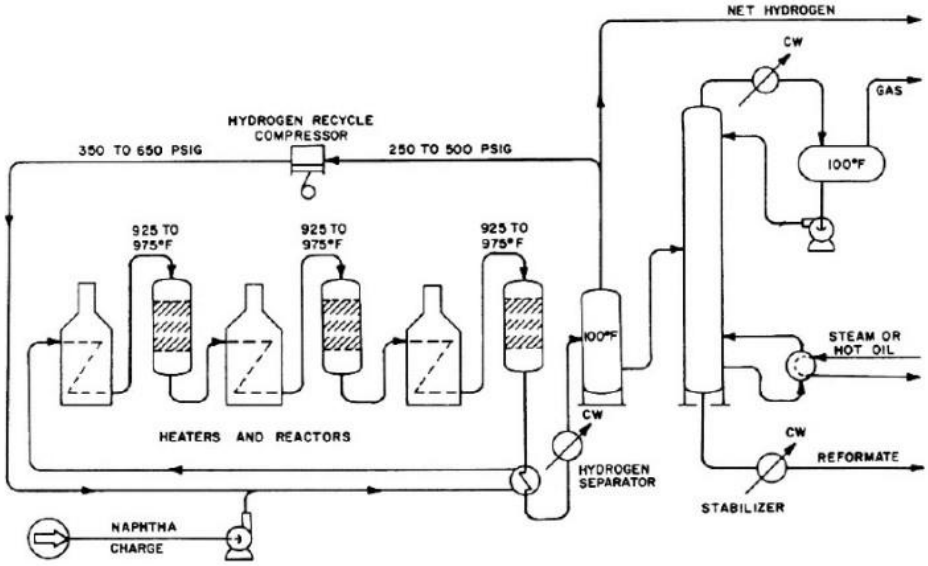

Figure 4. 1 Simplified semi-regenerative catalytic reforming process flowsheet (Gary and Handwerk, 2001)

4.3 Process Variables

There are several major process variables relating to the performance of a unit. The process variables include operating conditions, feedstock properties, and catalyst selectivity, activity and stability. These factors and their influence are briefly explained in this section.

❖ Operating conditions

The key operating conditions such as reactor pressure, reactor temperature, space velocity, hydrogen/hydrocarbon (H_2/HC) molar ratio can strongly affect the performance of a reforming process and product quality.

➢ Reactor Pressure:

In general, average reactor operating pressure is referred to as reactor pressure. The reactor pressure affects reformer yields, reactor temperature requirement, and catalyst stability. As can be seen later in the reaction pathways, major reforming reactions favour low pressure, at the expense of high coke yield for quicker catalyst deactivation.

➢ Reactor Temperature:

The operating temperature is the primary control for product quality. The typical temperature range of catalyst reforming processes is from 490 to 525 ℃ (Meyer, 2004).

➢ Space Velocity:

Space velocity is defined as the amount of naphtha processed over a given amount of catalyst over a given length of time. It is an indication of the contact time between reactants and catalyst. There are two terms of space velocity: liquid hourly space velocity (LHSV) and weight hourly space velocity (WHSV). The typical space velocity for modern refiners is between 1.0 h^{-1} and 2.0 h^{-1} (LHSV) (Wu, 2010).

➢ Hydrogen/Hydrocarbon Molar Ratio:

The H_2/HC ratio is the ratio of moles of hydrogen in the recycle gas to moles of naphtha fed to the unit. H_2/HC ratio affects length of catalyst life. The typical H_2/HC molar ratio ranges from 3 to 8.

❖ Feedstock Properties

In general, the feed to a catalytic reforming process is heavy straight-run naphtha with the boiling range between 80 ℃ to 180℃. Feedstock with a low initial boiling point less than 70℃ (ASTM D86) contains light components that are difficult to be converted to valuable aromatics. Heavy fractions with a boiling point higher than

180℃ are undesirable since it would produce excessive carbon lay-down on the reformer catalyst, and the corresponding gasoline products often exceed the maximum specification of end boiling point. Table 4.1 gives two kinds of typical composition of naphtha reforming feed.

Table 4. 1 Compositions of two typical feeds (Gary, 2001)

	Paraffinic (Arabian Light)	Naphthenic (Nigeria)
RON	50	66
Average molecular weight	114	119
Sulphur (wtppm)	500	350
Paraffins (vol%)	66.8	29.3
Naphthenes (vol%)	21.8	61.85
Aromatics (vol%)	11.4	8.85

❖ Catalyst Selectivity, Activity and Stability

Reformer catalyst is very important to a reforming unit and can affect other process variables significantly. Catalyst selectivity can be defined as the amount of desired product that can be yielded from a given feedstock. Activity of catalyst is the ability to promote a desired reaction with respect to reaction rate, space velocity, or temperature. A more active catalyst can produce reformate with the desired octane number at a lower temperature. Catalyst stability is a measure of length of catalyst life in a semi-regenerative process.

4.4 Reformate Properties

A typical product from naphtha catalytic reforming contains mainly C5+ reformates, hydrogen, and some light hydrocarbons such as methane, ethane, propane and butanes. Recently, the byproducts of hydrogen and light hydrocarbons have also

become more and more valuable to the market. Table 4.2 shows a typical product composition from a paraffinic feed on a bimetallic catalyst at 15 bar. The yield of desired C5+ reformate reaches 82.5 wt% and the product with less value as methane and ethane is lower than 5wt%.

Table 4. 2 Typical product distribution from paraffinic feed at 15 bar with RON of 98 (George, 2004)

Product	Yield (wt% / feed)
H_2	2.5
CH_4	1.7
C_2H_6	3.1
C_3H_8	4.2
C_4H_{10}	6.0
C5+	82.5

According to the literature, naphthenes and olefins concentrations are lower than 1% wt except for low pressure processes (Wu, 2010). Table 4.3 shows a detailed composition analysis combining carbon number and PIONA series. Aromatics, especially C_7 to C_{10} aromatics as the main contributor to octane number, are close to 70 % wt. Reformates normally do not contain any sulphur content ($S \leq 0.1$ ppm).

Table 4. 3 Typical composition of reformate at low operating pressure (George, 2004)

wt %	nP	iP	O	N	A	sum
4	0.57					0.57
5	1.51	2.37	0.1			3.98
6	1.69	3.97	0.16	0.19	2.34	8.35
7	2.5	8.42	0.35	0.4	14.16	25.83
8	1.16	4.91	0.44	0.34	26.28	33.13
9	0.26	1.04	0.08	0	21.08	22.46
10	0.07	0.28	0	0	4.76	5.11
11	0	0.02	0	0	0.55	0.57
sum	7.76	21.01	1.13	0.93	69.17	100

4.5 Review of Existing Modelling Work

Various kinetic models for reforming reactions have been developed over the past decades. The level of sophistication of these models varies from three rough lumps to very detailed mechanistic level models involving hundreds of reaction species and thousands of reactions.

In a lump approach, many different molecules are classified into a single group or lump, and then assumed to behave identically as a single compound with the average properties of that lump. The earliest kinetic model for reforming was reported by Smith (1959), which assumes that the complex feedstock is the mixture of three lumps: paraffins (P), naphthenes (N) and aromatics (A). The kinetic network of this model accounts for dehydrocyclisation of paraffins to naphthenes, dehydrogenation of naphthenes to aromatics and hydrocracking of aromatics to paraffins. Krane et al (1959) further improved this model by splitting up each PNA lump into carbon number based groups. This modified model has 20 lumps and 53 reactions. But key factors such as the effect of some reaction variables have been ignored in these

simplified lumping models.

Henningsen et al (1970) introduced a network considering different reaction rates between C5 and C6 naphthenes and activity factor of catalyst deactivation. Jenkins et al. (1980) considered empirical correction factors for acid and pressure in the rate expression. Ancheyeta (1994, 2011) also introduced a similar pressure correction term to account for pressures other than 300 psig specified in the Krane et al. model. The model proposed that naphthenes with six-carbon ring are the primary precursor to benzene (Figure 4.2) and considered non-isothermal operating conditions.

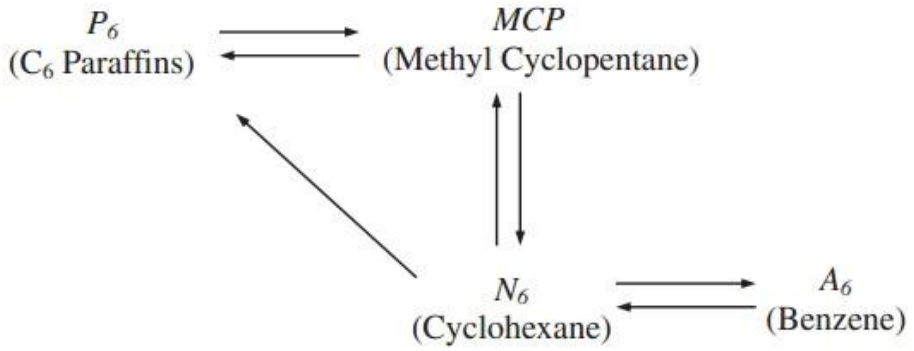

Figure 4. 2 Reaction network of benzene formation (Ancheyta, 2000)

Krane's original model and Anchyeta's modification model do not include the inhibition and decrease in catalyst activity due to a variety of factors. Kmak (1972) gave the earliest model treating the reaction network as a catalytic system. Marin et al. (1983) refined Kmak model by extending the reaction network covering the carbon number range from C5 to C10 with Hougen-Waston Langmuir-Hinshelwood (WHLH) rate equations. Taskar et al. (1997) proposed a model containing 35 pseudocomponents connected by a network of 36 reactions, and further divided isoparaffins into single-branched paraffins and multi-branched paraffins due to the verity of their physical properties.

4.6 Chemical Reactions Network

A large number of reactions occur in catalytic reforming over the bifunctional catalysts that contains a metal and an acid function. Table 4.4 lists some major

reactions observed in the reforming process (Chang, et al., 2012). All these reactions can contribute to octane number enhancement except hydrocracking, which converts valuable C_5^+ molecules into light gases and results in a decrease in reformate yield.

Table 4. 4 Major reactions of catalytic reforming process

Dehydrogenation of naphthenes to aromatics	MCH → TOL + H_2
Dehydrocyclisation of paraffins to aromatics	P_7 → TOL + H_2
Isomerisation of normal paraffins to isoparaffins	NP → IP
Isomerisation of cycloalkanes	MCP → MCH
Hydrocracking reactions	P_n → P_{n-i} + P_i

The major reaction such as dehydrogenation of naphthenes in the first reactor is the fastest, and isomerisation is moderately fast, while dehydrocyclisation of paraffins and hydrocracking are the slowest. The dehydrogenation of naphthenes is the major reaction to produce aromatic components and can achieve thermodynamic equilibrium under industrial operating conditions. The dehydrocyclisation of normal-paraffins is also an important reaction for aromatics formation and increases reformate octane number substantially. Other desirable reactions such as saturation of olefins and isomerisation of paraffins also have positive impact on reformate quality. At the same time, some undesirable reactions to form lighter paraffins, for instance, cracking of paraffins and naphthenes and dealkylation of side chains on naphthenes and aromatics, are need to be inhibited by choosing appropriate reactiing conditions.

4.6.1 Dehydrogenation of Naphthenes to Aromatics

The transformation from alkylcyclohexanes to corresponding aromatics is the fastest and most principle reaction in a reforming process.

$$N_n \rightarrow A_n + H_2 \tag{4.1}$$

This reaction results in an increase of molecules in the forward direction of the

reaction and is hence sensitive to system pressure. Chemical equilibrium is shifted to the forward direction under low-pressure conditions. Because dehydrogenation reactions are highly endothermic and cause a temperature drop during reaction processing, inter-heaters are needed between catalyst beds to keep a high reactant temperature for the reaction to proceed. Besides, low space velocity and low hydrogen-to-hydrocarbon molar ratios can also promote the reaction to the right direction.

4.6.2 Isomerisation and of Paraffins and Naphthenes

The reactions of isomerisation occur on the acid alumina sites with moderate rates at commercial operating temperatures. The transformations from normal paraffins to iso-paraffins are highly desired during catalytic naphtha reforming by the positive contribution for octane number from the produced iso-paraffins. The isomerisation of naphthenes, such as the conversion of methylcyclopentane (MCP) into cyclohexane, can provide the reactant of benzene formation and increase the octane number of reformates.

The distribution between isomers of paraffins can be calculated by thermodynamic equilibrium approach (Rodriguez, and Ancheyta, J., 2011).

For the isomerisation reaction between paraffins as following:

$$NP_i \leftrightarrow IP_i \tag{4.2}$$

The equilibrium constant (K_i) is related to the standard Gibbs energy change (ΔG^0) and temperature of reaction:

$$\ln K_i = -\frac{\Delta G^0}{R\,T} \tag{4.3}$$

where R is the universal constant of gases.

ΔG^0 can be determined with

$$\frac{\Delta G^0}{R\,T} = \frac{\Delta G^0 - \Delta H_0^0}{R\,T_0} + \frac{\Delta H_0^0}{R\,T} + \frac{1}{T}\int_{T_0}^{T}\frac{\Delta Cp}{R}dT - \int_{T_0}^{T}\frac{\Delta Cp}{R}\frac{dT}{T} \tag{4.4}$$

Where Cp is heat capacity and Cp of a component on temperature T can be calculated as following:

$$Cp_i = A_i + B_iT + C_iT^2 + D_i3 \quad (4.5)$$

By substituting Eq.(4.5) in Eq.(4.4), the integral parts can be estimated with the following forms:

$$\int_{T_0}^{T} \Delta CpdT = \Delta A(\tau - 1)T_0 + \frac{\Delta B}{2}(\tau^2 - 1)T_0^2 + \frac{\Delta C}{2}(\tau^3 - 1)T_0^3 + \frac{\Delta D}{2}(\tau^4 - 1)T_0^4 \quad (4.6)$$

$$\int_{T_0}^{T} \frac{\Delta Cp}{T} dT = \Delta A \ln(\tau) + \Delta B(\tau - 1)T_0 + \frac{\Delta C}{2}(\tau^2 - 1)T_0^2 + \frac{\Delta D}{3}(\tau^3 - 1)T_0^3 \quad (4.7)$$

Where

$$\tau = \frac{T}{T_0} \quad (4.8)$$

The required thermodynamic data are given in Table 4.5 for the above calculation procedure (Ancheyta, J., 2011).

Table 4. 5 Thermodynamic data of various paraffins (Reid, 1977)

Name	A	B	C	D	H^o	G^o
n-Butane	2.266	7.91E−02	−2.65E−05	−6.74E−10	−30.15	−4.10
i-Butane	−0.332	9.19E−02	−4.41E−05	6.92E−09	−32.15	−4.99
n-Pentane	−0.866	1.16E−01	−6.16E−05	1.27E−08	−35.00	−2.00
2 Methyl butane	−2.275	1.21E−01	−6.52E−05	1.37E−08	−36.92	−3.54
2,2 Dimethyl propane	−3.963	1.33E−01	−7.90E−05	1.82E−08	−39.67	−3.64
n-Hexane	−1.054	1.39E−01	−7.45E−05	1.55E−08	−39.96	−0.06
2 Methyl pentane	−2.524	1.48E−01	−8.53E−05	1.93E−08	−41.66	−1.20
3 Methyl pentane	−0.570	1.36E−01	−6.85E−05	1.20E−08	−41.02	−0.51
2,2 Dimethyl butane	−3.973	1.50E−01	−8.31E−05	1.64E−08	−44.35	−2.30
2,3 Dimethyl butane	−3.489	1.47E−01	−8.06E−05	1.63E−08	−42.49	−0.98
n-Heptane	−1.229	1.62E−01	−8.72E−05	1.83E−08	−44.88	1.91
2 Methyl hexane	−9.408	2.06E−01	−1.50E−04	4.39E−08	−46.59	0.77
3 Methyl hexane	−1.683	1.63E−01	−8.92E−05	1.87E−08	−45.96	1.10
2,2 Dimethyl pentane	−11.966	2.14E−01	−1.52E−04	4.15E−08	−49.27	0.02
2,3 Dimethyl pentane	−1.683	1.63E−01	−8.92E−05	1.87E−08	−47.62	0.16
2,4 Dimethyl pentane	−1.683	1.63E−01	−8.92E−05	1.87E−08	−48.28	0.74
3,3 Dimethyl pentane	−1.683	1.63E−01	−8.92E−05	1.87E−08	−48.17	0.63
3 Ethyl pentane	−1.683	1.63E−01	−8.92E−05	1.87E−08	−45.33	2.63
n-Octane	−1.456	1.84E−01	−1.00E−04	2.12E−08	−49.82	3.92
2 Methyl heptane	−21.435	2.97E−01	−2.81E−04	1.10E−07	−51.50	3.05
3 Methyl heptane	−2.201	1.88E−01	−1.05E−04	2.32E−08	−50.82	3.28
4 Methyl heptane	−2.201	1.88E−01	−1.05E−04	2.32E−08	−50.69	4.00
2,2 Dimethyl hexane	−2.201	1.88E−01	−1.05E−04	2.32E−08	−53.71	2.56
2,3 Dimethyl hexane	−2.201	1.88E−01	−1.05E−04	2.32E−08	−51.13	4.23
2,4 Dimethyl hexane	−2.201	1.88E−01	−1.05E−04	2.32E−08	−52.44	2.80
2,5 Dimethyl hexane	−2.201	1.88E−01	−1.05E−04	2.32E−08	−53.21	2.50
3,3 Dimethyl hexane	−2.201	1.88E−01	−1.05E−04	2.32E−08	−52.61	3.17
3,4 Dimethyl hexane	−2.201	1.88E−01	−1.05E−04	2.32E−08	−50.91	4.14
3 Ethyl hexane	−2.201	1.88E−01	−1.05E−04	2.32E−08	−50.40	3.95
2,2,3 Trimethyl pentane	−2.201	1.88E−01	−1.05E−04	2.32E−08	−52.61	4.09
2,2,4 Trimethyl pentane	−1.782	1.86E−01	−1.02E−04	2.19E−08	−53.57	3.27
2,3,3 Trimethyl pentane	−2.201	1.88E−01	−1.05E−04	2.32E−08	−51.73	4.52
2,3,4 Trimethyl pentane	−2.201	1.88E−01	−1.05E−04	2.32E−08	−51.97	4.52
2 Methyl 3 ethyl pentane	−2.201	1.88E−01	−1.05E−04	2.32E−08	−50.48	5.08
3 Methyl 3 ethyl pentane	−2.201	1.88E−01	−1.05E−04	2.32E−08	−51.38	4.76
n-Nonane	0.751	1.62E−01	−4.61E−05	−7.12E−09	−54.74	5.93
2,2,3 Trimethyl hexane	−10.899	2.52E−01	−1.71E−04	4.75E−08	−57.65	5.86
2,2,4 Trimethyl hexane	−14.405	2.64E−01	−1.84E−04	5.23E−08	−58.13	5.38
2,2,5 Trimethyl hexane	−12.923	2.62E−01	−1.85E−04	5.39E−08	−60.71	3.21
3,3 Diethyl pentane	−16.067	2.69E−01	−1.91E−04	5.51E−08	−55.44	8.38
2,2,3,3 Tetramethyl pentane	−13.037	2.60E−01	−1.81E−04	5.12E−08	−56.70	8.20
2,2,3,4 Tetramethyl pentane	−13.037	2.60E−01	−1.81E−04	5.12E−08	−56.64	7.80
2,2,4,4 Tetramethyl pentane	−16.099	2.79E−01	−2.06E−04	6.15E−08	−57.83	8.13
2,3,3,4 Tetramethyl pentane	−13.117	2.61E−01	−1.82E−04	5.15E−08	−56.46	8.15
n-Decane	−1.890	2.30E−01	−1.26E−04	2.70E−08	−59.67	7.94
3,3,5 Trimethyl heptane	−16.808	2.94E−01	−2.07E−04	5.86E−08	−61.80	8.02
2,2,3,3 Tetramethyl hexane	−14.052	2.94E−01	−2.11E−04	6.17E−08	−61.66	11.28
2,2,5,5 Tetramethyl hexane	−14.890	2.97E−01	−2.14E−04	6.25E−08	−68.32	4.66

With calculated K_i of all paraffin isomers, the formulae to calculate the composition (y_i) of all isomers can be determined as:

$$y_i = \frac{K_i}{1+\sum_{i=1}^{n_{isomers}} Ki} \quad (4.9)$$

The distribution between isomers can be used to lump all paraffins together to adopt the kinetic model of PNA lumps, and to obtain a detailed reformate composition matrix after modelling simulation.

Isomerisation is favoured by high temperature, low pressure and low space velocity.

4.6.3 Dehydrocyclisation of Paraffins

The dehydrocyclisation reaction formula is shown in Eq (4.10):

$$P_n \rightarrow N_n \quad (4.10)$$

where n ranges from 6 to 12.

The difficulty to promote the paraffin dehydrocyclisation is molecular rearrangement of paraffins to naphthenes. Only paraffins with at least a six-carbon straight chain can cyclise to cycloalkanes and this kind of conversion requires both metal and acid functions of catalyst. With the increasing of carbon number, the reaction becomes easier since the probability of ring formation increases, however partially offset by hydrocracking to lighter paraffins (Wu, 2010). Dehydrocyclisation yield is increased by low pressure and high temperature.

4.6.4 Hydrocracking and Dealkylation

Both hydrocracking of paraffins and dealkylation of aromatics and naphthenes result in producing lighter liquid and gas products with hydrogen consumption. The conditions of high temperature, high pressure and low space velocity promote these reactions.

The hydrocracking reactions are exothermic and mainly occur in the last section of the reactor due to the exothermic nature of the reaction. It is necessary to control the hydrocracking reactions so that high quality and yield of products can be obtained.

Dealkylation of naphthenes and aromatics makes the side chains on the naphthene or aromatic ring smaller or removes the alky groups completely.

4.7 Development and Validation of MTHS Based Catalytic Reforming Model

4.7.1 Kinetic Network and Parameter Regression

A kinetic model proposed by Ancheyta (2011) is modified in this work. The kinetic model considers the whole naphtha range fraction at a molecular level, and the isomerisation of MCP (methylcyclopentane) to cyclohexane. All reactions are assumed to be pseudo-first order with respect to hydrocarbons. The kinetic network is shown in Figure 4.3. This network contains 71 reactions and 25 reacting components.

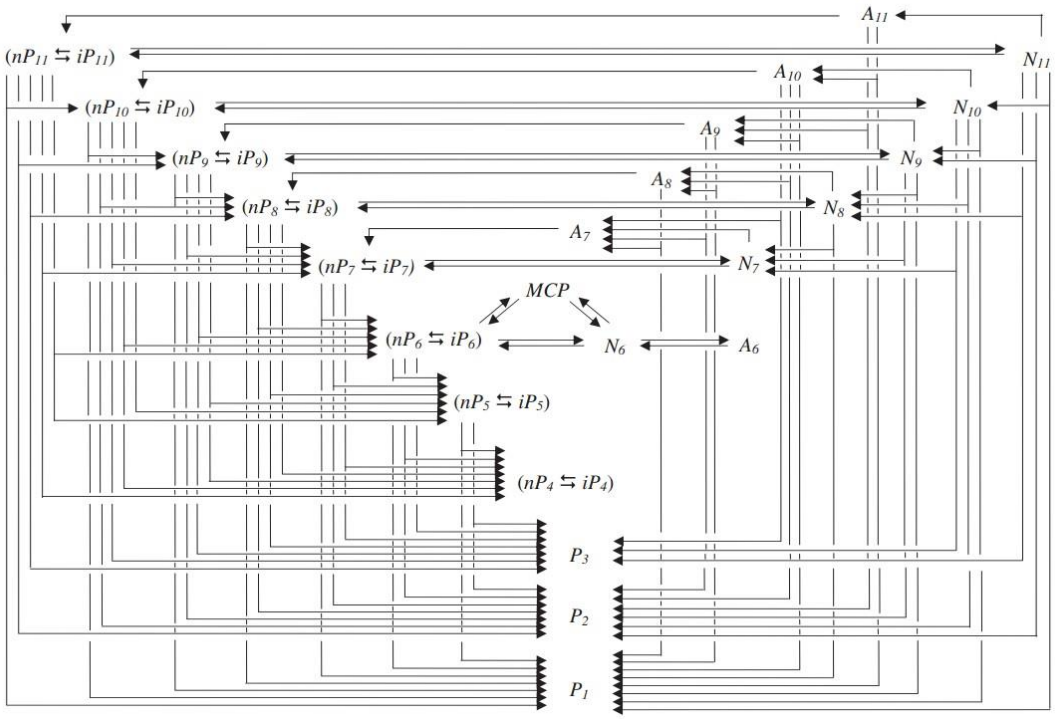

Figure 4. 3 Kinetic network of proposed reforming model (Ancheyta, 2011)

The reaction rate of all lumps can be generally determined by the following equation.

$$\frac{dC}{dt} = -kC \tag{4.11}$$

Where k is the kinetic parameter of each reaction; C is the concentration of the reactant. The influence of temperature and pressure on kinetic parameters is considered by an Arrhenius-type variation of the rate constants with activation energy values for each type of reaction as well as a factor for pressure effect. The equation (Ancheyta, 2000) for the combined effect is expressed as follows:

$$k_i = k_i^0 exp\left[\frac{E_{Aj}}{R}\left(\frac{1}{T_0}-\frac{1}{T}\right)\right]\left(\frac{P}{P_0}\right)^{\alpha_k} \quad (4.12)$$

The values of activation energies (E_{Aj}) for each reaction j and pressure effect factors α_k are given in Table 4.6. Under the standard conditions of T_0 = 766 K, P_0 = 300 psig, H_2/oil ratio of 2-8 mol/mol, and WHSV of 0.7 – 5.0h^{-1}, kinetic constants (k_i) based on the report of Krane et al. (1959) are chosen as the initial guess.

Table 4. 6 Activation energies and pressure effect factors of each reaction

Reaction	Number of reactions	E_{Aj} (kcal/mol)
Paraffins		
$P_n \rightarrow N_n$	5	45
$P_n \rightarrow P_{n-i} + P_i$	21	55
Subtotal	26	–
Naphthenes		
$N_n \rightarrow A_n$	5	30
$N_n \rightarrow N_{n-i} + P_i$	6	55
$N_n \rightarrow P_n$	5	45
Subtotal	16	–
Aromatics		
$A_n \rightarrow A_{n-i} + P_i$	6	40
$A_n \rightarrow P_n$	4	45
$A_n \rightarrow N_n$	1	30
Subtotal	11	–

Reaction	α_k
Isomerization	0.370
Dehydrocyclization	−0.700
Hydrocracking	0.433
Hydrodealkylation	0.500
Dehydrogenation	0.000

n: number of atoms of carbon ($1 \leqslant i \leqslant 5$).

Due to the difference in gasoline representation methodology, kinetic parameters need to be re-regressed in this work. The regression is based on information available in the literature. The regression result is shown in Table 4.8 under operating conditions listed in Table 4.7. Kinetic rate constants are assumed to be fixed within a reactor. Therefore, considering the influence of temperature on kinetic parameters (reactor pressures are the same), kinetic parameters in Reactor 2 and Reactor 3 could be calculated. The objective is to minimise the difference of product distribution between the data from the literature (Anchetya, 2000) and calculated.

Table 4. 7 Reactor operating conditions for kinetic regression

Reactor No.	Temperature(K):	Pressure(psi)	WHSV
Reactor 1	763.15	149.49	5.6433
Reactor 2	773.15	149.49	14.1043
Reactor 3	783.15	149.49	28.2486

Table 4. 8 Kinetic parameters of the proposed model

ID	Reaction step	k (h^{-1})	ID	Reaction step		ID	Reaction step	k (h^{-1})
1	P11→N11	0.0155	25	P8→2P4	0.0054	49	N8→N7+P1	0.0007
2	P10→N10	0.0113	26	P7→P6+P1	0.0025	50	N11→A11	0.6296
3	P9→N9	0.0217	27	P7→P5+P2	0.0013	51	N10→A10	0.4734
4	P8→N8	0.0164	28	P7→P4+P3	0.0024	52	N9→A9	0.3827
5	P7→N7	0.0070	29	P6→P5+p1	0.0013	53	N8→A8	0.2207
6	P6→N6	0.0000	30	P6→P4+P2	0.0012	54	N7→A7	0.3528
7	P6→MCP	0.0034	31	P6→2P3	0.0012	55	N6→A6	0.6800
8	P11→P10+P1	0.0086	32	P5→P4+P1	0.0019	56	A11→P11	0.0014
9	P11→P9+P2	0.0104	33	P5→P3+P2	0.0023	57	A10→P10	0.0016
10	P11→P8+P3	0.0167	34	N11→P11	0.0050	58	A9→P9	0.0010
11	P11→P7+P4	0.0184	35	N10→P10	0.0054	59	A8→P8	0.0011
12	P11→P6+P5	0.0282	36	N9→P9	0.0054	60	A7→P7	0.0007
13	P10→P9+P1	0.0013	37	N8→P8	0.0025	61	A11→A10+P1	0.0006
14	P10→P8+P2	0.0050	38	N7→P7	0.0019	62	A11→A9+P2	0.0006
15	P10→P7+P3	0.0248	39	N6→P6	0.0096	63	A10→A9+P1	0.0006
16	P10→P6+P4	0.0114	40	MCP→P6	0.0008	64	A10→A8+P2	0.0006
17	P10→2P5	0.0051	41	N11→N10+P1	0.0136	65	A10→A7+P3	0.0000
18	P9→P8+P1	0.0039	42	N11→N9+P2	0.0135	66	A9→A8+P1	0.0006
19	P9→P7+P2	0.0072	43	N11→N8+P3	0.0081	67	A9→A7+P2	0.0007
20	P9→P6+P3	0.0187	44	N10→N9+P1	0.0125	68	A8→A7+P1	0.0001
21	P9→P5+P4	0.0082	45	N10→N8+P2	0.0133	69	A6→N6	0.0008
22	P8→P7+P1	0.0022	46	N10→N7+P3	0.0083	70	MCP→N6	0.0656
23	P8→P6+P2	0.0081	47	N9→N8+P1	0.0177	71	N6→MCP	0.0035
24	P8→P5+P3	0.0030	48	N9→N7+P2	0.0259			

4.7.2 Mathematical Model of Catalytic Reformer

The regressed kinetic model is incorporated in a fixed-bed one-dimensional pseudo-homogeneous adiabatic reactor model. Under the general reactor operating conditions, radial and axial dispersion effects were found to be negligible. Therefore, the mixture could be assumed as plug-flow in the reactor (Taskar, 1997). Several assumptions are made for the development of the mathematical model (Wu, 2010),

including: (1) the reactor is operated in an adiabatic and steady-state condition; (2) velocity keeps as constant across the reactor section; (3) radial deviation of concentrations do not exist in a reactor.

Temperature profiles and reformate composition through each reactor bed are presented by the following ordinary differential equations (eq. 4.13 - eq. 4.14) (Froment, 1990).

Reformate composition:

$$\frac{dF_i}{dw} = \sum_{j \in J} \gamma_{j,i} r_j \quad \forall i \in I \tag{4.13}$$

Temperature profile:

$$\frac{dT}{dw} = \frac{\sum_{j \in J} r_j(-\Delta H_j)}{\sum_{j \in I} F_i C_{pi}} \tag{4.14}$$

where F_i stands for molar flow rate of component i, and w is catalyst weight. $\gamma_{j,i}$ is the stoichiometric coefficient of component i in reaction j. r_j is the reaction rate of reaction j. T is the reactor temperature along with catalyst weight, and ΔH_j stands for the reaction heat of reaction j. Cp_i is the specific heat capacity of component i.

The pressure is decreasing along reactor bed gradually. This pressure drop could be described by the Ergun equation (Fogler, 1992), which is shown in eq. 4.15 for the prediction of power cost used to compress the recycle hydrogen to a reactor pressure, which could be an important consideration in future process optimisation.

$$\frac{dP}{dw} = -\frac{G}{\rho d_p \varepsilon^3}\left[\frac{150(1-\varepsilon)\mu}{d_p} + 1.75G\right]\frac{1}{A_c \rho_c} \tag{4.15}$$

where P stands for pressure along with the catalyst weight, and G is the superficial mass velocity of gas mixture; d_p is the diameter of catalyst particle; ρ is the density of the gas mixture; ε is for void fraction of catalyst bed; and μ is for the viscosity of the gas mixture. A_c is cross sectional area of the bed, and ρ_c is the

density of catalyst.

Apart from the mathematical models of catalytic reforming kinetic and reactor, the characterisation method proposed in Chapter 3 is incorporated here as well. The analysis information of naphtha feed is usually reported in bulk properties such as distillation profile and density, which is not suitable for the proposed process model. Therefore, the bulk property information needs to be transferred into molecular-level information by the proposed MTHS method firstly, and then could be adopted in the CR model.

4.7.3 Validation and Result Discussion

The case from Ancheyta (2000) is chosen to validate the proposed MTHS based catalytic reforming model. A hydrodesulfurised straight-run naphtha with boiling temperature range of 82℃ to 168℃ from a commercial naphtha HDS unit is fed to the reforming unit. The feedstock composition determined by GC analysis is presented in Table 4.9.

Table 4. 9 Composition of the feedstock (Ancheyta, 2000)

Mol%	Normal Paraffins	Iso-Paraffins	Naphthenes	Aromatics
C5	3.80	3.40		
C6	4.40	6.70	3.63	0.80
C7	3.20	6.20	5.80	3.22
C8	6.36	6.51	4.71	4.71
C9	5.09	8.31	3.56	4.21
C10	2.97	6.22	0.60	2.70
C11	2.20		0.40	0.30

The semi-regenerative catalytic reforming process contains three reactors with different inlet temperatures of 490, 500 and 510℃ with independent temperature

control and space velocities (WHSV) of 17.72, 7.09, and 3.54 h^{-1} respectively. Each reactor is operated in isothermal mode at pressure of 149.49 psi, H_2/HC molar ratio of 6.5. The reactor configuration is shown in Figure 4.4.

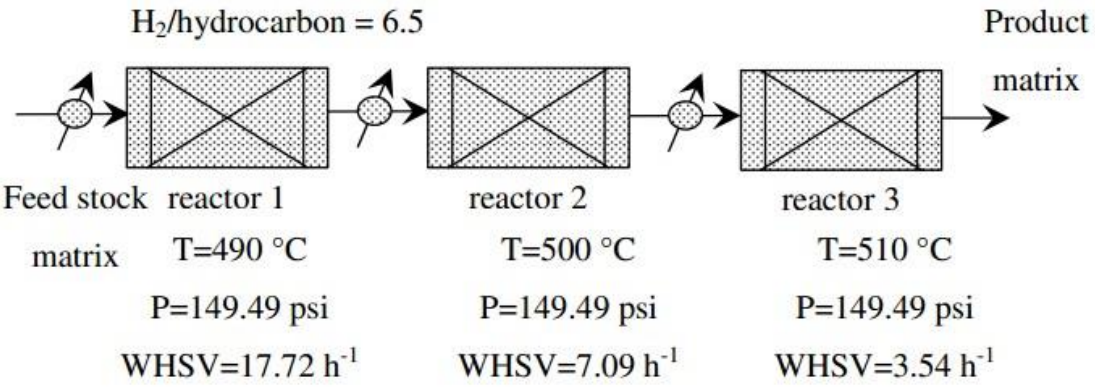

Figure 4. 4 Reaction Configuration and Operating Conditions

Before the simulation, the molecular composition is converted to bulk properties of the feedstock at the beginning. Then a new composition matrix based on homologous series and temperature is generated and listed in Table 4.10. By applying the kinetic model with regressed kinetic parameters listed in Table 4.8 for Reactor 1, the composition of stabilised reformate is transformed to the MTHS matrix and the corresponding bulk properties can be estimated sequentially.

Table 4.10 Pseudo-component based MTHS matrix of feedstock (vol%)

	Temperature in K	n-paraffins	i-paraffins	naphthenes	aromatics	vol%
PC1	282.15	0.21	0.15			0.36
PC2	293.15	1.45	2.12			3.57
PC3	313.15	1.55	2.12			3.67
PC4	333.15	1.67	2.14	0.50		4.31
PC5	353.15	2.39	2.23	2.84	0.55	8.01
PC6	373.15	3.28	3.74	3.74	2.05	12.80
PC7	393.15	5.46	7.48	3.71	2.87	19.51
PC8	413.15	6.51	8.92	3.25	3.10	21.78
PC9	433.15	4.73	6.48	2.67	2.65	16.54
PC10	453.15	2.42	3.32	2.09	1.84	9.67
PC11	464.26	0.09	0.12	0.10	0.08	0.39

The calculated properties data based on the modified MTHS method and the data

based on composition in the literature are compared in Table 4.11.

Table 4. 11 Comparison of predicted and measured properties of feed and product

	Feedstock		Absolute Error	Product		Absolute Error
Properties	Measured	Calculated		Measured	Predicted	
SG	741.46	741.33	-0.13	795.28	798.14	2.86
RVP (psi)	3.11	3.23	0.12	4.32	4.41	0.09
RON	62.76	61.69	-1.07	96.39	98.63	2.24
MON	58.95	58.40	-0.55	89.21	90.58	1.37
Benzene (vol%)	0.48	0.55	0.07	4.59	4.78	0.19
P (vol%)	69.24	68.03	-1.21	39.21	36.35	-2.86
N (vol%)	17.11	18.83	1.72	1.71	3.08	1.37
A (vol%)	13.65	13.13	-0.52	59.08	61.54	2.46

The results show a good agreement between the calculated values of this work and the data generated by correlations in the literature. The calculated composition of PNA compounds and bulk properties with the proposed model agrees reasonably well with measured information from literature. The biggest different is 2.24 in production RON prediction. Compared with the measurements, the model clearly over-predicts the conversion of paraffins, while under-predicts the conversion of naphthenes. The total amount of aromatics increases dramatically through the catalytic reforming unit as well as the RON and MON values. Approximately half of paraffins in the feedstock are converted during the process. 3.08 vol% of naphthenes remains in reformate which is initially around 18% of the reactant.

The comparison of distillation curves of the feedstock and the product are shown in Figure 4.5.

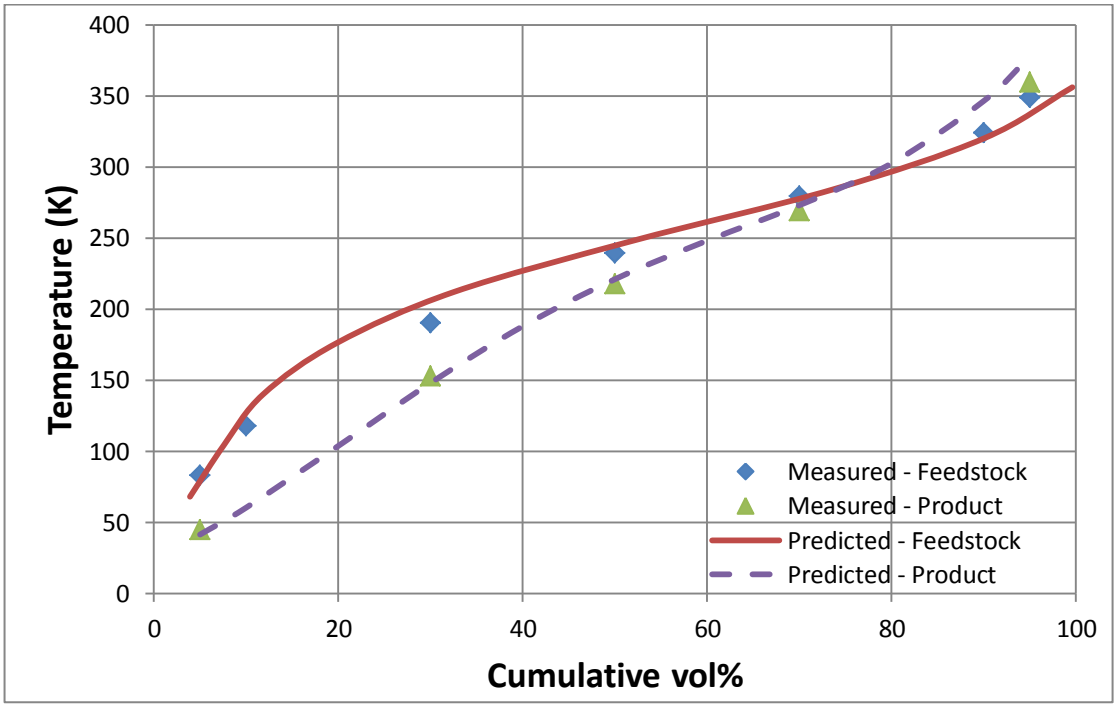

Figure 4. 5 Comparison of the feedstock distillation profile

Most of the boiling points of the two figures show good agreements of the predicted curves. But there are obvious deviations near the final boiling point of both the feedstock and the product. This deviation would be caused by the inherited correlation calculation errors or the distillation curve regression by gamma cumulative distribution.

Due to the fact that only a single operating point is available from the literature, it is not possible to regress kinetic rate constants for the reactions involved. Therefore, some inaccuracy from the predicted results is expected. In practice, such a model should always be turned by regression analysis with multiple operating points, which can improve the accuracy significantly.

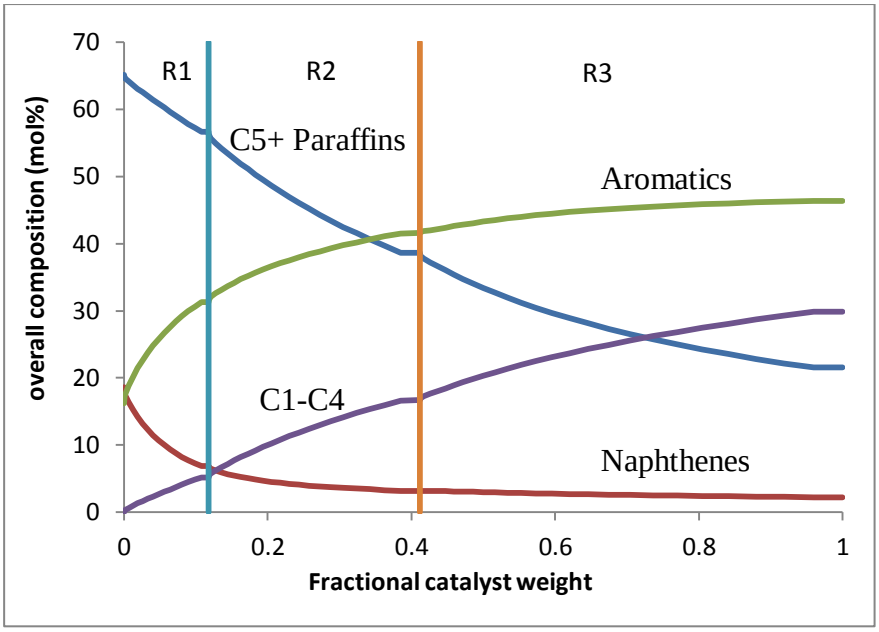

Figure 4. 6 Composition profile through the reactors

The reformate composition curves against fractional catalyst weight is shown in Figure 4.6. The left part describes the reactions occurred in reactor 1. In this reactor, formation reactions of aromatics proceed very fast. The increase speed slows down during the second and third reactors. Naphthenes reduce in the first part due to the reaction of naphthenes dehydrogenation. The amount of C5+ paraffins decreases gradually through the whole catalyst reforming procedure because of the dehydrocyclisation and cracking reactions. Cracked components show a smooth lift while the fractional catalyst weight increasing.

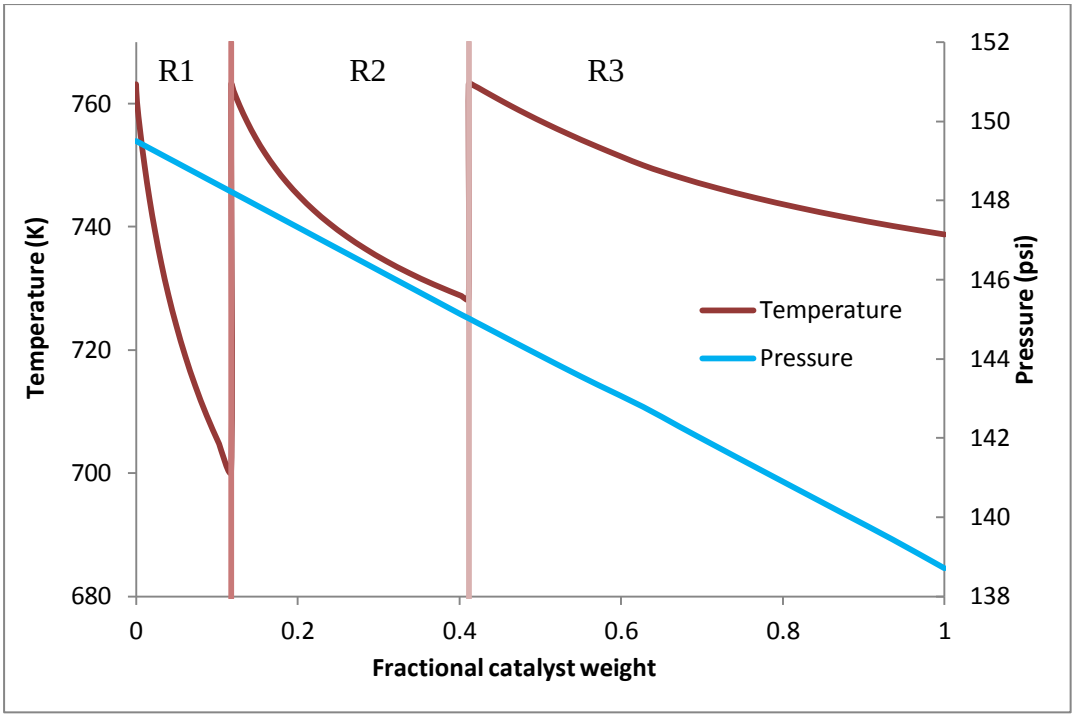

Figure 4. 7 Temperature and pressure profile under the adiabatic operating mode

Figure 4.7 shows the changing trend of temperature and pressure through reactions. As the reactions of catalyst reforming are mostly endothermic, the temperature drops in all three reactors with different rates. The major reaction taking place in the first reactor is dehydrogenation of naphthenes, which is strongly endothermic and very fast and results in a sharp decrease of reactor temperature. After reheated of the reactant, isomerisation mostly occurs in the second reactor, and causes a moderate temperature drop. The temperature drop across the last reactor is relatively low due to the cracking of paraffins and dealkylation of naphthenes and aromatics. The operating pressure decreases smoothly between continuous reactors from 149.49 psi to 138.70 psi. Overall, the predicted trends of composition profile, temperature profile and pressure profile meet the expected reaction performance of catalytic reforming processes.

4.8 Sensitivity Analysis of Operating Conditions

As mentioned before, operating condition is one of the major process variables that could heavily affect the reforming product yield and quality, as well as the catalyst life. To achieve the target of process operating optimisation, the influence on reformate yield and product ON is analysed in this section.

4.8.1 Reactor Pressure

The increasing in the reactor pressure reduces the hydrogen and reformate yield, and slightly decreases product octane number. High pressure prefers hydrocracking reaction and could slow down other reactions such as dehydrogenation, dehydrocyclisation. Figure 4.8 and Figure 4.9 show the influence of reactor pressure on product distributions, and reformate yield and quality under the reactor temperature of 783.15K, respectively.

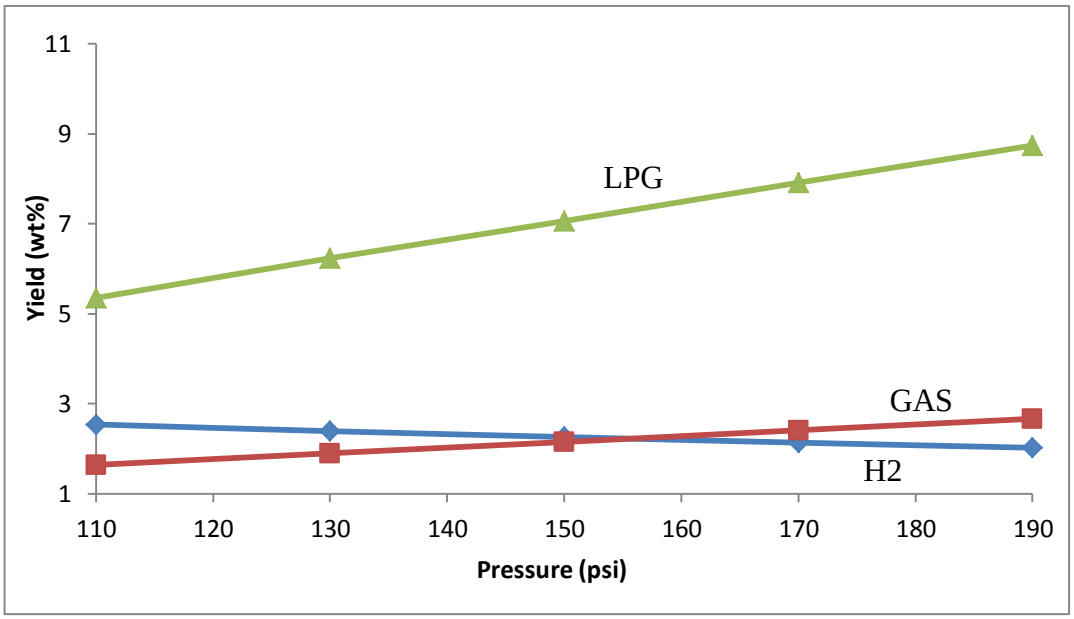

Figure 4. 8 Influence of pressure on product distribution.

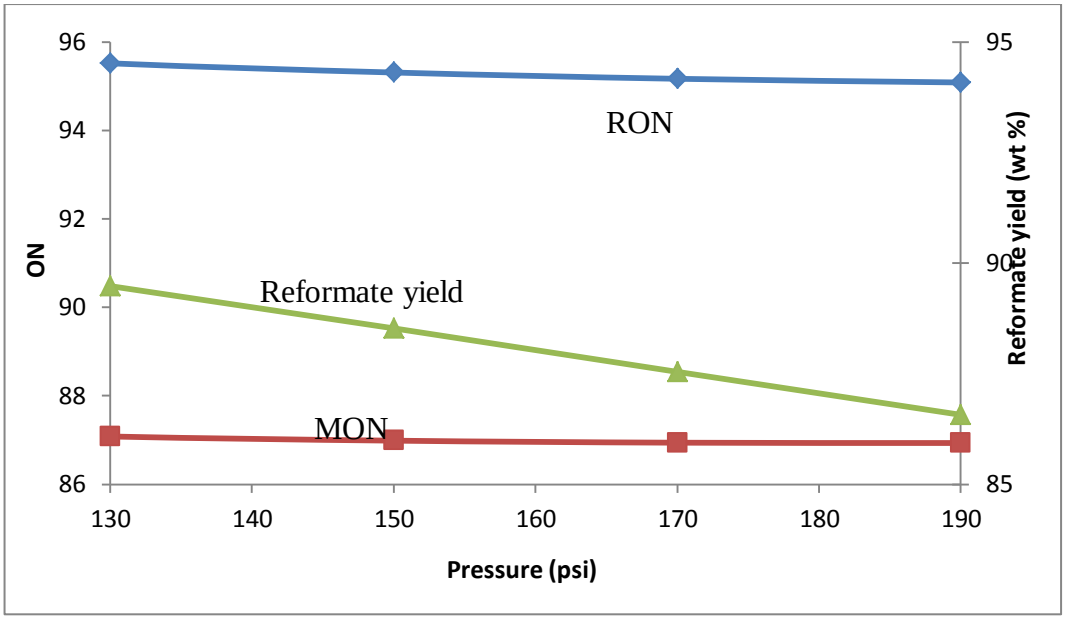

Figure 4. 9 Influence of pressure on the reformate yield and quality.

4.8.2 WHSV

To produce reformate with a certain ON, reactor temperature and space velocity are controlled together. The greater the space velocity, the higher the temperature is required. When the reactor temperature is fixed, the increase of WHSV causes the reduction in LPG, and hydrogen yield. With the increasing of WHSV, higher reformate yield can be achieve with the loss of ON. Figure 4.10 and 4.11 show the influence of WHSV on product distribution, and reformate yield and ONs, respectively.

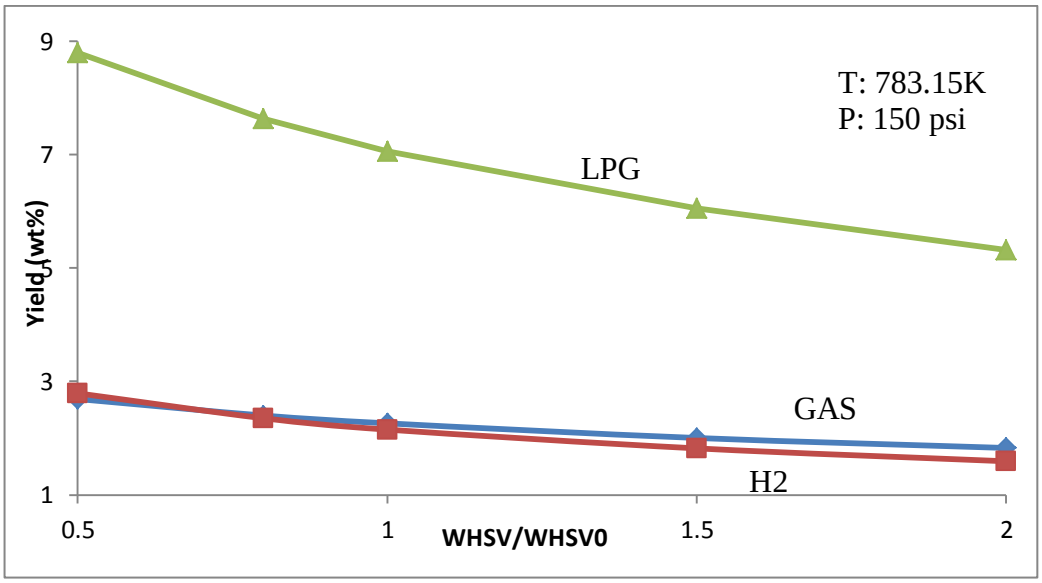

Figure 4. 10 Influence of WHSC on product distribution.

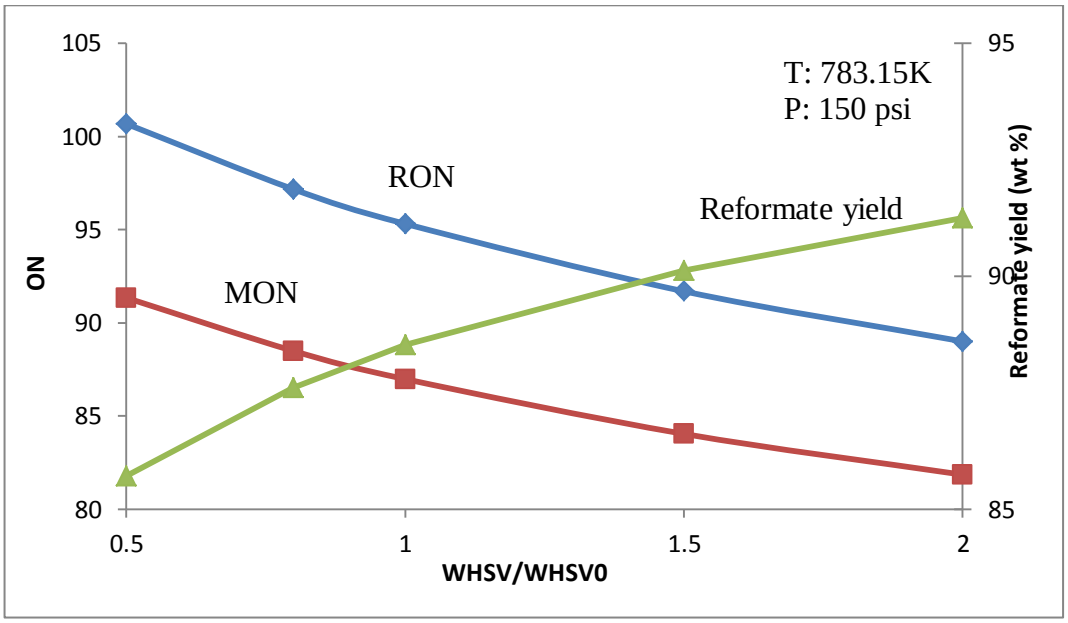

Figure 4. 11 Influence of WHSV on the reformate yield and quality.

4.8.3 Reactor Temperature

As mentioned before, the reactor temperature is the most process variable in catalytic reforming. High temperature could lead to an enhancement of ONs. All reaction rates are increased when reactor temperature is increasing. The undesired hydrocracking reaction occurs to a large extent at high temperatures and could reduce the reformate yield. Therefore, for the trade-off between reformate yield and quality, the reactor temperature is necessary to be controlled carefully. Figure 4.12 and Figure 4.13 show the influence of reactor temperature on product distribution, and reformate yield and ONs, respectively.

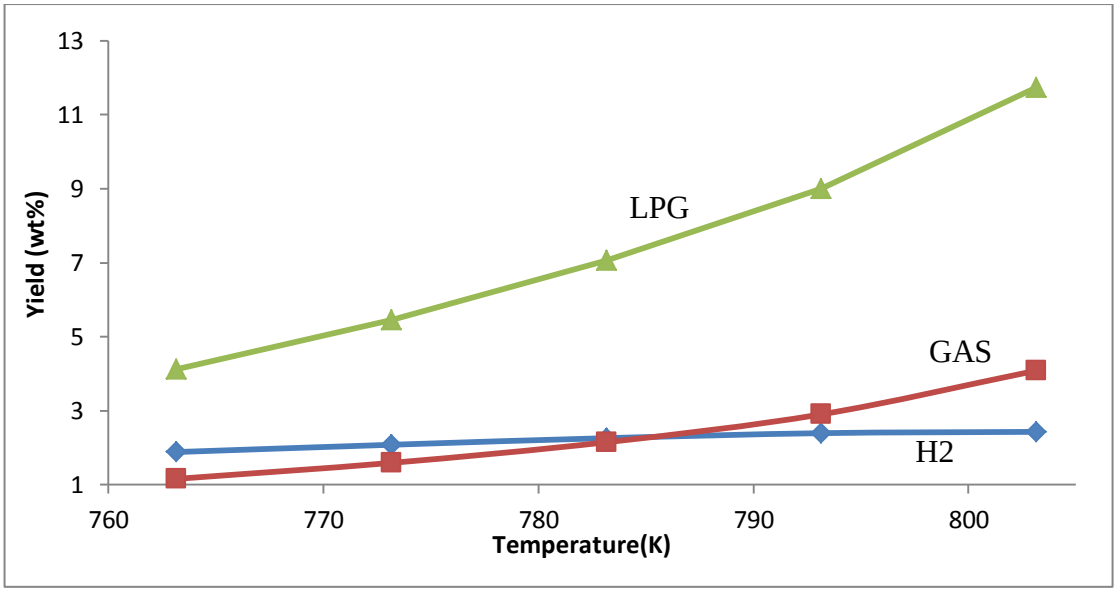

Figure 4. 12 Influence of reactor temperature on product distribution.

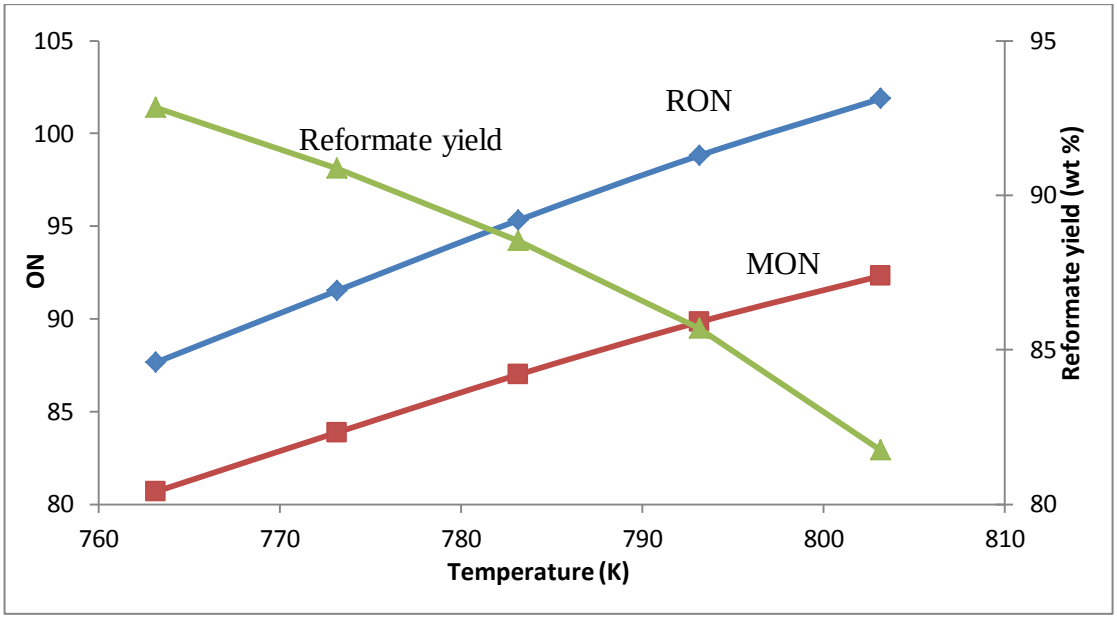

Figure 4. 13 Influence of reactor temperature on the reformate yield and quality.

From the above sensitivity analysis, it shows that the predicted results match the common understanding of the catalytic reforming mechanism. In reality, if multiple operating points are available, they can be used to turn the kinetic coefficients to improve the accuracy of model prediction.

4.9 Summary

Modified gasoline catalytic reforming kinetic and reactor models are developed based on the developed MTHS method for characterisation of naphtha feed and reformate. The model considers the most important reactions of reforming process in terms of homologous series (paraffins, naphthenes, aromatics), and provides a method to estimate inner distribution of paraffins. The temperature and pressure influence on the kinetic constants has been considered by an Arrhenius-type equation. The reactor model from Wu (2010) is incorporated in this work. A case study of a semi-regenerative unit containing three reactors has compared the result from the proposed molecular model with the measured data obtained from the literature. The case study illustrates the proposed model with acceptable accuracy.

The successful development of the MTHS-based catalytic reforming model based on existing molecular-level process models from other researchers demonstrates the flexibility of the MTHS characterisation method, shows a possibility to connect models of different refining processes from different researchers with some modifications. It also shows that an overall refinery molecular management could be achieved by adopting existing process models based on the same characterisation methodology, which can then lead to reaction and separation simulation and optimisation to be carried out on the same modelling framework.

4.10 Nomenclature

List of sets

i	component index
n	carbon number
j	reaction index

List of symbols

k	kinetic parameter of each reaction
t	time
C	concentration
T	operating temperature
E_{Aj}	activation energies
F	molar flow rate of component
$\gamma_{j,i}$	stoichiometric coefficient of component i in reaction j
ΔH_j	reaction heat of reaction j
Cp_i	specific heat capacity of component i
P	pressure
d_p	diameter of catalyst particle
ρ	density of the gas mixture
ε	void fraction of catalyst bed
μ	viscosity of the gas mixture
A_c	cross sectional area of the bed
ρ_c	density of catalyst

Chapter 5 Molecular Modelling of Gasoline Blending

5.1 Introduction

Gasoline blending is an integral part of refinery operations to convert intermediate process streams to high-value gasoline that can yield up to 60-70% of a refinery's profit. Due to the complex gasoline specifications, gasoline range fraction from a refining unit is not permitted to go to the fuel market directly, since its properties cannot meet all the requirements. Besides, different marketing locations served by a refinery may have different performance and regulatory specifications that may also be varying seasonally. And the most important, the economic requirements and multiple internal inventories need to be satisfied in gasoline manufacture. Therefore, refiners need to select optimal combinations of various intermediate streams, which are called blend recipes, to produce on-specification finished products. A simplified refinery layout related to gasoline blending is shown in Figure 5.1. The objective of gasoline blending is to find the optimal recipe meeting product demands and specifications by using available blending components at the lowest cost and maximum overall profit. Because even a small amount of feedstock saving will produce a substantial increase in profit for a refiner. For example, around $100,000 profit could be made if a refiner sells one billion gallons of gasoline per year and saves one one-hundredth of a cent per gallon (Gary and Handwerk, 2001).

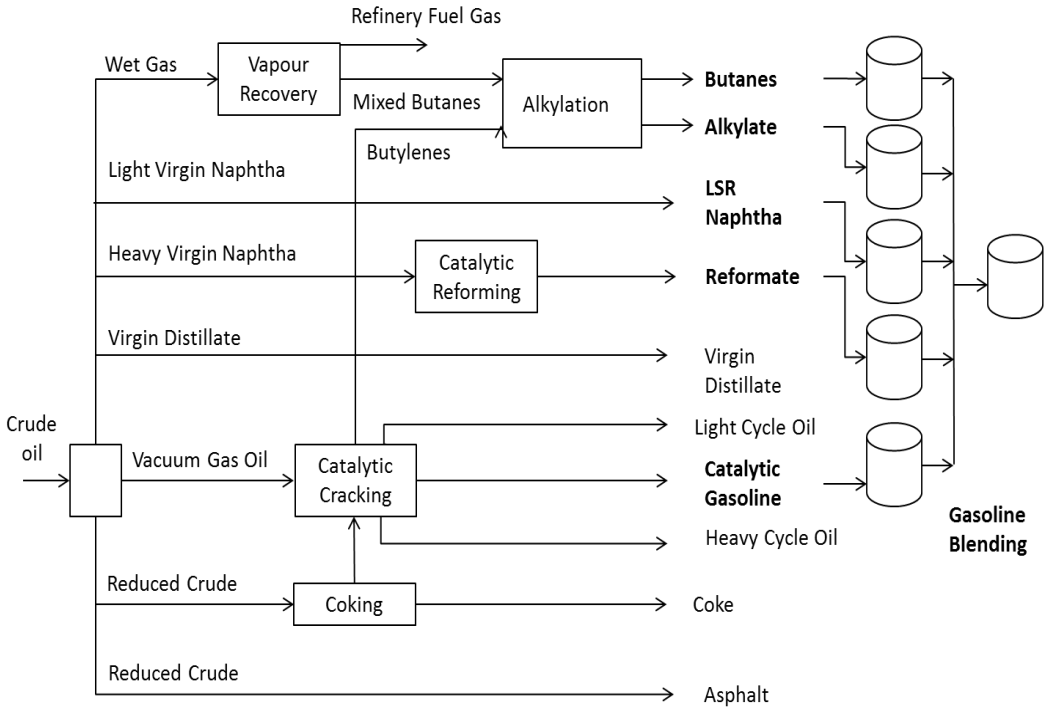

Figure 5. 1 Simplified petroleum refinery flowsheet (Gupta, 2008)

According to the flowsheet (Figure 5.1), different refining streams are blended to make final gasoline products. Only a small portion of the distillates from distillation unit can go directly to gasoline blending. Most of the outputs from distillation are sent to other processing units for upgrading. These more valuable mid-products with varying qualities are then sent to intermediate storage tanks from where they are blended into final gasoline products. A large refinery can have more than 20 blending components that are blended into several grades of gasoline (Wu, 2010). Major blending components are the products of:

- Catalytic Reforming unit
- Fluid Catalytic Cracking unit
- Isomerisation unit
- Alkylation unit
- Other units such as Visbreaking, Coking, Hydrotreating and Hydrocracker.

Apart from this, different additives such as oxygenates, antioxidants, anti-rust agents, detergents, lubricants, etc. are used to further improve the gasoline products' quality to meet the product specifications.

Our aim is to develop a common characterisation methodology that could provide a

consistent platform for each refining process and petroleum fraction. Therefore, the developed framework (Chapter 3) needs to be tested and validated with a gasoline blending model. In this chapter, a MTHS based gasoline blending model is developed and validated, and applied to a gasoline blending case.

5.2 Gasoline Product Specifications

Gasoline product specifications relate to two main factors: the environmental concerns and the internal combustion engine performance. The environmental legislations are putting more and more emphasises on air pollution, especially the impact on air quality caused by gasoline or gasoline-powered vehicles. Vehicle exhaust usually contains CO, CO_2, NO_x, VOC, SO_x and other toxics emissions. Tables 5.1 and 5.2 show the air quality standards, and it can be seen that most air pollutants in these tables can be found in vehicle exhaust.

Carbon monoxide (CO) is the result of incomplete combustion of fuel and its formation is very dependent on the air/fuel ratio. In pre-1990, oxygenates were added in gasoline to increase the amount of combustion air, but it is proven to have no effect on CO emission from newer vehicles (Aye, 2003).

Table 5. 1 U.S. Ambient Air Quality Standards (Chevron, 2009)

Criteria Pollutant	Averaging Time	Maximum Average Concentration	
		Federal Standard	California Standard
Ozone, ppm	1-hour 8-hour	– 0.075	0.09 0.070
Carbon monoxide (CO), ppm	1-hour 8-hour	35 9	20 9.0
Nitrogen dioxide (NO_2), ppm	1-hour Annual	– 0.053	0.18 0.030
Sulfur dioxide (SO_2), ppm	1-hour 24-hour Annual	– 0.14 0.030	0.25 0.04 –
Suspended particulate matter (PM_{10}), $\mu g/m^3$	24-hour Annual	150 –	50 20
Suspended particulate matter ($PM_{2.5}$), $\mu g/m^3$	24-hour Annual	35 15	– 12
Lead, $\mu g/m^3$	30-day Quarterly	– 1.5	1.5 –
Sulfates, $\mu g/m^3$	24-hour	–	25
Hydrogen sulfide, ppm	1-hour	–	0.03
Vinyl chloride, ppm	24-hour	–	0.01

Table 5. 2 European Union Ambient Air Quality Standards (Chevron, 2009)

Pollutant	Legal Nature*	Concentration, max	Averaging Period	Effective Date	Permitted Exceedences Each Years
Sulfur dioxide (SO_2), $\mu g/m^3$	Limit	350 125 20	1-hour 24-hour Annual and winter**	Jan. 1, 2005 Jan. 1, 2005 July 19, 2001	24 3 –
Nitrogen dioxide (NO_2), $\mu g/m^3$	Limit	200 40	1-hour Annual	Jan. 1, 2010 Jan. 1, 2010	18 –
Nitrogen oxides (NO_X), $\mu g/m^3$	Limit	30	Annual	July 19, 2001	–
Suspended particulate matter (PM_{10}), $\mu g/m^3$	Limit	50 40	24-hour Annual	Jan. 1, 2005 Jan. 1, 2005	35 –
		50 20	24-hour Annual	Jan. 1, 2010 Jan. 1, 2010	7 –
Lead (Pb), $\mu g/m^3$	Limit	0.5	Annual	Jan. 1, 2005	–
Carbon monoxide (CO), $\mu g/m^3$	Limit	10	Maximum daily 8-hr mean	Jan. 1, 2005	–
Benzene, $\mu g/m^3$	Limit	5	Annual	Jan. 1, 2010	–
Ozone, $\mu g/m^3$	Target	120	Maximum daily 8-hr mean	Jan. 1, 2010	25 days averaged over 3 years
Arsenic (As), ng/m^3	Target	6	Annual	Dec. 31, 2012	–
Cadmium (Cd), ng/m^3	Target	5	Annual	Dec. 31, 2012	–
Nickel (Ni), $\mu g/m^3$	Target	20	Annual	Dec. 31, 2012	–
PAH as Benzo(a)pyrene, ng/m^3	Target	1	Annual	Dec. 31, 2012	–

Carbon dioxide (CO_2) is converted from fuel combustion when the air is sufficient. CO_2 is regarded as one of the main greenhouse gases that may endanger public health or welfare.

Nitrogen Oxides (NO_x) are the generic term for several reactive gases containing nitrogen and oxygen in various ratios. Around 90 percent of NO_x emissions are man-made, in which, gasoline-powered motor vehicles contribute about 19 percent (U.S. EPA, 2002)

Exhaust VOC: The vast majority of gasoline is burned before combustion gases exit the engine in a properly operating vehicle. But a small fraction, typically 1 percent to 5 percent, escapes the combustion chamber unburned. These VOC emissions consist primarily of unburned hydrocarbons, but partially burned oxygen-containing compounds such as aldehydes are also present in small amounts. Most are removed by a vehicle's catalytic converter.

Sulphur Oxides (SO_x) are produced primarily from the combustion of fuels containing sulphur. SO2 is a moderate lung irritant. Both SO2 and NOX are major precursors to acidic deposition (acid rain).

Most hydrocarbons are nontoxic at low concentrations, with benzene a notable exception. Toxic organics related to gasoline and gasoline vehicles include benzene, formaldehyde, polycyclic organic matter (POM), 1,3-butadiene, and Acetaldehyde. Considering these issues, specifications have restricted the upper bound of some pollutant contents such as benzene and sulphur.

On the other hand, the spark-ignition engine performance is another key factor when determining the gasoline specifications. Usually a desired engine for a vehicle is the one that starts easily when cold, warms up rapidly, and runs smoothly under all conditions; delivers adequate power without knocking; with little engine deposits and uncontaminated. Some of these expectations could be met by proper vehicle design and maintenance, however, the influence of gasoline is remarkable.

For example, to enable good driveability in different seasonal, altitude, and location conditions, vapour pressure and distillation profile are restricted. Both of these properties belong to the volatility that are used to describe a gasoline's tendency to vaporise, which is a key gasoline characteristic. Gasoline that vaporises easily allows

a cold engine to start quickly and warm up smoothly. Warm-weather gasoline is blended to vaporize less easily to prevent engine vapour lock and other hot fuel handling problems.

Another characteristic of gasoline that could improve the driveability is antiknock performance. Octane number (ON) is a measure of a gasoline's antiknock performance. Gasoline with higher ON is more capable to resist knocking as it burns in the combustion chamber. There are two laboratory test methods used to measure the octane number of a gasoline: the Research octane number (RON) and the Motor octane number (MON). Improving the octane number of gasoline could result in reducing power loss of the engine, improving fuel economy, and a reduction in environmental pollutants and engine damage (Bacon et al., 2009).

Although the gasoline properties of interest are listed in Section 3.3.3, we will just list the major properties again for the sake of completeness. Blending properties taken into consideration for the gasoline range fractions are:

1. Research Octane Number (RON),
2. Motor Octane Number (MON),
3. Reid Vapour Pressure (RVP),
4. Specific Gravity/Density,
5. Boiling Point Temperature,
6. Aromatics,
7. Olefin,
8. Benzene.

5.3 Review of Researches on Gasoline Blending

There are two types of blending operations, usually referred to as batch blending and in-line blending. In batch blending, blending components are blended one at a time, whereas in-line blending simultaneously mixes all components (, 2013). To avoid the trial-and-error procedure which is costly in time and feedstocks, it is necessary to predict priori certain properties of a proposed blending. Considering refinery

operating flexibility and daily feedstock change, the prompt adjustment of blending recipes must be made, which requires a fast and accurate blending method. With modern continuous stream analysers, many refiners prefer to use computer-controlled in-line blending to blend directly to tankers and pipelines rather than batch blending (Maples, 2000; Morris, 1986; Wenzel, 1991). Also, there could be multiple combinations of blending components for a blend that meets a particular required specification. And usually there are several specifications to be satisfied. These considerations have led to linear methods for most refiners to optimise their blends in the past. However, the complex nature of blending determines that simplified blending models could not provide enough accuracy and lead to a property give-away in some cases, which could cause great economic loss, especially for octane number give-away. Besides, the stringent gasoline specifications are putting more focuses on gasoline composition that can cause difficulties in existing blending models.

The core of gasoline blending modelling is the estimation of properties. Blending properties could be classified into two categories according to their blending pattern. A blending property that could be called additive property if it is the average of that same property on each of the blending components based on a weight-, volume- or mol-fraction(Maples, 2000), or in other words could be blended linearly.

Common additive properties include (Nelson, 1958; Agrawal, 2013):

- Specific gravity based on volume fractions of blending components
- Sulphur content based on weight fractions of blending components
- Olefins, benzene, aromatic, oxygen based on mass fractions of blending components
- API gravity

On the other hand, a number of properties of interest to the refiners are not additives and need to be treated non-linearly, that include:

- Octane number (RON, MON) and Anti-Knock Index (AKI)
- Reid vapour pressure (RVP)
- Distillation points

Additive properties that blend linearly could be calculated via the following

equations:

$$P_{b,w} = \sum_i W_i P_i \tag{5.1}$$

$$P_{b,v} = \sum_i V_i P_i \tag{5.2}$$

$$P_{b,x} = \sum_i X_i P_i \tag{5.3}$$

Properties that blend non-linearly could be classified into 3 types (Agrawal, 2013) for the following reasons:

- The blended properties of components depend on some nonlinear function of the same quality (Type 1);
- The blended properties of components may depend on the same properties of other blending components (Type 2);
- The blended properties of components are highly interactive, and depend on the same and other properties of other blending components (Type 3)

For properties blended as type 1, model could linearize the blended property of blending component by converting it into corresponding blending index from the blending components firstly to allow them to be blended linearly (Aye, 2003). A simple case of blending index is presented by following flash point calculation:

$$log_{10} BI_F = -6.1188 + \frac{2414}{T_F - 42.6} \tag{5.4}$$

$$BI_B = \sum x_{vi} BI_i \tag{5.5}$$

Where BI_F represents the flash point index; T_F is the flash point in Kelvin; BI_B is the

blend flash point index, once the blend flash point index is calculated it could be used in Eq. 5.4 to calculate the blend flash point (Riazi, 2005).

For properties blended as type 2, models are further extended from type 1. An example of a type 2 blending model is given as the ASTM-D86 distillation point calculation by the ethyl equation (Ethyl Corporation, 1981):

$$D86_{XB} = \sum_{i=1}^{n} v_i BV_{xi} \tag{5.6}$$

$$BV_{xi} = C0_x + C1_x A_i + C2_x A_i^2 + C3_x A_i^3 + C4_x A_i G_i + C5_x \frac{G_i}{A_i} + C6_x \frac{G_i}{A_i^2} + C7_x G_i \tag{5.7}$$

Where $D86_{XB}$ stands for the predicted temperature at a given point X, BV_{xi} is the temperature blending value of components *i* at a desired point X, A_i is the average boiling temperature (^oC) of component *i*, G_i is the components *i* ASTM severity (T90-T10), and $C0_x - C7_x$ are the coefficients for each included D86 distillation point need to be regressed.

And type 3 nonlinear blending models are the most complex because the highly interactive nature. For example, octane numbers (RON/MON) depend on the olefin, aromatic, and benzene contents of all the blending components in the pool.

Although it may fail to provide desired accuracy, linear blending models are still widely adopted in commercial software due to the high efficiency for calculations, such as GRTMPS (Haverly Systems), PIMS (Aspen Technology), and RPMS (Honeywell Hi-Spec Solutions). Linear models could also be compatible to the overall refinery optimisation easily. However, the nonlinear nature of gasoline blending determines the difficulty for linear models to predict blending properties with high accuracy and general application for wide selection of feedstocks. And the complexity of nonlinear blending model could be handled by some methods

(Agrawal, 2013). Therefore, there is an increasing need to develop and apply more accurate non-linear models for blending optimisation, especially for some key properties such as RON, MON and RVP.

5.3.1 Octane Number

Octane Number is defined as a volume percentage of i-octane in a blend of n-heptane and i-octane, which produces the same knock intensity at the test fuel under standard test conditions in an ASTM internal combustion engine. Two types of ONs are defined by ASTM to represent the fuel performance under different working conditions. The research octane number (RON), which is evaluated using ASTM D2699 test under the conditions of slower engine speed and lower fuel/air temperature, is used to represent the fuel performance for city driving, while the motor octane number (MON) is measured using the ASTM D2700 test under the faster engine speeds and higher fuel/air temperature to represent the fuel performance for highway driving (ASTM, 1989)

Early research on the octane number of hydrocarbons showed that ONs of aromatics and branched iso-paraffins are higher than those of the corresponding paraffins (Lovell, 1931). The American Petroleum Institute (API) analysed ONs of more than 300 hydrocarbon molecules and developed several gasoline composition based correlations (ASTM, 1958; API, 1986; Scott, E, J, 1958). The nonlinear interactions between different molecular types have been firstly studied (Scott, 1958). Anderson (1972) developed a linear ON prediction method for different gasoline using 31 molecular lumps based on the gas chromatographic (GC) analysis. However, a high average error around 2.8 is shown when predicting catalytically cracked naphthas due to the shortcoming of linear ON model. Since then, Researchers have been considering the nonlinear interactions between different chemical compounds of gasoline and putting emphasis on the enhancement of reliability of ON correlations (Rusin, 1981; Habib, 1989; Cotterman, 1989). Leeuwen (1994) correlates the GC analysed gasoline composition with ON by neural networks; Meusinger (1999) and Moros (2000) used genetic algorithms and neural networks to identify partial ONs of gasoline components based on the structural elements of the molecule. Other researches on chemical composition based ON methods include Twu and Coon (1997), and Albahri (2000). Ghosh (2006) developed a detailed composition based

ON prediction model covering variety of gasoline process streams based on the analysis of 1471 gasoline fuels with 57 hydrocarbon lumps from GC analysis. The model provides an acceptable accuracy within a standard error of 1 number for both RON and MON. Parameters of Ghosh's (2006) work are further regressed by Wu (2010) which is adopted in this work. Details of the ON model could be found in Appendix 3. In this method, the nonlinear interactions between paraffins and naphthenes and between paraffins and olefins are taken into consideration.

5.3.2 RVP

Two fundamental methods for predicting blended RVP are given in Stewart et al. (1959) and Vazques-Esparragoza et al. (1992). Stewart et al. (1959) presented one of the first theoretical approaches for predicting blended RVPs. The method uses component data (such as feedstock composition and component volatility), thermodynamic relationships, and a set simplified assumptions (i.e. presence of air and water vapour are ignored, absolute pressure is taken as the RVP, volatile components are assumed to have the density of butanes, and the non-volatile components are assumed to have the thermal expansion characteristics of n-octane) to predict the blended RVP of a mixture. Vazques-Esparragoza et al. (1992) presented an iterative procedure that extended Stewart's method. In this approach, the additivity of liquid and gas volumes is assumed and a different equation of state is used.

Furthermore, the Vazques-Esparragoza et al. (1992) approach requires that the molar composition of the feedstocks to be known. The computations required in both of these methods are complex in comparison to those required in other approaches. Two empirical approaches for predicting blended RVP are the interaction method by Morris et al. (1975) and the blending index approach by Gary (1994). The interaction approach has also been applied for predicting blended RVP. It is exactly the same as for predicting blended octane numbers. Chevron Research Company developed one of the easiest empirical methods to use, which is termed as the blending index method. In this approach, blended RVP's are predicted using the Reid vapour pressure blending indices (RVPBI), which blend linearly. Haskell and Beavon (1942) proposed a method, which involves the volumetric averaging of the component, RVP's except those of butanes. They assigned variables called "blending pressure

values" to the butanes which are calculated based on the RVP of the butanes and that of the de-butanised blend (blend with all components except the butanes).

Another simple approach uses molar averaging (not volumetric) of the component RVP's based on the blend composition (Stewart, 1959). The difficulty of obtaining molar composition of feedstocks readily makes this method unattractive. Comparisons of predictive accuracy of some of the methods can be found in Stewart (1959) who looked at the standard deviation of prediction error for 67 blends using different blended RVP prediction approaches. Table 5.6 presents the reported standard deviations. The methods based on fundamental principles provide more accurate predictions. However, these theoretical methods are rather tedious due to their computational requirements. The interaction method requires numerous parameters to be updated. Although not as accurate as the theoretical methods, the simplicity of the blending index method makes it attractive for use in gasoline blending models.

Table 5. 3 A comparison of accuracy of RVP blending models

Method	Standard Deviation (psi)
Stewart (1959)	0.76
Ideal Blending	1.3
Haskel and Beavon (1942)	1.01
Molar average	1.17

In this work, the blended RVP is calculated via blending index as following:

$$RVPI_i = (RVP_i)^{1.25} \tag{5.8}$$

$$RVP_b = [\sum V_i RVPI_i]^{0.8} \quad (5.9)$$

Where $RVPI_i$ represents the Reid vapour pressure index of component i; RVP_i is the Reid vapour pressure of component i; RVP_b is the Reid vapour pressure of blend; V_i stands for the volumetric fraction of component i *(Riazi, 2005)*.

5.4 Development and Validation of MTHS Based Gasoline Blending Model

The proposed characterisation methodology provides a platform for gasoline blending to be simulated and optimised at a molecular level. By adopting the modified MTHS matrix framework, gasoline fractions used in blending could be added to form a new matrix that represents the blending product. It is important to note that only when pseudo-components are cut at the same temperatures, matrices can be added directly. Because of the lack of data, the influence of additives such as MTBE has not been taken into consideration.

The first step of the molecular-level gasoline blending model is to transfer every blending feedstock into MTHS matrix. The boiling temperature cuts and homologous series division could be determined to keep the correspondence between all blending feedstocks. As molecules are fixed in certain boiling temperature range, volume fraction values of matrix entries within the same pseudo-component temperature cut and same homologous series from different feedstock matrices can be added with its blending ratio. Therefore, a blending product matrix can be obtained.

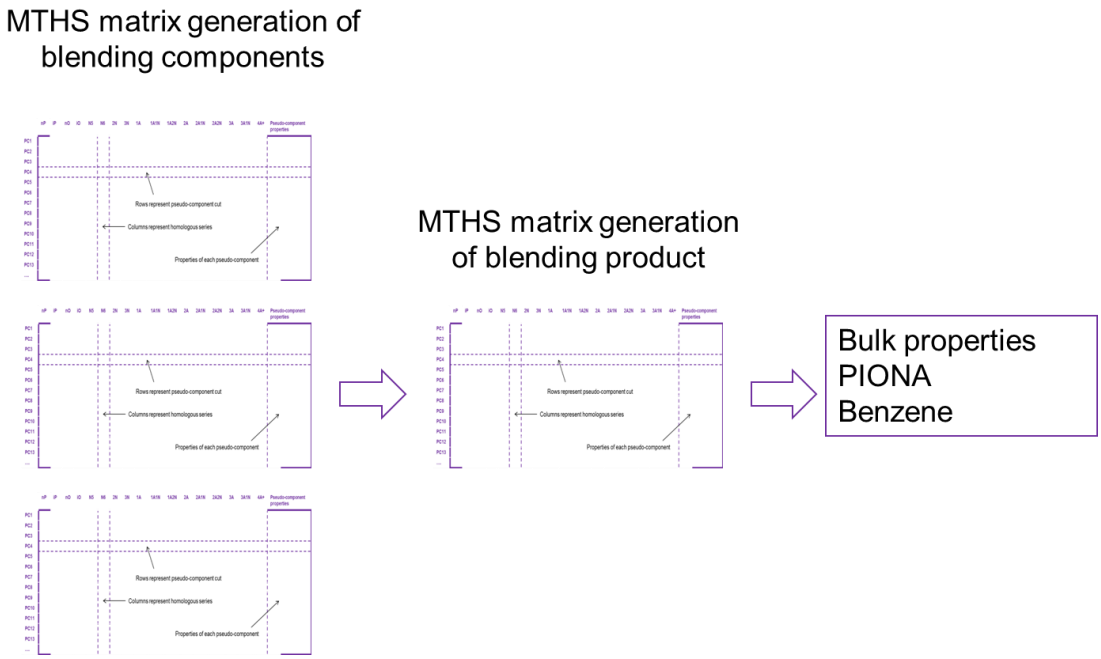

Figure 5. 2 MTHS matrix based gasoline blending method

Properties of blending products could be predicted through the proposed method from matrix composition. Blending rules used in this step for property calculation can be found in Table X.X.

5.4.1 Mathematical Model

As mentioned in the previous section, the objective of gasoline blending modelling is to produce on-specification finished gasoline products with maximum profit by optimising blending recipes with available blending feedstocks and additives. Main constraints in this problem comprise: (1) product specifications; (2) market demands; (3) feedstocks availability; (4) mass balance. As discussed before, due to the nonlinear nature of some properties in blending, the problem is formulated as an NLP model.

The mathematical model is shown as follows:

The objective function is to maximum the profit of all products:

$$\text{Profit} = \sum (F_p \times C_p) - \sum (F_j \times C_j) \qquad (5.10)$$

where subscript p represents blending product; subscript j represents blending

feedstock; F is the volume of product/feedstock; and C is the price of product/feedstock.

Subject to:

(1) Product specifications:

$$\theta_{p,k} = f(\theta_{j,k}, x_{i,j}) \tag{5.11}$$

$$\forall i \in \text{PIONA}, \forall j \in J, \forall k \in \theta$$

$$\theta_{p,k}^{min} \leq \theta_{p,k} \leq \theta_{p,k}^{max} \tag{5.12}$$

$$\forall p \in P, \qquad \forall k \in \theta$$

(2) Market demands:

$$F_p^{min} \leq F_p \leq F_p^{max} \tag{5.13}$$

(3) Feedstock availability:

$$F_j^{min} \leq F_j \leq F_j^{max} \tag{5.14}$$

(4) Mass balance:

$$F_p = \sum F_{j,p} \tag{5.15}$$

$$F_j = \sum F_{j,p} \tag{5.16}$$

where subscript p represents blending product; subscript j represents blending feedstock; F is the volume of product/feedstock.

5.4.2 Validation of MTHS Based Gasoline Blending Model

A verification case from an Asian refinery is studied to show the accuracy of properties prediction of blending products. Three blending components are mixed together to produce the gasoline product. Blending feedstock 1 is an alkylate stream, feedstock 2 is an H/S LCN stream, and feedstock 3 is a raffinate stream. Measured bulk properties of blending components and gasoline product, including RON, MON, RVP, density, D86, Olefin, Aromatic, and Benzene contents as well as blending ratio, are shown in Table 5.4. To illustrate the proposed methodology, matrices of all blending components are established and mixed together to form the product matrix. Once the product matrix is obtained, bulk properties of the blending product can be calculated by the proposed methodology. The calculated properties are compared with the measured properties of blending product to show the feasibility of the model of gasoline blending recipe simulation.

Table 5. 4 Measured properties of blending components and product

	Feed1	Feed2	Feed3	Product	Predicted	Absolute error	Relative error %
RON	95.6	92.6	75.0	93.7	92.6	1.1	1.2
MON	88.0	82.0	74.0	81.7	82.7	1.0	1.2
RVP(kPa)	32	63	70	59	59	0.0	0
Density 15^{o}C, kg/L	701.2	732.8	670.3	735.2	725.9	9.3	0.3
IBP ^{o}C	38.0	32.9	34.7	N/A	30.1		
10% ^{o}C	82.6	51.6	51.6	53.0	53.07	0.1	0.1
50% ^{o}C	106.8	93.3	64.0	93.9	93.5	0.4	0.4
90% ^{o}C	136.6	161.6	78.5	169.9	159.5	1.4	0.8
FBP ^{o}C	215.6	189.5	95.5	196.8	199.07	2.3	1.2
Olefins content (vol%)	0.17	38.90	4.80	32.30	32.20	0.1	0.3
Aromatics content (vol%)	0.19	20.04	3.00	21.80	24.10	2.3	10.6
Benzene content (vol%)	0	0.88	3.00	N/A	0.85		
Blending ratio	12.85	83.25	3.90				

The recipe simulation result is listed in Table 5.4. In addition, the errors are given in Figure 5.3 to illustrate the prediction accuracy of proposed MTHS based gasoline blending model and the linear model. Compared the predicted properties with measured values, an acceptable precision could be seen. The proposed model is better in most properties prediction. Results from the linear model are slightly better when predicting MON, density, and T50 boiling point, but the differences of relative

error are less than 1%. The validation illustrates the reliability of the proposed model, and the applicability will be illustrated in a gasoline blending recipe optimisation with a case study in Section 5.5.

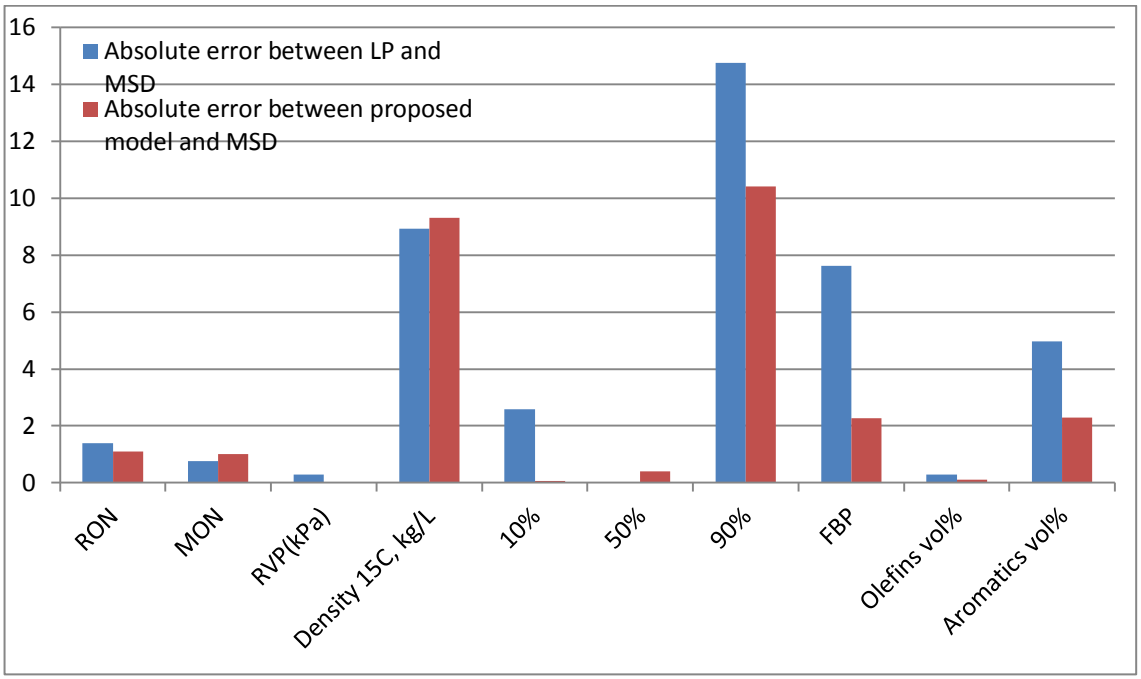

Figure 5. 3 Comparison of the validation results

In practice, the model coefficients in the matrix transformation are normally further tuned by carrying out a series of lab tests to obtain more accurate molecular information, before the model is applied for new predictions. With that, it is expected that the accuracy level for the MTHS method will be significantly improved.

5.5 Case Study

To demonstrate the effectiveness of the proposed blending model, blending feedstocks used in Section 5.4 are chosen for case study in this section. These 3 feedstocks are blended to produce a finished gasoline product with the listed specifications shown in Table 5.6. We assume that there is no feedstock cost, and streams not used in blending could be sold to the market with the price listed in Table5.5.

Table 5. 5 Assumed feedstock availability and price

	Availability (t)	Price ($)
Stream 1	500	1129/t
Stream 2	500	967/t
Stream 3	500	484/t

Table 5. 6 Product specifications

	RON^{lo}	MON^{lo}	RVP^{up} (psi)	A^{up} (v%)	$Olefin^{up}$ (v%)	$Benzene^{up}$ (v%)	Price ($)
Product	93	81	60	25	15	0.8	1048/t

By adopting the proposed method, a reasonable blending recipe is generated to fulfil all constraints and property boundaries. The recipe based on the proposed method is shown in Table 5.7 with the one based on linear blending model.

Table 5. 7 Comparison of generated blending recipes

	Stream 1	Stream 2	Stream 3
Availability (t)	500	500	500
Blending quantity (t)	500	364	85
Blending quantity (t) (Linear)	500	500	61

The product properties and profit predicted by the MTHS based model and linear blending model are compared in Table 5.8. The profit is calculated by the price of

product and feedstock sold to the market. The result demonstrates the feasibility and capability to optimise the blending recipe within the constraints and make more profit.

Table 5. 8 Comparison of predicted product properties and profit

	RON	MON	RVP (psi)	A (v%)	Olefin (v%)	Benzene (v%)	Output (t)	Profit ($)
Product	93.13	84.59	47.84	7.83	15.00	0.61	949.69	1.33E+6
Product (Linear)	93.00	84.37	48.80	9.7	18.69	0.59	1061.12	1.32E+6

From the results, it can be seen that the maximum olefin content becomes the limiting constraint when using the MTHS based method, while it is the minimum RON that becomes the limiting constraint for the linear model. This observation shows that it is very important to use accurate blending models to avoid economic losses.

5.6 Summary

Product blending is one of the most important steps in refining operation. Most refining products are blended from intermediate process streams. Due to the varying properties of blending components from upstream units and tightened product specifications, the problem of product blending becomes more and more challenging for modern refiners. Therefore, it is necessary to make sure that the developed molecular characterisation framework can be applied to product blending.

An application of the proposed characterisation methodology has been illustrated by the developed gasoline blending model with a validation case in this chapter. The proposed model is applied to a gasoline blending case to show its feasibility and benefits. An acceptable accuracy has been reached in prediction of blending product properties such as RON, MON, RVP, density, D86 and key components of olefins, aromatics and benzene. The successful implementation of the developed

characterisation method for gasoline blending, together with its implementation to process modelling shown in Chapter 4, demonstrates that it can be used as a common platform to simulate and optimise refining operation at the molecular level.

5.7 Nomenclature

List of sets

i	blending component for blending index calculation
j	blending feedstock
p	blending product
k	properties

List of symbols

BI_F	blending index of flash point
T_F	flash point
$RVPI_i$	Reid vapour pressure index of component i
RVP_i	the Reid vapour pressure of component i;
RVP_b	Reid vapour pressure of blend
V_i	volumetric fraction of component i
F	volume of product/feedstock
C	price of product/feedstock

Chapter 6 Conclusions and Future Work

6.1 Conclusions

In this work, a non-experimental characterisation methodology is developed to obtain molecular level information of light petroleum fractions by using the basis of the MTHS matrix framework. Both the matrix representation methodology and transformation methodology are enhanced by this method. By adopting the pseudo-component approach and embedding chemistry information into it instead of using carbon number in the matrix framework, the matrix can be easily extended to heavier fractions without the loss of accuracy, and become more compatible for general process modelling applications. The statistic distribution is also an improvement of the previous approach, which highly improves the usability of the modified method. The pseudo-component based characterisation method provides a consistent platform for modelling refining processes from distillation units to reactors, and could be further linked with petrochemicals.

A molecular level model of catalytic reforming process has been developed based on the proposed characterisation approach in this work. A modified kinetic network of the CR reaction is illustrated to incorporate the modified MTHS matrix and the effects of operating temperature and pressure. The re-regressed kinetic model is employed in a reactor model and validated with a case study of a semi-regenerative reforming process. Besides, influences of operating conditions such as reactor pressure, space velocity and reactor temperature are analysed. The successful practice shows the possibility of the incorporation of different refining process models for reaction and separation by the same characterisation basis.

The characterisation method is also adopted in the proposed gasoline blending model to show its applicability. The successful implementation of the pseudo-component based MTHS method to gasoline blending, together with the successful development of the catalytic reforming model shows that it is now possible to adopt the new MTHS method as the common basis for overall refinery modelling and simulation.

6.2 Future Work

Up to now, the characterisation method has been developed based on Pseudo-component concept and homologous series type matrix and further combined with a catalyst reforming model and a gasoline blending model.

There are still many aspects could be explored to improve and expand the content in the thesis. As the first level of molecular management, the proposed molecular characterisation method could be extended to heavier petroleum fractions. Although the developed MTHS method is applied to a diesel range fraction, the influence of heteroatoms has not been studied, which is crucial in heavy petroleum characterising and processing.

Beside, a series of refining processes is waiting ahead for modelling based on the new MTHS method, such as hydrotreating, catalytic cracking, etc. Due to the importance of blending operation in a modern refiner, blending models, such as diesel blending and crude oil blending, are necessary to develop.

The eventual objective is to set up an overall refinery model based on the new MTHS method to achieve the molecular management in refinery simulation and optimisation.

Abbreviations

ADU	atmospheric distillation unit
AKI	anti-knock index
API	American Petroleum Institute
ASTM	America society of testing and measurements
BTX	benzene, tolunen, xylene
CARB	California Air Research Board
CCI	calculated Cetane index
DBE	double bond equivalent
DOF	degree of freedom
EOS	equations-of-state
FBP	final boiling point
FCC	fluidised catalytic cracking
GC	gas chromatography
HEI	Health effects institute
HPLC	high performance liquid chromatography
HDS	hydrodesuphurised
IBP	initial boiling point
LCO	light cycle oil
LHSV	liquid hourly space velocity
LP	linear programming
LPG	liquefied petroleum gas
MCP	methyl cyclopentane
MMT	Methylcyclopentadienyl Manganese Tricarbonyl
MON	motor octane number
MS	mass spectroscopy
MTHS	molecular type homologous series
NLP	non-linear programming
NMR	nuclear magnetic resonance
PC	pseudo-component

PDF	probability density function
PIONA	normal paraffin, iso-paraffin, olefin, naphthene, aromatic
RON	research octane number
RVP	Reid vapour pressure
SARA	saturates, aromatics, resins, and asphaltenes
SRGO	straight-run gas oil
SRN	straight-run naphtha
TBP	true boiling point
VGO	vacuum gas oil
VOC	volatile organic compound
VR	vacuum residue
WHSV	weight hourly space velocity

References

A Grade Premium Unleaded Gasoline Specifications, Megallan, 2014. Web. 08 Apr. 2015 <https://www.magellanlp.com/uploadedFiles/Commercial_Info_Assets/Product_Pipeline_Specifications/A%20GRADE%20PREMIUM%20UNLEADED%20GASOLINE.pdf>

A Primer on Gasoline Blending, EPRINC, 2009, Web. 08 Apr. 2015 http://eprinc.org/2009/06/a-primer-on-gasoline-blending/

Agrawal, S.S., Fuel Blending Technology and Management, Chapter 19, in the book: Riazi, M. R., Eser, S., Agrawal, S., Pena Diez, J. L. ,Petroleum Refining and Natural Gas Processing, ASTM MNL58, ASTM International, 2013.

Ahmad, M.I., Integrated and multi-period design of diesel hydrotreating process, Ph.D. Thesis, University of Manchester, 2009

Albahri, T.A., Structural Group Contribution Method for Predicting the Octane Number of Pure Hydrocarbon Liquids, Ind. Eng. Chem. Res, 42, 657, 2003

Albahri, T.A., Molecularly Explicit Characterization Model (MECM) for Light Petroleum Fractions. Industrial & Engineering Chemistry Research, 44, pp9286 – 9298, 2005

Altgelt, K.H., Boduszynski, M.M., Composition and Analysis of Heavy Petroleum Fractions, Chemical Industries, Vol.54, 1994

Anderson, P. C.; Sharkey, J. M.; Walsh, R. P. Calculation of Research Octane Number of Motor Gasolines from Chromatographic Data and a New Approach to Motor Gasoline Quality Control.J. Inst. Pet., 59, 83, 1972

Ancheyta, J., Aguilar,R. Oil Gas J., Jan. 31, 93-95, 1994

Ancheyta, J., Kinetic Modelling of Naphtha Catalytic Reforming Reactions, Energy & Fuels, 14,1032-1037, 2000

Ancheyta, J., Modelling and simulation of catalytic reactors for petroleum refining, Wiley & Sons, New Jersey, 2011

Athier, G., Floquet, P., Pibouleau, L., Domenech, S., Process optimization by simulated annealing and NLP procedures Application to heat exchanger network synthesis, Computers & Chemical Engineering 21, S475-S480, 1997

Aye, M., Molecular modelling for cleaner fuel production, Department of Process Integration, UMIST, Manchester, 2003

Aye, M. S., Zhang, N., A Novel Methodology in Transformation Bulk Properties of Refining Streams into Molecular Information, Chem. Eng. Sci., 60, pp6702-6717, 2005

Bacon, J.; et al., Motor Gasolines Technical Review, Chevron, 2009

Behrenbruch, P., Dedigama, T., Classification and Characterisation of Crude Oils Based on Distillation Properties, Journal of Petroleum Science and Engineering, 57: 166-180, 2007

Boyoung P., Correlation of Breast Cancer Incidence with the Number of Motor Vehicles and Consumption of Gasoline in Korea, Asian Pac J Cancer Prev, 15 (7), 2959-2964 , 2014

Campbell, D.M., Stochastic modelling of structure and reaction in hydrocarbon conversion, Ph.D. Thesis, University of Delaware, Newark. 1998

Cordes, W., Rarey, J., A New Method for the Estimation of the Normal Boiling Point of Non-electrolyte Organic Compounds, Fluid Phase Equilibria, 201 :409-433, 2002

Constantinou, L., Gani, R., O'Connell, J.P., Estimation of the acentric factor and the liquid molar volume at 298 K using a new group contribution method. Fluid phase Equil., 104: 11, 1995

Cotterman, R.L., Bender, R., Prausnitz, J.M., Phase equilibria for mixtures containing very many components-development and application of continuous thermodynamics for chemical process design, Ind. Eng. Chem. Process Des. Dev. 24, 194-203, 1985

Chang, A., Pashikanti, K., Liu, Y.A., Refinery Engineering, Wiley-VCH Verlag & Co. KGaA, Germany, 2012

Chen, J. W., Process and Engineering of Fluid Catalytic Cracking, Chinese Petrochemical Publisher: China, 1995

Christensen, G., Apelian, M. R., Hickey, K. J., and Jaffe, S. B., Future directions in modelling the FCC process: an emphasis on product quality. Chem. Eng. Sci. 54:2753-2764, 1999

EPA, Air Trends September 2003 Report: National Air Quality and Emissions Trends Report, 2003 Special Studies Edition, U.S., 2003

EPA, Integrated Science Assessment for Particulate Matter (Final Report), U.S. Environmental Protection Agency, Washington, DC, EPA/600/R-08/139F., 2009

Flory, P.J., Molecular size distribution in linear condensation polymers. J. Am. Chem. Soc., 58, 1877. 1936

Froment, G.F., Modelling of Catalytic Reforming Unit; Chem.Eng.Sci., 42,1073-1087,1987

Froment, G., Bischoff, K., Chemical Reactor Analysis and Design. 2nd edition: John Wiley & Sons, Singapore, 1990

Gary, J., Handwerk, G., Petroleum refining technology and economics, 4th edition, McGraw-Hill, New York, 1979

Gary, J. H., Handwerk, G. E., Petroleum Refining Technology and Economics, 3rd Edition Marcel Dekker, Inc., New York, 1994

Giechaskiela, B., 1, Maricqb, M., Ntziachristosc, L., Dardiotisd, C., Wange, X.L., Axmannf, H., Bergmanna, A., Schindlerg, W., Review of motor vehicle particulate emissions sampling and measurement: From smoke and filter mass to particle number, Journal of Aerosol Science, Volume 67, Pages 48–86, 2014

Glinzer, O., General Vapor Pressure Correlation for N-Alkanes: With Applications for Simulated Distillation Extension to Characterization of Technical Distillation Residue. Erdoel and Kohle, 38, 5, 213-220. 1985

Gomez-Prado, J., Zhang, N., Theodoropoulos, C., Characterisation of Heavy Petroleum Fractions Using Modified Molecular-type Homologous Series (MTHS) Representation, Energy, 33: 974-987, 2008

Gray, R.D. Jr., Heidman, J.L., Springer, R.D., Tsonopoulos, C., Characterisation and Property Prediction for Heavy Petroleum and Synthetic Liquids, Fluid Phase Equilibrium, 53: 355-376, 1989

Haagen-Smit, A. J., Fox, M. M., Ozone Formation in Photochemical Oxidation of Organic Substances, Industrial & Engineering Chemistry 48 (9), 1484-1487, 1956

Hay, G., Loria, H., Satyro, M. A., Thermodynamic Modelling and Process Simulation through PIONA Characterisation, Energy Fuels, 27, 3578−3584, 2013

Henningsen, J., Bundgaard, N.M., Chem. Eng., 15, 1073-1087, 1970

Heck, R. H., Contribution of Normal Paraffins to the Octane Pool. Energy Fuels, 3, 109, 1989

HEI, Understanding the health effects of ambient ultrafine particles, HEI Perspectives 3 Health Effects Institute, Boston, Massachusetts, 2013

Hou, S., Long, J., Zhang, N., Molecular reconstruction model of vacuum gas oil I model estimation, Shiyou Xuebao, 28, 6, 889-894, 2012

Hu, S., Zhu, X.X., A general framework for incorporating molecular modelling into overall refinery optimisation, Applied Thermal Engineering, 21, 1331-1348 , 2001

Hu, S., Zhu, X.X., Molecular Modelling and Optimisation for Catalytic Reforming. Chem. Eng. Commun., 191, 500-512, 2004

Ingber, L., Very fast simulated Re-annealing, Math Comput. Modelling, 12, 967-973, 1989

Jabr, N., Alatiqi, I. M., Fahim, M. A., An Improved Characterization Method for Petroleum Fractions, Can. J. Chem. Eng., 70, pp765 – 773, 1992

Jaffe, S. B., Control of Gasoline Manufacture. U.S. Patent 4, 251,-870, 1981

Jenkin, J.H., Stephens, T.W., Kinetics of catalytic reforming. Hydrocarbon Proc., 1(59), 163-167, 1980

Joback, K.G., A unified approach to physical property estimation using multivariate statistical techniques, S.M. Thesis, Department of chemical engineering, Massachusetts Institute of technology, Cambridge, MA,1984

Joback, K.G., Reid, R.C., Chem. Eng. Comm., 57, 233, 1987

Katz, D.L., Brown, G.G., Vapour pressure and vaporization of petroleum fractions, Ind. Eng. Chem., 25,1373-1384,1933

Kirkpatrick, S., Gellat, C.D., Vecchi, M.P., Optimisation by simulated annealing. Science, 220,671-680, 1983

Klein, M.T., Molecular modelling in heavy hydrocarbon conversions, CRC/Taylor & Francis, 2006

Kmak, W.S., A kinetic simulation model of the power forming process, AIChE Meeting, Houston, TX, 1972

Knock characteristics of motor fuels by the research method, American Society for Testing and Materials Test Method D2699, American Society for Testing and Materials, West Conshohocken, PA, 1989

Knocking characteristics of pure hydrocarbon, Special Technical Publication No. 225; American Society for Testing and Materials, West Conshohocken, PA, 1958

Korsten, H., Characterization of hydrocarbon systems by DBE concept. AIChE J., 43, 6, 1559-1568, 1997

Krane, H.G., Groh,A.B., Shulman,B.D., Sinfelt,J.H., Reactions in Catalytic Reforming of Naphthas, Proceedings of the 5th world petroleum congress, 39-51,1959

Li, S., WANG, B.C, HE, J., The U.S. refining industry's status and outlook , PetroChina International Co., Ltd. International Petroleum Economics, 2013

Liguras, D.K., Allen, D.T., Interfacing structural characterisations and kinetic models: a case study using FCC. Poster at the Engineering Foundation Conference on Chemical Reaction Engineering, Santa Barabara, California, March, 1987

Lin, S., Petroleum Refining Engineering, 3rd Ed. Petroleum Industry Press, Beijing, 2000

Lovell, W. G., Campbell, J. M., Boyd, T. A., Detonation Characteristics of Some Aliphatic Olefin Hydrocarbons, Ind. Eng. Chem. 23, 555, 1931

Lugo, H. J., Ragone, G., Zambrano, J., Correlations between Octane Numbers and Catalytic Cracking Naphtha Composition, Ind. Eng. Chem. Res, 38, 2171, 1999

Maples, R. E., Petroleum Refinery Process Economics, 2nd Ed. Penn Well Corporation, Tulsa, 2000

Marafi, A., Al-Hendi, A., Al-Mutawa, A., Stanislaus, A., Studies on hydrotreating of diesel streams from different Kuwait crudes for ultralow sulfur diesel production, Energy & Fuels, 21, pp3401-3405, 2007

Marin, G.B., Froment, G.F., The Development and Use of Rate Equations for Catalytic Refinery Processes, EFCE Publ. Ser., Vol 2. , No.27, C 117, 1983

Marrero-Marejon, J., Pardillo-Fontdevila, E., AIChE J., 45:615, 1999

Metropolis, N., Rosenbluth, A., Rosenbluth, M., Teller, A., Teller, E., J. Chem. Phys. 21, 1087, 1953

Meusinger, R., Moros, R., Determination of quantitative structure octane rating relationships of hydrocarbons by genetic algorithms, Chem. Intell. Lab. Syst, 46, 67, 1999

Meusinger, R., Moros, R., Determination of octane numbers of gasoline compounds from their chemical structure by 13C NMR spectroscopy and neural networks, Fuel, 80, 613, 2001

Meyer, R.A., Handbook of Petroleum Refining Processes. 3rd edition, McGraw-Hill, 2004

Morris, W.E., Oil& Gas Journal, September 8, pp.112-114, 1986

Motor Gasoline Technical Review, Chevron, 2009. Web, 08 Apr. 2015 <http://www.chevron.com/documents/pdf/MotorGasTechReview.pdf>

Petroleum Refining, Encyclopædia Britannica. Encyclopædia Britannica Online, Encyclopædia Britannica Inc., 2015, Web. 08 Apr. 2015 <http://www.britannica.com/EBchecked/topic/454440/petroleum-refining/81813/Gasoline-blending>.

Peng, B., Molecular modelling of petroleum processes. Ph.D. Thesis, University of Manchester Institute of Science and Technology, 1999

Poling, B. E.; Prausnitz, J. M.; O'Connell., The Properties of Gases and Liquids. 5th ed., McGRAW-HILL, New York, 2001

Quann, R.J., Modelling the chemistry of complex petroleum mixtures, Environmental Health Perspectives 106 (6), 1441-1448, 1998

Read, R.C., The Enumeration of Acyclic Chemical Compounds, Chemical Applications of Graph Theory, A.T. Academic Press, Inc., 1976

Riazi, M. R., and Daubert, T.E., Characterisation parameters for petroleum fractions, Industrial and engineering chemistry research, Vol. 26, 755-759, 1987

Riazi, M. R., Characterization and Properties of Petroleum Fractions, ASTM, 2005

Refinery capacity report, U.S. Energy Information Administration, June 2013

Reliance commissions world's biggest refinery, The Indian Express, December 26, 2008

Rodriguez,M.A., Ancheyta,J., Detailed description of Kinetic and Reactor Modelling for Naphtha Catalytic Reforming. Fuel, 90, 3492-3508, 2011

Rose, L.M., Distillation Design in Practice. Elsevier, New York, 1985

Rossini, F.D., Chemical Thermodynamics, Wiley, New York, 1950

Rusin, M.H., Chung, H.S. and Marshall, J.F., "A transformation method for calculating the research and motor octane numbers of gasoline blends".Ind. Eng. Chem. Fund., (20) 1981

Sasano,Y., Measuring method of research octane number of gasoline by gas chromatograph and its apparatus, JP Patent 09-318613, 1997.

Scott, E. J. Y., Knock Characteristics of Hydrocarbon Mixtures.Proc. API DiV. Refin. 1958, 38, 90, 1958

Shariati, A., Peters, C.J., Moshfeghian, M. A systematic approach to characterize gas condensates and light petroleum fractions, Fluid Phase Equilibria, 154 (2), 165-179, 1999

Sull, D.R. Westrum, E.F and Sinke, G.C., The chemical Thermodynamics of organic compounds, Wiley, New York, 1969

Smith, J.M., Van Ness, H. C., Abbott, M.M., Introduction to Chemical Engineering Thermodynamics, Mc-Graw Hill, 5th Ed., New York, 1996

Smith, R.B., Kinetic analysis of naphtha reforming with platinum catalyst. Chem. Eng. Prog., 55(6), 76-80, 1959

Sotelo-Boyas, R., Froment, G.F., Fundamental Kinetic Modelling of Catalytic Reforming, Ind. Eng. Chem. Res., 48, 1107-1119, 2009

Speight, J. G., The Chemistry and Technology of Petroleum, 3rd ed., Marcel Dekker, New York, 1998

Statistical Review of World Energy 2013, BP, 2013
http://www.bp.com/en/global/corporate/about-bp/energy-economics/

Sun, J., Molecular modelling and integration analysis of hydroprocesses, PhD thesis, University of Manchester, 2004

Table European Union specifications for gasoline (Official Journal of the European Communities)

Table Clean Air Act and CARB specifications (U.S.A.)

Taskar, U., Riggs, J.B., Modelling and optimization of a semiregenerative catalytic naphtha reformer, AIChE J. 43, pp740–753, 1997

Teng, S.T., Williams, A.D., Urdal, K., Detailed hydrocarbon analysis of gasoline by GC-MS (SI-PIONA). Journal of High Resolution Chromatography 17, 469-475, 1994

Twigg, M. V., Progress and future challenges in controlling automotive exhaust gas emissions， Applied Catalysis B: Environmental Volume 70, Issues 1–4, 31 January, Pages 2–15, 2007

Twu, C. H., Coon, J. E., Estimate octane numbers using an enhanced method, Hydrocarbon Process, 76, 65, 1997

Van, G., Hudebine, D., Reyniers, M.F., Wahl, F., Verstraete, J.J., Marin, G.B., Molecular reconstruction of naphtha steam cracking feedstocks based on commercial indices. Comput. Chem. Eng. 31, 1020-1034, 2007

Van Leeuwen, J. A., Jonker, R. J., Gill, R., Octane number prediction based on gas chromatographic analysis with non-linear regression techniques, Chem. Intell. Lab. Syst., 24, 325, 1994

Washington, D.C., API Technical Data Book on Petroleum Refining, API, 1986

Washington, D.C., American Petroleum Institute. Technical data book – petroleum refining; 6th Ed, 1997

Waston, K. M., Nelson, E. F., Murphy, G. B., Characterisation of Petroleum Fractions, Industrial and Engineering Chemistry, Vol. 27, 1460-1464, 1935

Watkins, R. N., Petroleum Refinery Distillation, 2nd Ed. Gulf Publishing Company, Houston, 1979

Wenzel, F.W., Serpemen, Y., and Hubel, A., On-line gasoil blending: an important tool to improve refining profitability, Oil&Gas Journal, March 18 p.62, 1991

Whitson, C.H., Characterizing hydrocarbon plus fraction, Soc. Pet. Eng. J. 683-694 (August), 1983

Wu, Y., 2010. Molecular management for refining operations, PhD thesis, University of Manchester, Manchester, 2010

Wu, Y., Zhang, N., Molecular Characterization of Gasoline and Diesel Streams. Ind. Eng. Chen. Res., 49: 12773-12782, 2010

Zhang, L., Hou, Z., Horton, S. R., Klein, M. T., Shi, T., Zhao, S., Xu, C., Molecular Representation of Petroleum Vacuum Resid, Energy Fuel. 28, 1736–1749, 2014

Zhang,Y., A molecular approach for characterisation and property predictions of petroleum mixtures with applications to refinery modelling. Ph.D. Thesis, University of Manchester Institute of Science and Technology, 1999

Appendix 1 Pseudo-component generation in GAMS

```
sets
NumD volume fraction of D86    %  /N1*N51/
PseComp                        /P1*P36/
CutInter                       /I1*I6/
parameters
include inc\%CompName%.in
ontext
spg0 /727.5368/

Frac(NumD)
/
N1      5
N2      10
N3      30
N4      50
N5      70
N6      90
N7      995
/

TempF(NumD)
```

```
/
N1    99.26937683
N2    107.1682011
N3    144.7152758
N4    202.0536914
N5    283.7767904
N6    381.0613384
N7    428.7695349
/
TempTBP(NumD)
;
loop (NumD$(TempF(NumD)>0),TempTBP(NumD)=(TempF(NumD)-32)/1.8;);
variables
a
b
c
d
T2(NumD)
diff
;

scalar NoPseudo the number of pesudocomponent /35/;
scalar iter number of binary search tries /0/;
scalar       persents   /0/   ;
scalar       cutT    /0/;
scalar Tpre number of binary search tries /0/;
```

```
scalar Vpre                    /0/;

scalar vc /0/

positive variable Frac2;



Equations

      D86predict(NumD)  predict D86

      diffcal       material balance


;

D86predict(NumD)$(TempTBP(NumD)>0)..          Frac2(NumD)       =e=
a/10000000*power(TempTBP(NumD),3)+     b/1000*power(TempTBP(NumD),2)+
c/1000*TempTBP(NumD)+d;

diffcal..              diff=e=sum(NumD$(Frac(NumD)>0),power(((Frac2(NumD)-
Frac(NumD) )/Frac(NumD) )*100,2))  ;

*eq3..                          100=g=    a/10000000*power(TempTBP('N7'),3)+
b/1000*power(TempTBP('N7'),2)+ c/1000*TempTBP('N7')+d;

*eq4..        100 =g= Frac2('N7');

*D86predict(NumD)$(Frac(NumD)>0)..T2(NumD)                              =e=
a/10000000*power(Frac(NumD),3)+              b/1000*power(Frac(NumD),2)+
c/1000*Frac(NumD)+d;

*diffcal..             diff=e=sum(NumD$(TempTBP(NumD)>0),power(((T2(NumD)-
TempTBP(NumD) )/TempTBP(NumD) )*100,2))  ;


 Model D86reg1 /D86predict, diffcal/ ;

 Solve D86reg1 using NLP minimizing diff ;

display TempTBP ;
```

```
display a.l, b.l,c.l,d.l;

display Frac2.l;

*display T2.l;
```

Appendix 2 Group definition in group contribution method

2550 components are chosen to construct the structural groups from the Dortmund Data Bank (DDB).And around 16000 components were stored in form of connection tables. The structural groups of hydrocarbons used to represent petroleum streams in the thesis could be found in the following Table.

Group 14	Description	Name	ID/PR	Occurs
$-CH_3$	CH_3- not connected to either N, O, F or Cl	CH_3-(ne)	1/75	Decane
	CH_3- connected to either N, O, F or Cl	CH_3-(e)	2/73	Demethoxymethane, methyl butyl ether
	CH_3- connected to an aromatic atom	CH_3-(a)	3/74	Toluene, p-methyl-styrene
$-CH_2-$	$-CH_2-$ in a chain	$-C(c)H_2-$	4/82	Butane
	$-CH_2-$ in a ring	$-C(r)H_2-$	9/83	Cyclopentane
>CH-	>CH- in a chain	>C(c)H-	5/88	2-Methylpentane
	>CH- in a ring	>C(r)H-	10/87	Methylcyclohexane
>C<	>C< in a chain	>C(c)<	6/90	Neopentane
	>C< In a chain connected to at least one aromatic carbon	>C(c)< (a)	8/79	Ethylbenzene, diphenylmethane
	>C< in a chain	>C(c)< (e)	7/78	Ethanol

	connected to at least one N, O, Cl or F			
	>C< in a ring	>C(r)<	11/89	Beta-pinene
	>C< in a ring connected to at least one aromatic carbon	>C(r)<(Ca)	14/77	Indene, 2-methyl tetralin
	>C< in a ring connected to at least one N or O which are not part of the ring or one Cl of F	>C(r)< (e,c)	12/80	Cyclopentanol, menthol
	>C< in a ring connected to at least one N or O which are part of the ring	>C(r)< (e,r)	13/81	Morpholine,nicotine
=C(a)<	Aromatic =CH-	=C(a)H-	15/76	Benzene
	Aromatic =CH< not connected to either O, N, Cl or F	=C(a)< (ne)	26/86	Ethylbenzene, benzaldehyde
	Aromatic =C< with three aromatic neighbours	(a)=C(a)<(2a)	28/85	Naphthalene, quinolone
	Aromatic =C< connected to either O, N, Cl or F	=C(a)<(e)	27.84	Aniline, phenol
>C=C<	H_2C=C< (1-ene)	H_2C(c)=C<	61/33	1-Hexene
	>C=C< both C have at least one non-H neighbours	>C(c)=C(c)<	58/38	2-Heptene, mesityl oxide

	Non-cyclic >C=C< connected to at least one aromatic C	>C(c)=C(c)<C(a)	59/35	Isosafrole, cinnamic alcohol
	Cyclic >C=C<			
	Non-cyclic >C=C<	>C(r)=C(r)<	62/36	Cyclopentadiene
	substituted with at least one F, Cl, N or O	-(e)C(c)=C(c)<	60/34	Trans-1,2-dichloroethylene, perfluoroisoprene

Appendix 3 Octane Number Prediction Method

The prediction procedure including two steps: regression and prediction. Instead of calculating ONs of each matrix entry, Wu adopted 5 lumps of PIONA for ON regression. And an ON blending model developed by Ghosh (2006) is incorporate in this work to predict ONs of a petroleum stream. The methodology procedure is presented as Figure A.1.

There are two main assumptions that adopted in this method: hydrocarbons belonging to a same homologous series could blend linearly (API, 1997; Scott, 1958; Ghosh, 2006). For example, paraffins blend linearly with other paraffins; olefins blend linearly with other olefins. Another assumption is that fractions and ONs of PIONA lumps could be correlated with bulk properties such as TBP curve and density.

Based on the first assumption, the ON of a stream could be presented as the function of fractions and ONs of PIONA lumps, shown as Equation A.1:

$$ON = f(x_i, ON_i) \quad \forall i \in PIONA \tag{A.1}$$

where x_i is the fraction of i lump, and ON_i for ON of lump i.

Based on the second assumption, a correlation that is analogous to the equation for cetane number calculation is proposed here. The quadratic equations correlate the fractions and ONs of PIONA lumps with TBP and density as Equation A.2 and A.3. Parameters are regressed by the proposed methodology.

$$\begin{aligned} x_i^{pred} = {} & a_{1,i}^f B_N^2 + a_{2,i}^f T_{10N}^2 + a_{3,i}^f T_{50N}^2 + a_{4,i}^f T_{90N}^2 + a_{5,i}^f B_N T_{10N} \\ & + a_{6,i}^f B_N T_{50N} + a_{7,i}^f B_N T_{90N} + a_{8,i}^f T_{10N} + a_{9,i}^f T_{50N} \\ & + a_{10,i}^f T_{90N} + a_{11,i}^f B_N + a_{12,i}^f \end{aligned} \tag{A.2}$$

$$\forall i \in PIONA$$

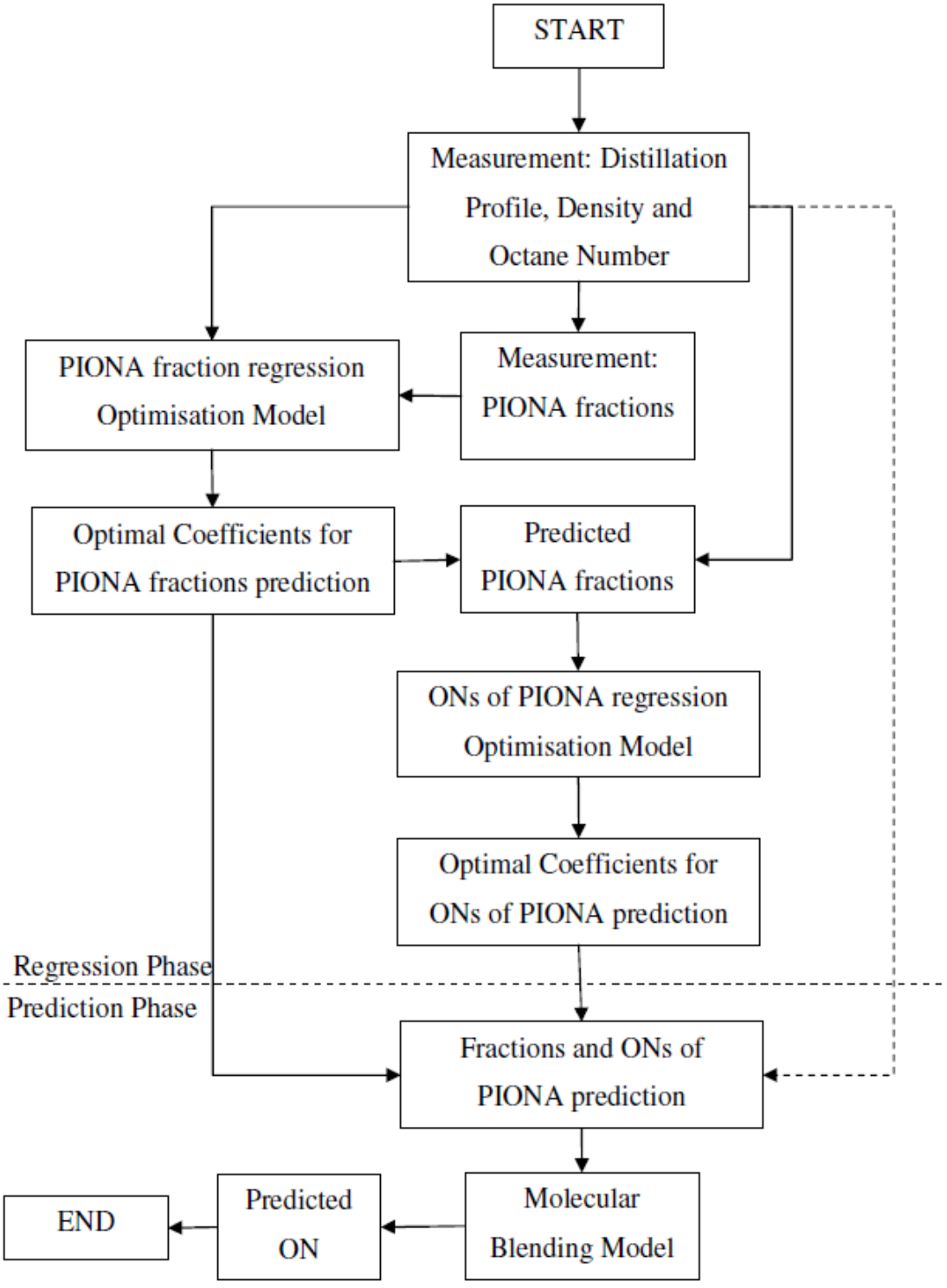

Figure A.1 the methodology of predicting ON of gasoline stream

and

$$
\begin{aligned}
ON_i^{pred} = {} & a_{1,i}^{ON} B_N^2 + a_{2,i}^{ON} T_{10N}^2 + a_{3,i}^{ON} T_{50N}^2 + a_{4,i}^{ON} T_{90N}^2 \\
& + a_{5,i}^{ON} B_N T_{10N} + a_{6,i}^{ON} B_N T_{50N} + a_{7,i}^{ON} B_N T_{90N} \\
& + a_{8,i}^{ON} T_{10N} + a_{9,i}^{ON} T_{50N} + a_{10,i}^{ON} T_{90N} + a_{11,i}^{ON} B_N \\
& + a_{12,i}^{ON} \qquad \forall i \in PIONA
\end{aligned} \tag{A.3}
$$

where

$$B_N = e^{-3.5(d-\bar{d})} - 1 \tag{A.4}$$

$$T_{10N} = \frac{T_{10}}{100} \tag{A.5}$$

$$T_{50N} = \frac{T_{50}}{100} \tag{A.6}$$

$$T_{90N} = \frac{T_{90}}{100} \tag{A.7}$$

The initial guess of ON could be estimated by the following equations (Riazi, 2005):

$$RON_i^{Init} = a_i + b_i T + c_i T^2 + d_i T^3 + e_i T^4 \tag{A.8}$$

The coefficients is shown in Table A.2 which is different with the values from Riazi's book (2005) in normal paraffin, naphthene via an re-regression, and one more set of coefficients for olefin is added in the table.

The detailed gasoline composition-based octane blending model (Ghosh, 2006) adopted here is as Equation A.2:

$$ON = \frac{\sum_{i \in PIONA} x_i^v \beta_i ON_i + I_{PI} \sum_{i \epsilon PI} x_i^v \beta_i ON_i}{\sum_{i \epsilon PIONA} x_i^v \beta_i + I_{PI} (\sum_{i \epsilon PI} x_i^v \beta_i - \sum_{i \epsilon PI} x_i^v)} \tag{A.9}$$

where β_i is the adjustable parameters and represent whether a molecule contributes beneficially or detrimentally to the ON of the gasoline fuel.

$$I_{PI} = \frac{k_{PN}^{a} x_N^{v} + k_{PO}^{a} x_O^{v}}{1 + k_{PN}^{b} x_N^{v} + k_{PO}^{b} x_O^{v}} \tag{A.10}$$

RON	a	b	c	d	E
P	1514.96	-3893.45	1211.06	3649.12	-2507.33
I	95.93	-157.53	561.00	-600.00	200.00
	92.07	57.63	-65.00	0.00	0.00
	109.38	-38.83	-26.00	0.00	0.00
	97.65	-20.80	58.00	-200.00	100.00
O	517.85	-1064.06	181.02	1237.31	-777.67
N	3.70	390.92	-493.28	98.66	82.24
A	145.67	-54.34	16.28	0.00	0.00

Table A.2 Coefficients for Equation

Values of parameters could be found in Table A.1

molecular class	molecular lumps	β(RON)	β(MON)
n-paraffins	nC_4-nC_{12}	2.0559	0.3092
i-paraffins	C_4-C_{12} mono-, di-, and trimethyl-*i*-paraffins	2.0204	0.4278
naphthenes	C_5-C_9 naphthenes	1.6870	0.2821
aromatics	benzene$-C_{12}$ aromatics	3.3984	0.4773
olefins/cyclic olefins	C_4-C_{12} linear, branched, and cyclic olefins	8.9390	10.0000
oxygenates	MTBE, EtOH, TAME	3.9743	2.0727
interaction parameters	$k_{PN}^{(a)}$, $k_{PN}^{(b)}$, $k_{PO}^{(a)}$, $k_{PO}^{(b)}$	0.2, 2.4, 0.4, 3.6	0.2, 2.4, 0.4, 3.6

Table A.1 Average values of the adjustable parameters

Appendix 4 Kinetic Network Code for Catalytic Reforming

```
function dydt = Rxn( t, y, flag, k )
% This function convert reaction network into ODEs and then it was
% dilivered to ODE solver to sovle it

dydt=zeros(size(y));

dydt(1)=k(34)*y(12)+k(58)*y(19)-(k(1)+k(2)+k(3)+k(4)+k(5)+k(6))*y(1);
dydt(2)=k(2)*y(1)+k(39)*y(13)+k(61)*y(20)-
(k(7)+k(8)+k(9)+k(10)+k(11)+k(12))*y(2);
dydt(3)=k(3)*y(1)+k(8)*y(2)+k(44)*y(14)+k(65)*y(21)-
(k(13)+k(14)+k(15)+k(16)+k(17))*y(3);
dydt(4)=k(4)*y(1)+k(9)*y(2)+k(14)*y(3)+k(48)*y(15)+k(68)*y(22)-
(k(18)+k(19)+k(20)+k(21)+k(22))*y(4);
dydt(5)=k(5)*y(1)+k(10)*y(2)+k(15)*y(3)+k(19)*y(4)+k(51)*y(16)+k(70)*y(23)-
(k(23)+k(24)+k(25)+k(26))*y(5);
dydt(6)=k(6)*y(1)+k(11)*y(2)+k(16)*y(3)+k(20)*y(4)+k(24)*y(5)+k(53)*y(17)+k(
56)*y(18)-(k(27)+k(28)+k(29)+k(30)+k(31))*y(6);
dydt(7)=k(6)*y(1)+2*k(12)*y(2)+k(17)*y(3)+k(21)*y(4)+k(25)*y(5)+k(29)*y(6)-
(k(32)+k(33))*y(7);
dydt(8)=k(5)*y(1)+k(11)*y(2)+k(17)*y(3)+2*k(22)*y(4)+k(26)*y(5)+k(30)*y(6)+k
(32)*y(7);
dydt(9)=k(4)*y(1)+k(10)*y(2)+k(16)*y(3)+k(21)*y(4)+k(26)*y(5)+2*k(31)*y(6)+k
```

```
(33)*y(7)+k(38)*y(12)+k(43)*y(13)+k(64)*y(20);

dydt(10)=k(3)*y(1)+k(9)*y(2)+k(15)*y(3)+k(20)*y(4)+k(25)*y(5)+k(30)*y(6)+k(3
3)*y(7)+k(37)*y(12)+k(42)*y(13)+k(47)*y(14)+k(60)*y(19)+k(63)*y(20)+k(67)*y(
21);

dydt(11)=k(2)*y(1)+k(8)*y(2)+k(14)*y(3)+k(19)*y(4)+k(24)*y(5)+k(29)*y(6)+k(3
2)*y(7)+k(36)*y(12)+k(41)*y(13)+k(46)*y(14)+k(50)*y(15)+k(59)*y(19)+k(62)*y(
20)+k(66)*y(21)+k(69)*y(22);

dydt(12)=k(1)*y(1)-(k(34)+k(35)+k(36)+k(37)+k(38))*y(12);

dydt(13)=k(7)*y(2)+k(36)*y(12)-(k(39)+k(40)+k(41)+k(42)+k(43))*y(13);

dydt(14)=k(13)*y(3)+k(37)*y(12)+k(41)*y(13)-(k(44)+k(45)+k(46)+k(47))*y(14);

dydt(15)=k(18)*y(4)+k(38)*y(12)+k(42)*y(13)+k(46)*y(14)-
(k(48)+k(49)+k(50))*y(15);

dydt(16)=k(23)*y(5)+k(43)*y(13)+k(47)*y(14)+k(50)*y(15)-(k(51)+k(52))*y(16);

dydt(17)=k(27)*y(6)+k(57)*y(18)+k(71)*y(24)-(k(53)+k(54)+k(55))*y(17);

dydt(18)=k(28)*y(6)+k(55)*y(17)-(k(56)+k(57))*y(18);

dydt(19)=k(35)*y(12)-(k(58)+k(59)+k(60))*y(19);

dydt(20)=k(40)*y(13)+k(59)*y(19)-(k(61)+k(62)+k(63)+k(64))*y(20);

dydt(21)=k(45)*y(14)+k(60)*y(19)+k(62)*y(20)-(k(65)+k(66)+k(67))*y(21);

dydt(22)=k(49)*y(15)+k(63)*y(20)+k(66)*y(21)-(k(68)+k(69))*y(22);

dydt(23)=k(52)*y(16)+k(64)*y(20)+k(67)*y(21)+k(69)*y(22)-k(70)*y(23);

dydt(24)=k(54)*y(17)-k(71)*y(24);

dydt(25)=(k(1)-(k(2)+k(3)+k(4)+k(5)+k(6)))*y(1)+(k(7)-
(k(8)+k(9)+k(10)+k(11)+k(12)))*y(2)...

    +(k(13)-(k(14)+k(15)+k(16)+k(17)))*y(3)+(k(18)-
(k(19)+k(20)+k(21)+k(22)))*y(4)...

    +(k(23)-(k(24)+k(25)+k(26)))*y(5)+(k(27)+k(28)-(k(29)+k(30)+k(31)))*y(6)...

    -(k(32)+k(33))*y(7)+(3*k(35)-(k(34)+k(36)+k(37)+k(38)))*y(12)+(3*k(40)-
(k(39)+k(41)+k(42)+k(43)))*y(13)...
```

```
+(3*k(45)-(k(44)+k(46)+k(47)))*y(14)+(3*k(49)-
(k(48)+k(50)))*y(15)+(3*k(52)-k(51))*y(16)+(3*k(54)-k(53))*y(17)...

-(4*k(58)+k(59)+k(60))*y(19)-(4*k(61)+k(62)+k(63)+k(64))*y(20)-
(4*k(65)+k(66)+k(67))*y(21)-(4*k(68)+k(69))*y(22)...

-4*k(70)*y(23)-3*k(71)*y(24)-k(56)*y(18);



end
```